AD-A033 037 MARYLAND UNIV COLLEGE PARK COMPUTER SCIENCE CENTER F/G 4/2
CLOUD PATTERN CLASSIFICATION FROM VISIBLE AND INFRARED DATA.(U)
FEB 76 J PARIKH F44620-72-C-0062
UNCLASSIFIED TR-442 AFOSR-TR-76-1137 NL

1 OF 2
AD
A033037

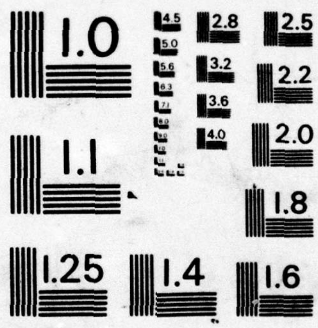
1.0
1.1
1.25
1.4
1.6
1.8
2.0
2.2
2.5
2.8
3.2
3.6
4.0
4.5
5.0
5.6
6.3

403 018

COMPUTER SCIENCE TECHNICAL REPORT SERIES

UNIVERSITY OF MARYLAND
COLLEGE PARK, MARYLAND
20742

AFOSR - TR - 76 - 1137

TR-442 February 1976

F44620-72C-0062

CLOUD PATTERN CLASSIFICATION FROM VISIBLE AND INFRARED DATA

JoAnn Parikh
Computer Science Center
University of Maryland
College Park, MD 20742

ABSTRACT

This report describes progress in the development of the area classification portion of a computer vision system for cloud pattern analysis. The ultimate goal of the vision system is to extract meteorologically significant cloud regions from a time sequence of dual-channel geosynchronous satellite images. The question explored by this paper is to what extent single-stage and multistage statistical pattern recognition techniques may be employed in the classification of clouds from a single dual-channel image.

See 1473

ACKNOWLEDGEMENTS

I would like to acknowledge my indebtedness to the members of the National Environmental Satellite Service (NESS), of the University of Maryland Picture Processing Laboratory, and of the University of Maryland Laboratory for Pattern Analysis without whom this study would not have been possible.

For both meteorological advice and technical assistance in obtaining the data base for this study, I would like to thank Mr. Arthur L. Booth and Mr. Henry Drahos of NESS. In addition, meteorological insights into problems of cloud pattern analysis provided by Mr. Lester F. Hubert and Mr. Andrew Timchalk proved invaluable.

The programming assistance provided by Mr. Robert Kirby, Ms. Joan Weszka, and Mr. Kenneth Hayes of the University of Maryland Picture Processing Laboratory is deeply appreciated.

For the privilege of being the first user of the Maryland Interactive Pattern Analysis Classification System (MIPACS), I wish to thank Dr. Laveen Kanal, Mr. George Stockman, and Mr. Ashok Kulkarni of the University of Maryland Pattern Analysis Laboratory. Their interest and participation in this project resulted in an extensive analysis of multistage classification designs. For his comments throughout the course of this study and his criticism on portions of this report relating to multistage pattern classification systems, my special thanks to

Mr. Ashok Kulkarni.

The continual guidance of my advisor, Dr. Azriel Rosenfeld, and the support of Dr. Laveen Kanal and Dr. Ashok Aqrawala have provided the inspiration to continue the arduous task of investigating many cloud pattern classification designs.

Special thanks to Ms. Shelly Rowe who typed both the text and the numerous statistical tables and mathematical formulae in this report.

1. Introduction

The success or failure of global numerical weather prediction models hinges upon two basic factors: adequate formulation of the system of hydrodynamic and thermodynamic equations modeling the dynamics of the atmosphere, and accurate determination of the set of initial variables input to the numerical prediction model. A detailed description of numerical weather prediction models can be found in [1]. This set of variables includes horizontal wind velocity estimates for each pressure height (vertical level) of the forecasting model. A global set of wind velocity estimates can be obtained only by supplementing weather station estimates (available primarily for the Northern Hemisphere) extracted from radiosonde data, aircraft reports, and dropsonde data with automatically extracted wind velocity estimates obtained from observation of cloud motion in consecutive pairs of geostationary satellite images. The subject of this report is the design, implementation, and testing of an automatic cloud classification system for preprocessing geostationary satellite images used in wind velocity estimation. Currently, this classification is done by meteorologists with the aid of time sequence movie loops in addition to the pairs of images.

Deterioration in the quality of automatic wind velocity estimates can often be traced either to incorrect estimation of the variables relating infrared measurements to cloud-top temperatures or to violation of the basic assumption that the observed cloud motion corresponds to the horizontal wind

flow. References [2], [3], [4], [5] discuss the problem in further detail. Identification followed by rejection of satellite image areas containing cumulonimbus clouds eliminates from consideration for wind velocity estimation a major non-advective cloud type whose motion is affected by strong vertical currents. Variables which affect both classification accuracy and accuracy of conversion of infrared measurements into cloud-top temperatures are size of cloud elements, number of breaks or holes in the cloud elements, location of cloud elements relative to viewing angle of the sensor, presence of atmospheric gases such as water vapor, carbon dioxide, and ozone along the radiation path, and opaqueness of the cloud elements. If the cloud elements do not entirely fill the field of view of the sensor or if there are breaks or holes in the clouds smaller than the sensor's resolution, the satellite-derived temperature will be warmer than the actual temperature. Identical cloud patterns viewed at different angles may appear to have different temperature profiles. The sensor when viewing the cloud patterns at a direct angle may measure a larger proportion of surface radiation in the image window than when viewing the cloud pattern at an oblique angle, thus making it appear that the cloud pattern viewed directly is warmer than the cloud pattern viewed obliquely. Radiation from sea-surface and clouds involves absorption and re-emission at a lower temperature by several atmospheric gases along the path from sea-surface or clouds to satellite sensor. The longer the radiation path or the higher the concentration of water vapor

(water vapor concentration in the tropics is particularly high) and other gases, the colder the satellite-derived temperature will appear to be. If the absorptivity of these gases is negligible, and if the clouds are continuous and opaque to terrestrial radiation (i.e., emissivity, E, is assumed to be unity), then the satellite-derived temperature closely approximates the cloud-top temperature.

Cloud emissivity (E) is a variable which must be estimated when relating the radiance or temperature (B_T) measured by infrared satellite sensors to the temperature (B_c) of a cloud. The vertical location of a wind vector estimated from the movement of cloud c is determined by entering the temperature B_c and the location P_c of the cloud into the National Meteorological Center (NMC) data base (stored on an IBM 360/195 system of vertical temperature profiles). The pressure altitude, rounded off to the nearest 10 mb, becomes the vertical location of the wind vector. The temperature B_c of the cloud is related to the infrared satellite reading B_T for cloud c by the following equation:

$$B_c = [B_T - B_s(1-E)]/E$$

where

B_T = radiance at satellite

B_c = radiance from cloud

B_s = radiance from surface below the cloud (either sea-surface and/or underlying clouds)

E = emissivity of cloud c

When the value of the emissivity is unity, the satellite-derived temperature equals the cloud-top temperature. The

range of possible values for E is maximal for cirrus clouds where values of emissivity can range from .35 up to unity. The choice of cloud tracers for cirrus clouds should be restricted to sufficiently opaque patches which appear white in both visible and infrared images. The problem of restriction of cloud tracers is not as acute for middle clouds (where emissivity values range typically between .7 and unity) or for low clouds (which generally have high values of emissivity).

The identification of areas containing predominantly cirrus clouds alerts the wind extraction program to check the opacity of cloud tracers in both visible and infrared data. Areas containing multi-layered clouds present additional processing problems to a wind extraction program in that movement of cloud elements within the window cannot be integrated into one wind velocity vector. The task of the classification program in preprocessing satellite VISSR (Visible and Infrared Spin Scan Radiometer) data is summarized in Table 1.

The four classes of clouds enumerated in Table 1 are:

Class 1 -- cumulonimbus clouds

Class 2 -- low clouds, i.e., cumulus, cumulus congestus, stratocumulus, and stratus

Class 3 -- cirrus clouds

Class 4 -- mixed clouds -- cirrus with low clouds, cirrus with middle clouds, and cirrus with low and middle clouds

An area on a satellite image was classified as Class 1 if cumulonimbus clouds occurred in any part of the area, re-

gardless of their amount, and whether or not cumulus or cirriform clouds were also present. An area was classified as Class 2 if predominantly single-layered low clouds were present and as Class 3 if predominantly single-layered cirrus clouds were present. An area was classified as Class 4 if it contained multiple-layered cloud elements.

This research evaluates the ability of various features and statistical classification methods to separate sample areas selected from VISSR images into the above four classes. A sub-problem, the design of a pattern classification system to separate samples from classes 1, 2, and 3, was also investigated. Section 2 describes the characteristics of the NOAA-1 satellite data set. Section 3 describes the feature selection phase of the pattern classification study. Section 4 describes the classifier selection phase of the pattern classification study. Section 5 presents conclusions and plans for further research.

A pattern recognition system may be decomposed into three different parts:

1) choice of decision logic structure, i.e., whether all classes are to be separated at once or whether one or more classes are to be sequentially separated from the remaining classes
2) choice of classifier(s), and
3) choice of features.

Eight different decision trees, representing alternatives for sequential cloud pattern identification, were examined during the course of this study. Four different classifiers

-- maximum likelihood, multiclass one-against-the-rest, multiclass voting, and Fisher using sample "a priori" probabilities -- were applied at various nodes of the decision tree structures. A total of 334 feature statistics -- 46 first-order statistics and 288 second-order or texture statistics -- were extracted from 243 sample cloud observations. The sample cloud observations were divided into four classes labelled "low" clouds, "mix" clouds, "cirrus" clouds, and "cumulonimbus" clouds. For each feature a measure of class separation, the Fisher Distance, was calculated for each of the six two-class combinations. This measure was used as a guide in the selection of those combinations of features assigned to a given decision tree node.

Maximum likelihood two-level classification for identification of the four classes using a selected combination of seven features at the first level and six features at the second level resulted in 91.4% of the samples being correctly classified. If areas which contained "mix" samples could be processed by scene analysis techniques, the above four-class problem would reduce to the three-class problem of identification of "low", "cirrus", and "cumulonimbus" clouds. Maximum likelihood single-level classification for identification of these three classes using only two features resulted in 98.7% of the samples being correctly classified.

2. Characteristics of the Digital Satellite Data and Class Category Map for Sample Tropical Cloud Patterns

2.1 Description of NOAA-1 Visible and Infrared Ingest Data

The digitized satellite data for the sample cloud patterns analyzed in this study resulted from analog-to-digital processing of scanning radiometer signals received from the NOAA-1 spacecraft on May 3, 1971 (Orbit 1798). The NOAA-1 polar orbiting satellite was in operation from December 11, 1970 until August 19, 1971. NOAA-1 was launched into an approximately 790 n.mi., sun-synchronous orbit, i.e., the orbital plane precessed about the Earth's polar axis in the same direction and at the same average rate as the Earth's annual revolution about the sun, thereby minimizing annual variation in satellite sun angle. The ascending node (longitude at which the satellite crosses the Equator from south to north) crossing was at 1500 hours local mean solar time.

The prime imagery sensors of NOAA-1 are two-channel scanning radiometers sensitive to energy in the 0.52 to 0.72μm visible spectrum and to energy in the 10.5 to 12.5μm atmospheric infrared "window". Energy is gathered by a 5 inch elliptical scan mirror set at an angle of 45° to the scan axis and rotating at 48 rpm. The rotating mirror provides an optical scan of a 3,622 n.mi. long area of the earth perpendicular to the direction of spacecraft motion. The infrared window radiation is collected into a thermistor bolometer, the size of which (5.3

milliradians) defines the Instantaneous Field of View. The visible energy is detected by a silicon photo voltaic detector, the size of which together with its field stop limits the Instantaneous Field of View for visual data to approximately 2.8 milliradians. Since the mirror rotates at a constant angular rate, the geometic resolution of the ground field of view decreases as the distance from the subsatellite point increases. Resolution near the subpoint is approximately 4 n.mi. for the infrared channel, decreasing to 8 n.mi. by 12 n.mi. where the zenith angle (angle between normal to earth's surface and satellite) is beyond 60°; and 2 n.mi. for the visible channel, decreasing to 4 n.mi. by 8 n.mi. for a zenith angle beyond 60°. At the subpoint, successive infrared channel scan lines are contiguous and overlap as the distance from the subpoint increases. There is a 2 n.mi. gap between visible channel data lines at the subpoint. This gap disappears for distances more than 750 n.mi. from the subpoint. Descriptions of the NOAA-1 spacecraft and operational products available from ITOS scanning radiometer data can be found in [3], [6], [7], and [8].

The process of converting raw scanner signals into raw ingest data available on tape is described in [8]. Electrical and thermal or brightness calibrations are then applied to the data (see Appendix B, [8]). Further corrections, such as corrections of infrared data for atmospheric attenuation ("limb darkening" correction) as

a function of local zenith angle, or sun normalization corrections of the visual data to compensate for differences in solar illumination, were not made. For the data selected for this study, the effects of atmospheric attenuation and varying sun-angle were considered minimal and thus neglected. From each scan line, only the central 1120 points, for which no curvature correction and no limb darkening correction were considered necessary, were chosen. Also, there was no problem of sun glint for this particular area of data.

The region of data selected consists of a pair of infrared and visual data arrays of 1120 x 960 points, covering an area of approximately 25° of latitude and 30° of longitude over the tropical eastern Pacific Ocean west and South of Baja California. Latitude limits are 26.7° N to 1.1° S. Values from the visible spectrum represent measurements of albedo ranging from 0 (black) to 255 (white). Values from the infrared spectrum represent effective blackbody radiative temperature measurements ranging from 160.0 (white)to 330.0 (black) degrees Kelvin. The infrared values were rounded to the nearest degree and re-scaled by a shift of -160. In order to obtain the pictures shown in Figs. 1 and 2, each scan line was doubled. For a region from the given pictures consisting of a 32x32 matrix of points, the areal dimension is approximately 54x96 n.mi. The vertical dimension of 96 n.mi. was obtained by multiplying the average resolution of a point (3 n.mi.) by 32, the number of vertical lines in a 32x32

array. The average resolution was taken as the average of a 2 n.mi. visible resolution and a 4 n.mi. infrared resolution. For the horizontal dimension, points did not represent contiguous fields of view. The sampling rate of the digitizer was approximately 1.7 samples per field of view, resulting in approximately 18 contiguous fields of view for 32 points. Multiplying 18 (the number of contiguous fields of view) by 3 n.mi.,one obtains an approximate horizontal dimension of 54 n.mi. A description of the data and of the accompanying cloud category map prepared by meteorologists from the National Environmental Satellite Service is given in [9].

2.2 Description of the Cloud-Truth Analysis for NOAA-1 Satellite Data

This section summarizes the description given in [9] of the method of preparation of the cloud category map, shown in Figure 3, for the satellite cloud data of Figures 1 and 2. Two meteorologists, furnished with ungridded enlargements of the infrared and visual NOAA-1 satellite cloud data, gridded enlargements (with the 1120x960 data arrays gridded into 35x30 observations each containing 32x32 data points), and near-time coincident movie loops of visual imagery from the ATS-1 satellite, were asked initially to identify all possible cloud types observable in the given region. The analysis resulted in a categorization of each of the 1050 sample areas of pairs of 32x32 infrared and visual matrices into one of the following

eight groups:

(1) no observable clouds

(2) cumulus/cumulus congestus

(3) stratocumulus/stratus

(4) cumulonimbus

(5) cirrus

(6) cirrus with low clouds

(7) cirrus with middle clouds

(8) cirrus with low and middle clouds

Within any particular group, the cloud amount for the predominant cloud type was variable; for example, an observation with a very small amount of cumulus cloud content was classified into group 2 rather than group 1. Also, whenever cumulonimbus clouds occurred in combination with any other cloud type, regardless of amount of cumulonimbus present, the observation was classified as cumulonimbus. The observations were then automatically classified as described in [9]. The number of correct classifications was 675 out of 1050. The 375 misclassified observations were re-examined by the two meteorologists, and 184 of the 375 samples were re-classified with the new classifications for 115 of the 184 samples in agreement with the corresponding automatic classifications. The group frequencies for the sample observations at the conclusion of this final analysis were

(1) group 1 - 113 samples

(2) group 2 - 258 samples

(3) group 3 - 155 samples

(4) group 4 - 117 samples

(5) group 5 - 174 samples

(6) group 6 - 182 samples

(7) group 7 - 38 samples

(8) group 8 - 13 samples

The resultant cloud category map in which each of the 1050 observations is identified by its group label (from "1" to "8") is shown in Figure 3.

Since the areas chosen for wind velocity estimation usually consist of 64x64 data points, every four sample 32x32 observations from the 1050 sample observations were combined together to form 255 new sample observations (each consisting of 64x64 data points) of which 243 contained cloud data. The cloud category map of Figure 3 was then reduced to the cloud category map of Figure 4. Any 4x4 configuration in the original cloud category map of Figure 3 which contained only 1's, 2's, or 3's and at least one 2 or 3 was labelled as "L" for "low cloud" in the cloud category map of Figure 9. Any 4x4 combination which contained one or more 6's, 7's, or 8's was labelled as "M" for "mixed cloud". Any 4x4 combination which contained one or more 4's was labelled as "Cb" for "cumulonimbus cloud". Any 4x4 combination which contained only 5's or 5's and 1's was labelled as "Ci" for "cirrus cloud". A 4x4 combination containing one or more 5's combined with one or more 2's or 3's was also classified as mixed cloud. Finally, any 4x4 combination containing all 1's

(no observable clouds) was not processed. The group frequencies for the four cloud types of the cloud category map of Figure 4 are

(1) low clouds - 86 samples

(2) mixed clouds - 87 samples

(3) cirrus clouds - 24 samples

(4) cumulonimbus clouds - 40 samples

The cloud category map of Figure 4, together with the 243 sample pairs of visual and infrared 64x64 data points, form the data base used to investigate the optimal design for a statistical cloud classification system for wind velocity estimation.

3. Feature Selection

3.1 First Order and Second Order (Textural) Statistical Features

First order statistical features of an image are features which describe or characterize the density function p(g) of the image gray levels. For comparison of finite images, each with the same number of gray levels, the histogram or frequency distribution of gray level values in the image can be used as the basic function whose properties are to be described by a given set of features.

For the classification of cloud patterns, the first order statistical features chosen to describe the infrared and visual histograms were the mean; the standard deviation; the gray level values with cumulative frequency percentages of 0%, 10%, ...,100%; and the differences between pairs of gray level values with cumulative frequency percentages of 0% and 100%, 10% and 90%, 0% and 50%, 50% and 100%, 20% and 80%, 30% and 70%, and 40% and 60%. Feature definitions for both first order and second order statistical features may be found in Appendix A.

Second order (textural) statistical features of an image are features which describe or characterize the joint density function $p_{\rho,\theta}(g_1,g_2)$ of pairs of gray levels separated from each other in the orientation or direction θ by a distance of ρ. That is, textural features characterize the spatial dependency of gray levels [10]. For textures composed of "elements" (e.g., small pieces of relatively constant gray level), if ρ is small compared to the element size, then $p_{\rho,\theta}(g_1,g_2)$ will tend to be high for $|g_1-g_2|$ small, and low otherwise; thus, measuring $p_{\rho,\theta}$

for various values of ρ provides information about texture element sizes. For ρ large compared to the element size, or if there are no significant texture elements, $p_{\rho,\theta}(g_1,g_2)$ will essentially be the probability that two randomly chosen image points have gray levels g_1 and g_2, respectively. In such cases second order statistics will not provide any useful information beyond that available from first order statistics.

Historically, textural features have been used to characterize cloud types. Expressions such as "fibrous appearance" have been used to characterize cirrus clouds; altocumulus is described in terms of "regularly arranged small elements [which] usually have an apparent width of between one and five degrees"; cirrocumulus is said to be "composed of very small elements in the form of grains, ripples, etc., merged or separate, and more or less regularly arranged" [11].

Textural features have been employed not only in manual but also in automatic cloud pattern analysis systems. In 1968, Darling and Joseph [12] published a classic paper on comparison of various decision algorithms using a set of 28 discriminators, including "15 quantities [designed to] measure the general textural characteristics of the scene". Ever since then, texture features have been incorporated into major cloud pattern analysis studies. In 1972 Booth [9] found that for both visual and infrared images the average digital gradient, a textural feature, entered into the discriminant function calculation at the 1% screening level. Aggarwal and Duda [13] state that "in the cloud tracking problem there are measurable differences in brightness, boundary shape, and texture between clouds in diff-

erent layers."

The incorporation of textural features into this study is an attempt to investigate measurable differences in texture between four classes of clouds, chosen for their relevance to automatic wind velocity estimation programs. The calculation of these textural features is based on areas which may not and often are not uniformly covered by one particular cloud layer. Variable amounts of sea surface and other cloud types may be present in the given imagery. This problem is inherent in any regular partitioning of a satellite picture into areas large enough for subjective meteorological classification and may cause degradation in the calculation of textural features. As will be seen in Section 4.3, the results of this study strongly suggest that features such as brightness and standard deviation are far more significant in identification of cloud layers than textural features.

The textural features extracted from each of the 243 cloud observations for distances $\rho = 1, 2, 4, 8$ and directions $\theta = 0°$, $45°$, $90°$, $135°$ are:

1) mean of gray level difference values -- the expected value of the gray level difference, which ranges from 0 to 255;
2) contrast -- the expected value of the squared gray level difference ;
3) angular second moment -- the sum of the squares of the difference probabilities;
4) entropy -- the negative sum of the products of difference probabilities times their logarithms;

5) statistics (consisting of mean, standard deviation, minimum, maximum, and range) for each of quantities (1), (2), (3), and (4) calculated, for a given distance, over all four directions.

The definitions of the above 288 second-order statistical features (144 visual and 144 infrared) can be found in Appendix A. A discussion of the relationship between difference features and other textural features can be found in Section 2 and Appendix B of [14].

3.2 Class Comparison of Statistical Measures of Individual Features

For each of the four cloud classes (low, mix, cirrus, cumulonimbus), class means, standard deviations, minimums, maximums, medians, and ranges were calculated for each feature. Large differences between class mean values, coupled with small class standard deviations, indicate a feature likely to contribute to class separability. If the feature tends to be normally distributed, one would expect the median to closely approximate the mean. The minimum, maximum, and range values give some idea of the overlaps between feature values of the classes being compared.

The visual brightness feature values, shown in Tables 2-5, consistently reveal the same pattern of low (dark) values for cirrus cloud with little variation between samples, brighter values for low and mix clouds, and very bright values for cumulonimbus clouds (as evidenced by the minimum value of feature 113 and the mean value of feature 115). A large overlap occurs between the low and mix classes throughout the spectrum of visual

brightness features (note in particular feature 117), with mix clouds slightly brighter in general than low clouds.

This overlap between the low and mix classes occurs also in the values of infrared temperature features 302 and 314-320, shown in Tables 6-9. For standard deviation feature 302 and temperature range features 314-320, there is little variation in temperature values for low clouds, and increasing variation for mix, cirrus, and cumulonimbus clouds. The coldest (brightest) temperature values (feature 303) belong to cumulonimbus clouds. The next coldest values can be found in the mix and cirrus sample observations. Low clouds are generally warm.

Second-order visual difference statistics for distance 1 (Tables 10-13) measure factors such as the amount of local variation and the overall homogeneity of the images [10]. The mean texture features 121-129, representing normalized expected values of differences of neighboring gray levels for directions 0°, 45°, 90°, 135° and statistics on these expected values, are lowest for cirrus clouds, highest for cumulonimbus clouds, and approximately equal for low and mix clouds, with slightly higher values for mix clouds. Similar remarks apply to the contrast texture features 130-138, with features 130-133 representing expected values of squares of differences over the four directions, and the entropy texture features 148-156 which measure the complexity of an image. Entropy feature values are highest when there are many different difference values, i.e., for a more complex image, whereas a reverse pattern can be seen for ASM (angular second moment) features 139-147, which are lowest when there are many different difference values. For ASM

features 139-147, therefore, the highest values occur for cirrus clouds and the lowest values for cumulonimbus clouds, with considerable overlap between the values for low and mix clouds (with minimum values for mix clouds lower than minimum values for low clouds). The visual textural features seem to duplicate the same pattern of homogeneity vs. complexity exhibited by the visual brightness standard deviation feature 102. Comparing all four groups of textural features by standard deviations relative to mean values, the visual contrast features 130-138 in particular show an unusually large scattering around their mean values compared to the visual entropy features 148-156.

The second-order infrared difference statistics for distance 1 (Tables 14-17) measure local variations in temperature. The lowest values (smallest temperature variations) occur for low clouds and the highest values for the dense thunderstorm cumulonimbus clouds. Local temperature variation is greater for cirrus clouds than for mix clouds. This result can partially be explained by differences in emissivity values of the thin and dense portions of the cirrus clouds (with warmer temperatures for the more emissive, thin portions) and partially by the method of classifying a sample as "mix" cloud. (If, for example, a minimum of 1/4 of the sample consisted predominantly of multi-layered cloud regions and the other 3/4 of the sample was predominantly low cloud, the sample was classified as "mix".) In many "mix" samples, a large portion of the sample contained relatively homogeneous low clouds. The overlap between mix and cirrus feature values was particularly evident for the ASM

features 339-347 (in fact, for feature 339, mix clouds appear slightly more homogenous than cirrus clouds). The angular second moment features show the same reverse pattern of the mean, contrast, and entropy features as noted in the previous paragraph with the mean, contrast, and entropy texture features duplicating the temperature variation pattern of the infrared standard deviation feature 302.

3.3 Results of Application of the Fisher Distance Criterion to the Feature Selection Problem

The problem of selection of features for class separability consists of choosing, at each stage s_i of a classification decision, that set of K_{s_i} features which contributes most effectively to the final discrimination of cloud classes. In order to measure class separability, the underlying class distributions must be assumed and a given classification decision logic, including type of classifier at each level and classes of cloud patterns to be distinguished at each level, must be specified. If the classifier chosen is the Bayes classifier (rather than, for example, a nearest neighbor classifier), the Bayes probability of error is the optimum measure of feature effectiveness. For two classes w_1, w_2 the Bayes classifier (decision rule) for one-dimensional (single feature) feature vectors is:

$$\text{Decide } w_1 \text{ if } \frac{p(x/w_1)}{p(x/w_2)} > \frac{P(w_2)}{P(w_1)}$$

$$\text{Decide } w_2 \text{ if } \frac{p(x/w_1)}{p(x/w_2)} < \frac{P(w_2)}{P(w_1)}$$

where $p(x/w_i)$ for i=1, 2 are class-conditional probability

densities and $P(w_i)$ for i=1,2 are a priori probabilities. Let R_1 be the region in which $\frac{p(x/w_1)}{p(x/w_2)} > \frac{P(w_2)}{P(w_1)}$, i.e., the region in which the decision w_1 is made, and let R_2 be the region in which $\frac{p(x/w_1)}{p(x/w_2)} < \frac{P(w_2)}{P(w_1)}$, i.e., the region in which the de-decision w_2 is made. The threshold t between R_1 and R_2 for two normal distributions with means μ_1 and μ_2 and with equal standard deviations σ is found by setting

$$\frac{p(t/w_1)}{p(t/w_2)} = \frac{P(w_2)}{P(w_1)} .$$

Assuming equal a priori probabilities $P(w_1) = P(w_2) = \frac{1}{2}$ and substituting the expression for the univariate normal densities, it follows that

$$\frac{\frac{1}{\sqrt{2\pi\sigma}} e^{-\frac{1}{2}\frac{(t-\mu_1)^2}{\sigma}}}{\frac{1}{\sqrt{2\pi\sigma}} e^{-\frac{1}{2}\frac{(t-\mu_2)^2}{\sigma}}} = 1$$

and taking natural logarithms on both sides of the equation, it follows that

$$t^2-2\mu_1 t+\mu_1{}^2 = t^2-2\mu_2 t+\mu_2{}^2$$

or

$$t = \frac{\mu_2+\mu_1}{2} ,$$

i.e., the threshold lies midway between the means. If R_2 is the

region to the right of R_1, i.e., $\mu_2 > \mu_1$, then the Bayes probability of error is given by

$$P(\text{error}) = P(x \in R_2, w_1) + P(x \in R_1, w_2)$$

$$= \int_t^{\infty} p(x/w_1)P(w_1)dx + \int_{-\infty}^{t} p(x/w_2)P(w_2)dx$$

$$= \frac{1}{2}\int_t^{\infty} \frac{1}{\sqrt{2\pi}\sigma} e^{-\frac{1}{2}\left(\frac{x-\mu_1}{\sigma}\right)^2} dx + \frac{1}{2}\int_{-\infty}^{t} \frac{1}{\sqrt{2\pi}\sigma} e^{-\frac{1}{2}\left(\frac{x-\mu_2}{\sigma}\right)^2} dx$$

which, substituting $u = (x-\mu_1)/\sigma$, $du = dx/\sigma$, $v = -(x-\mu_2)/\sigma$, $dv = -x/\sigma$, gives

$$= \frac{1}{2}\int_{\frac{t-\mu_1}{\sigma}}^{\infty} \frac{1}{\sqrt{2\pi}} e^{-\frac{1}{2}\mu^2} du - \frac{1}{2}\int_{\infty}^{\frac{\mu_2-t}{\sigma}} \frac{1}{\sqrt{2\pi}} e^{-\frac{1}{2}v^2} dv$$

which, substituting for t, changing the order of integration of the second integral, and collecting terms, yields

$$= \frac{1}{\sqrt{2\pi}} \int_{\frac{\mu_2-\mu_1}{2\sigma}}^{\infty} e^{-\frac{1}{2}y^2} dy$$

Note that the larger the value of the integration limit $\frac{\mu_2-\mu_1}{2\sigma}$, the smaller the probability of error.

The Fisher distance feature selection criterion for evaluation of the ability of a single feature to separate classes w_1 and w_2 is given by $\left|\frac{\mu_2-\mu_1}{\sigma_1+\sigma_2}\right|$ where μ_i, σ_i are the mean and standard deviation of the feature for samples in class w_i, i=1,2. For normal distributions and equal standard deviations, the Fisher distance is an optimum feature selection criterion,

i.e., it is monotonically related to the probability of error as shown in the previous paragraph. Except for the equal covariance case, even for normal distributions, the calculation of the probability of error requires a numerical integration. Various alternatives to calculation of the probability of error have been proposed. Most of these feature selection criteria, for example, the Fisher distance feature selection criterion, are designed to increase as the between-class scatter increases or the within-class scatter decreases.

The extension of the feature selection algorithms to multiclass (more than two) separability and multi-feature separability is unfortunately not simple. According to Fukunaga [15], "no single criterion can be particularly indicative of multiclass separability". Sometimes an upper bound on the probability of error is used. Theoretical relationships between the best pair, etc. of features for class separability and the best single features for class separability are lacking. This problem is discussed in detail in Kanal [16] where it is stated that "the only way to ensure that the best subset of k features from a set of N is chosen is to explore all $\binom{N}{k}$ possible combinations". In practice, however, a feature selection criterion for single features is often used to discard the worst features and subsequent trials of combinations tend to concentrate on adding a feature to those which performed well in the next lower-dimensional feature vector space.

The Fisher distance feature selection criterion was applied first to the problem of deciding whether distance 1, distance 2, distance 4, or distance 8 second-order textural

statistics were most effective in discriminating between pairs of cloud classes. Fisher distance values for visual difference features 121-264 are given in Tables 20-23 for distances 1, 2, 4, 8, respectively, and Fisher distance values for infrared difference features 321-464 are given in Tables 24-27 for distances 1, 2, 4, 8. For each of the difference features and for each of the six two-class combinations, a comparison of the values of the Fisher distance for distance 1, distance 2, distance 4, and distance 8 was made. A final tally revealed that distance 1 was the best overall choice. Distance 8 infrared difference features performed slightly better than distance 1 features for separation of low and mix clouds. Distance 8 infrared difference features were also useful for separation of low from cirrus clouds and distance 8 visual difference features were useful for separation of low from cumulonimbus clouds and low from mix clouds. This suggests that a typical difference pattern between elements of low clouds prevails over a large area.

The values of the Fisher distances in Tables 20-27 can also be used to verify which channel best separates each of the six two-class combinations. The infrared channel is to be preferred for any two-class combination containing low clouds. Differences between the cirrus cloud observations and observations of either mix clouds or cumulonimbus clouds are more pronounced in the visible image than in the infrared, where cirrus clouds appear dark gray and mix and cumulonimbus bright. Fisher distance values for separation of mix from cumulonimbus clouds are approximately equal for both infrared difference

features and visual difference features, with infrared entropy features slightly better than the others.

Evaluation of distance 1 features for each of the two-class combinations pointed to the superiority of the infrared entropy features 348-356 for separation of low clouds from either mix, cirrus, or cumulonimbus and for separation of mix from cumulonimbus clouds. Visual entropy features 148-156 performed well in discrimination of cirrus from cumulonimbus and from mix clouds, with visual ASM features slightly better than visual entropy features 148-156 or visual mean features 121-129 for separation of cirrus from mix. Infrared mean features 321-329 were second-best to infrared entropy features for the two-class problems of low vs. mix, low vs. cirrus, and mix vs. cumulonimbus, with infrared ASM features 339-347 second-best for the low vs. cumulonimbus combination. Visual ASM features 139-147 were second-best for cirrus vs. cumulonimbus. As a result of the analysis of Tables 20 and 24, it was decided to discard the infrared and visual contrast features 330-338 and 130-138 and to discard the statistical features on the directions of the second-order textural features, since there seemed to be no specific improvement in the Fisher distance values of the statistical features over the Fisher distance values of the basic second-order features. The second-order textural features which were retained as input for various classification designs were mean features 121-124 and 321-324, ASM features 139-142 and 339-342, and entropy features 148-151 and 348-351.

The highest of the Fisher distance values for first-order

statistical features, shown in Tables 18 and 19, were significantly larger than the highest values for the textural features (Tables 20-27) for all two-class combinations except mix vs. cirrus, where horizontal visual ASM feature 139, horizontal visual mean feature 121, and horizontal visual entropy feature 138 performed better than any first-order visual statistical feature. The highest Fisher distance value for separation of mix fr m cirrus was found in Table 19 for feature number 313 which epresents sea-surface temperature. However, incorporation of any particular feature into classification design must be predicated on knowledge of the meteorological significance of the feature. The tendency of the cirrus samples to cluster in a particular geographical region contributed to the ability of the infrared feature 313 (see Table 19) to discriminate cirrus from either low clouds, mix clouds, or cumulonimbus clouds. After discarding feature 313, it can be seen that the visual feature 114, representing the difference between the darkest point and the brightest point in the visible image, is the best single individual feature for separation of cirrus from mix as well as cirrus from cumulonimbus and mix from cumulonimbus. For separation of low clouds from mix, from cirrus, or from cumulonimbus, the best single feature is infrared feature 314, representing the difference between the warmest and the coldest temperature in the infrared image. In addition to features 114 and 314, features 108, 113, 115, 116, 117, 118, 302, 303, 308, 315, 316, 317, and 318 were retained for further processing in the classification design phase. Features 465-470, based on analysis of quadrants of infrared images, were calculated sub-

sequent to initial classification design trials in an attempt to separate low clouds from mix clouds. Fisher distances for features 465-470 are recorded in Table 19 to facilitate comparison with previously computed features.

4. Design and Evaluation of Cloud Classification Systems

4.1 Construction of Classification Decision Logic

The design and evaluation of cloud classification systems for both the four class problem (separation of low, mix, cirrus, and cumulonimbus clouds) and the three class problem (separation of low, cirrus, and cumumlonimbus clouds) was accomplished by interactively processing features which were retained during the feature selection phase through various decision logic structures created by selecting specific options available on the University of Maryland Interactive Pattern Analysis and Classification System (MIPACS). The present implementation version of MIPACS, described in [17], offers the following options at each level of the decision process:

1) number of user classification categories $N_{\ell 1}, N_{\ell 2}, \ldots, N_{\ell m}$ to be used in design of classifier at the given level ℓ,
2) choice of which sample cases are to be inserted into each of the categories $N_{\ell 1}$, $N_{\ell 2}, \ldots, N_{\ell m}$,
3) choice of which features from the sample feature vector are to be used for the design of the classifier at level ℓ, and
4) choice of type of statistical classifier to be used at level ℓ.

The data file prepared by the user of MIPACS consists of a set of cases (or samples) in which each case number is associated with a case feature vector. The case number, for example, could refer to a given window of a satellite picture and the

case feature vector could contain statistics such as the mean visual gray level, mean infrared gray level, standard deviation of the visual gray levels in the window, and standard deviation of the infrared gray levels. The classification function ("CLASSIFY") of MIPACS processes every sample which is an element of a terminal node (terminal user classification category) of the classification decision tree through the classifiers stored at each level of the classification design until the sample arrives at a terminal bin. The sample is then said to be an element of a terminal automatic classification category.

Typically, the terminal user classification categories correspond to classes of samples labelled by experts in the particular discipline from which the samples were drawn. A two-level decision process in which the three terminal classes consist of samples labelled respectively by meteorologists as "low" cloud, "high" cloud, and "cumulonimbus" cloud could be specified by any one of the three distinct decision trees below:

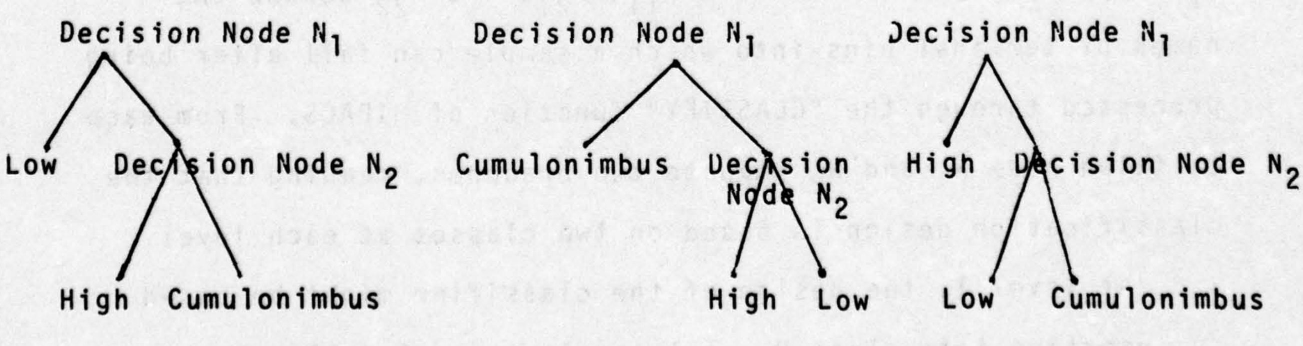

The tree on the left has the two levels shown below

Level 1

Decision Node N_1

Low	Decision Node N_2
(User Classification Category N_{11})	(User Classification Category N_{12})
(Automatic Classification Category A_{11})	(Automatic Classification Category A_{12})

and

Level 2

Decision Node N_2

High	Cumulonimbus
(User Classification Category N_{21})	(User Classification Category N_{22})
(Automatic Classification Category A_{21})	(Automatic Classification Category A_{22})

Classes N_{11}, N_{12} and N_{21}, N_{22} denote the classes of samples used to train the classifiers at Decision Node N_1 and Decision Node N_2 respectively. The classes A_{11}, A_{21}, and A_{22} denote the names of terminal bins into which a sample can fall after being processed through the "CLASSIFY" function of MIPACS. From each decision node N_1 and N_2 emanate two branches, meaning that the classification design is based on two classes at each level.

At level 1, the design of the classifier might be based on inserting into class N_{11} all sample cases labelled by meteorlogists as "low" cloud and on inserting into class N_{12}

all sample cases labelled as either "high" cloud or "cumulonimbus" cloud. At level 2, the design of the classifier might be based on class N_{21}, consisting of all samples labelled as "high" cloud, and on class N_{22}, consisting of all samples labelled as "cumulonimbus" cloud. For level 1, the infrared mean gray level and infrared standard deviation of gray levels might be the features chosen to separate the class of low clouds from the class of all high and cumulonimbus clouds. For level 2, the visual mean gray level might be chosen to separate the class of high clouds from the class of cumulonimbus clouds.

A maximum likelihood classifier could be selected by the user of MIPACS at level 1 and a Fisher linear discriminant could be chosen for level 2. The "CLASSIFY" function of MIPACS, operating at Decision Node N_1, would process every low cloud sample, every high cloud sample, and every cumulonimbus cloud sample sequentially through Decision Node N_1 and Decision Node N_2 (should the sample arrive at that node as a result of the maximum likelihood classifier stationed at Decision Node N_1) until the sample dropped into one of the terminal bins designated by A_{11}, A_{21}, or A_{22}. A confusion matrix of the form

(USER CLASSIFICATION CATEGORIES)	(AUTOMATIC CLASSIFICATION CATEGORIES) LOW (Class A_{11})	HIGH (Class A_{21})	CUMULONIMBUS (Class A_{22})
Low (Class N_{11})	10	2	1
High (Class N_{21})	4	5	0
CUMULONIMBUS (Class N_{22})	3	7	8

would then be flashed to the user of MIPACS. Interpretation of the figures in row 1 would be that out of 13 samples labelled by meteorologists as "low" cloud, the classification decision logic (specified in terms of choice of decision tree structure and choice of features and type of classifier for each level) had classified 10 samples as low cloud, 2 samples as high cloud (Type I error), and 1 sample as cumulonimbus cloud (Type I error). Interpretation of the figures in column 1 indicate that 10 low cloud samples were classified as low cloud, 4 high cloud samples as low cloud (Type II error), and 3 cumulonimbus cloud samples as low cloud (Type II error). Similar remarks apply to rows 2 and 3 and columns 2 and 3.

4.2 Description of Selected Cloud Classification Structures

In addition to the single stage decision structures classically employed in pattern recognition techniques, a variety of multistage decision tree structures were designed. Multistage decision tree classifiers, according to Wu [18], "have the potential for improving the classification accuracy and the computation efficiency" of single stage classifiers. Wu [18] notes, however, that theoretically "the conventional [single stage, maximum likelihood] procedure with the complete feature set is optimal in accuracy". The potential for improvement in accuracy offered by multistage decision trees stems from the problem of dimensionality.

As the number of features increases, the dimensionality problem is said to occur at the point when error involved in

density estimation increases faster than class separability. The dimensionality problem results from limited numbers of training samples. Single-stage classifiers which require large numbers of features for one-shot multiclass separability are more susceptible to the problem of dimensionality than sequential multistage decision tree classifiers which often require fewer features at each node. However, multistage decision tree classifiers suffer from the problem that at a given level, there may be one or more mixture classes which do not satisfy the assumption of normality typically assumed by statistical classifiers.

Just as the problem of feature selection cannot be simplified to selection of the best single features in one-dimensional space, the problem of design of a multiclass binary decision tree skeleton cannot be simplified to finding the best two-class combination for each decision level. Suppose, for example, that one could determine that a given set of features and classifier could separate cirrus from cumulonimbus clouds better than any set of features or classifier could separate any other pair of cloud classes. It would then seem logical to design a binary tree skeleton for the four-class problem as follows: Level 3 would involve a decision between cirrus and cumulonimbus clouds. Level 2 would involve a decision between whichever one of the remaining classes (low or mix) was best separated from the combination class of cirrus and cumulonimbus clouds, etc. Conversely, one might start top-down and find which one of the four

classes was best separated from a combination class of the other three. Unfortunately, this procedure fails to produce the optimal binary tree design for the specified number of levels and nodes because there is no simple relationship between the overall tree performance and the individual classification performances at decision nodes.

Even for statistically independent features, Kulkarni and Kanal [19] have shown that optimizing the average correct recognition rate at each node of a decision tree does not necessarily optimize the total tree performance. The total tree performance $P_c(T)$ for separation of four classes w_1, w_2, w_3, w_4 is given by

$$P_c(T) = \sum_{i=1}^{4} P(w_i)\, P_c(w_i)$$

where

$P(w_i)$ is the a priori probability of class w_i

$P_c(w_i)$ is the probability of correct recognition for class w_i.

For statistically independent features

$$P_c(w_i) = P_c(w_i/\text{Node } N_{p1}) \cdot P_c(w_i/\text{Node } N_{p2}) \cdots P_c(w_i/\text{Node } N_{pm})$$

where

Nodes N_{p1}, N_{p2},...,N_{pm} are nodes along a path from the root of the tree leading to the terminal node w_i

$P_c(w_i/N_{pj})$ is the probability of correct recognition of w_i at Node N_{pj}.

The average correct recognition rate $P_c(N_{pj})$ at Node N_{pj} is given by

$$P_c(N_{pj}) = \frac{\sum\limits_{w_i \varepsilon S} P(w_i) \cdot P_c(w_i/N_{pj})}{\sum\limits_{w_i \varepsilon S} P(w_i)}$$

where S is the set of all terminal nodes below N_{pj}. It can be seen that optimizing $P_c(N_{pj})$ does not necessarily optimize $P_c(T)$, which involves products of terms of the form $P_c(w_i/N_{pj})$ instead of linear combinations.

Kulkarni and Kanal [19] also prove that the optimal feature assignment at each node of a decision tree using a maximum likelihood rule does not necessarily result in the optimal overall feature assignment even for statistically independent features. Wu [18] mentions that "there are basically two problems in optimizing the performance of a decision tree... the complexity of the tree structure [and the fact that] the overall performance of proposed classifier structure cannot be predicted exactly".

Although there is no optimal method of designing a tree skeleton, selecting feature sets for each decision node, or selecting a classifier for each decision node other than exhaustive search, various suboptimal techniques are employed. Often the best feature subset in a lower-dimensional space is combined with another feature when increasing feature dimensionality. Tree design is often predicated on knowledge of the problem domain coupled with histogram or sequential clustering approaches (Wu [18]).

Histograms of individual features for each of the four classes were examined to determine whether or not there was any obvious design strategy which would necessitate more than four terminal nodes (i.e., more than one decision path for a given class). However, even for mix samples, there seemed no obvious class partition. Hence, it was decided to limit the design of the tree skeleton to trees with four terminal nodes, representing the four cloud classes, and also to consider only binary trees, i.e., to simplify the decision at each of the decision nodes to a two-way branch. This reduced the number of possible distinct trees to fifteen, three of the form  and twelve of the form 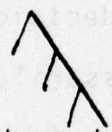

From these fifteen trees, four were selected which appeared likely to offer optimal performance at one or more stages of the decision tree structure. Although it was previously mentioned that maximizing classification performance at each individual node does not necessarily maximize overall tree performance, the suboptimal procedure of designing a tree stage by stage is often employed. A presentation of a search procedure which incorporates this stage by stage design concept can be found in Section 4.3 of Wu [18]. From a cursory scan of the mean values of several individual visual brightness features, it could be seen that there was good class separability between cirrus and cumulonimbus. Three of the four decision trees selected, trees 3-5 shown in Figures 7-9, at one stage of the decision process involved a separation between cirrus and cumulonimbus clouds. The fourth tree,

decision tree 6 shown in Figure 10, involved separation between cumulonimbus clouds and the remaining three cloud classes. It was found for various feature subsets that maximal one class vs. the rest separation was obtained when isolating cumulonimbus clouds from a mixture of the other three cloud classes.

Decision trees 7 and 8, shown in Figures 11 and 12, for the three-class problem were designed after initial four-class experiments indicated the problem of recognizing mix clouds. Decision tree 2 (Figure 6) resulted from an attempt to correct the confusion between mix and low clouds which was the largest single source of classification error for the single stage maximum likelihood classifier of decision tree 1, shown in Figure 5.

The maximum number of features used to separate two or more classes of multivariate normally distributed satellite data was determined by consideration of various theoretical and experimental results relating sample size, classification accuracy on an independent test set, and feature dimensionality. Two questions must be examined in this connection:

1) For a fixed number of training samples, what is the maximum number of features for which the estimate of the classification error on a design set is a reliable predictor of the expected error on an independent test set?
2) For a given problem domain and fixed sample sizes, what is the optimum feature dimensionality in the sense that as the number of features increases be-

yond this optimum, the experimental classification error on independent test sets tends to increase?

Several theoretical results, summarized in Kanal [16], can be applied to the solution of the first question. Foley [20] found that for multivariate normal distributions with equal known covariance matrices and estimated mean vectors, the ratio of number of training samples per class to number of features should be at least three to one. If the covariance matrices are equal but estimated from samples, Mehotra [21] recommended a minimum ratio of five to one. Fukunaga and Kessel [22] suggested that the ratio of total number of samples to number of features should be at least ten for the two-class equal covariance problem and greater than ten for the unequal covariance problem. Experimental results of Fu et al.[23] illustrated that for multispectral classes of remote sensing data, the optimum feature dimensionality was between three to five features for experiments involving 400 training samples per class and test sets of over 14,000 samples. Wu [18] uses a maximum feature dimensionality of four in most of his experiments on multispectral class separability.

In accordance with the criterion of a ten to one ratio for number of samples to number of features, the maximum number of features selected for classification of cloud pattern classes was seven, since the total number of samples in the smallest two classes (cirrus and cumulonimbus) was 24+46 = 70. From experiments on MIPACS, there appeared to be a degradation in classification results as the number of features increased

from five to six, suggesting that the maximum number of features for effective discrimination of cloud patterns is close to five -- a result similar to the experimental observations of Wu [18] on land use categories.

4.3 Evaluation of Cloud Classification Systems

For selected combinations of features, classifiers, and decision tree (Figures 5-12) the percentages of samples correctly classified (per class and per sum total) are presented in Tables 28-43. Confusion matrices corresponding to a given experiment number and given table number can be found in Appendix C. Each experiment within a given table for Tables 32-43 was representative of a collection of similar interactive experiments in which given features were interchanged with other features based on the same histogram. For example, feature 113 from the visual brightness histogram might have been substituted for feature 114.

The maximum likelihood classifier performed consistently better for the four-class problem than either the multiclass voting, multiclass one-against-the-rest, and Fisher classifier with sample a priori probabilities. The assumption of equal covariance matrices used in the latter three classifiers proved too restrictive for separation of the four cloud classes of low, mix, cirrus, and cumulonimbus. However, for the three-class problem (low, cirrus, and cumulonimbus), accuracy greater than 94% was obtained by all four types of classifiers.

For the four-class problem, a comparison of Experiment 1 in Table 43 with Experiment 1 in Table 33 shows a drop from 86% classification accuracy to 82% when a single-stage multiclass voting classifier was used in-

stead of a single-stage maximum likelihood classifier. A comparison of Experiment 2 in Table 43 with Experiment 1 in Table 40 shows a drop from 85% to 79% classification accuracy when multiclass voting classifiers were used at each stage of a multistage decision process instead of maximum likelihood classifiers, and a similar drop to 83% for the Fisher classifier with sample a priori probabilities. From Experiment 5 of Table 43, it can be seen that only 28% of the total number of samples were correctly classified when a multiclass one-against-the-rest classifier was substituted for a single-stage maximum likelihood classifier. The high reject rate of the multiclass one-against-the-rest classifier for the four-class problem contrasted with the accurate performance for the three-class problem illustrates the ambiguity introduced into the pattern analysis problem when non-uniformly covered cloud areas are to be identified.

The maximum feature dimensionality for classification of cloud patterns based on the limited number of training samples within a particular orbit can be seen from the single-stage maximum likelihood classification results in Tables 28-35 and Table 41 to be approximately 5 or less. For a feature dimensionality of 1, visual brightness features (Table 28) classified approximately 46%-53% of the samples correctly; visual difference features (Table 29) classified approximately 40%-47% correctly; infrared temperature features (Table 31), 60%-73%; and infrared

difference features (Table 32), 61%-68%. Infrared temperature features were obviously the best group of features, followed by infrared texture features. For feature combinations of three and four features (Table 32), classification results improved to approximately 84% and 86% respectively. Another 2% increase in classification accuracy to 88% occurred when the feature dimensionality was increased to 5. However, for various combinations of six features (Table 34), classification accuracy did not increase beyond 88% and only for a few select combinations of seven features (see Experiment 2, Table 35) did classification accuracy increase to 89%. This means that no major increase in classification accuracy beyond the five feature combinations was achieved until a two-stage classification process (see Table 36) for reducing the number of mix samples incorrectly classified as low samples was designed.

Accuracy was increased to 91.4% by combining a seven-feature four-class maximum likelihood classifier at level 1 of the classification process with a six-feature two-class (low vs. mix) maximum likelihood classifier at the second stage. Five of the six features which reduced the confusion between low and mix at the second level of the classification process were quadrant features, which were extracted in a crude attempt to predict how successful features which compared segments of a sample would be in separating uniformly covered from non-uniformly covered

cloud regions. The classification power gained from these simple features can also be seen by comparing the results of Experiments 2 and 3, Table 40, with the results of Experiment 1, Table 40.

An analysis of the sets of experiments, table by table, for Tables 28-36 leads to the following conclusions. The best single visual brightness feature (Table 28) was feature 113, the brightest point. There was little difference in the performance of the visual texture features (Table 29), with a slight preference for the diagonal directions. The best single infrared temperature features (Table 30) were whole sample and quadrant features involving determination of the coldest temperature, ranges between the coldest temperature and other points, and standard deviation. For infrared texture features (Table 31), the entropy features as a group proved superior to mean or angular second moment (ASM) features.

Comparison of Experiments 2 and 4 of Table 32 with Experiment 3 of Table 32 shows that at least one visual feature must be included for classification of cirrus and cumulonimbus clouds. For combinations of three features including one visual feature and two infrared features, similar results were obtained in Experiments 1 and 2 for one infrared temperature feature combined with one infrared texture feature and two infrared temperature features. One would have suspected prior to conducting the design experiment that the three-feature combination with the

texture feature would have given better results provided that the infrared texture feature was not highly correlated with the infrared temperature feature.

Experiments 3-7 of Table 32 illustrate the effect of leaving out one feature from the five-feature combination of Experiment 1 of Table 33. The five-feature combination (one visual and four infrared) of Experiment 1 of Table 33 [consisting of gray level difference between brightest and darkest points in the visual picture for a given sample area, standard deviation of temperature, coldest temperature, temperature difference between coldest and warmest temperatures, and temperature difference between the coldest 10% of the infrared temperatures and the warmest 10% of the infrared temperatures] was used as a standard feature set (see Table 43 and Experiments 1 of Tables 37-40) for comparison of various tree skeletons and classifiers because of its uniform ability to accurately separate cloud pattern regardless of classifier and/or tree skeleton design. Experiment 3 of Table 32 shows the result of excluding the visual brightness range. Experiment 4 illustrates the fact that most of the information contained in the infrared standard deviation feature can also be found in the infrared range features 314 and 315. The necessity of identifying the value of the coldest temperature for identification of cirrus and cumulonimbus is shown by Experiment 5. Experiments 6 and 7 and Experiment 8 of Table 33 illustrate

the essential redundancy for single-stage classification of including both the infrared range features from 0% to 100% and from 10% to 90%. Of the two ranges, the range from 10% to 90% performed slightly better in combination with other features. The incorporation of more than one range feature in feature combinations functioned more as a weighting factor than as an additional information source.

The five-feature standard combination, given in Experiment 1 of Table 33, resulted in 86% classification accuracy for single-stage maximum likelihood classification. When the quadrant standard deviation feature was substituted for the sample standard deviation feature (Experiment 2, Table 33), total classification accuracy remained the same. Experiments 3, 5, and 8 vary the proportion of visual to infrared features in Experiments 2, 4, and 7 from 1 and 4 to 2 visual and 3 infrared features. In each of Experiments 3, 5, and 8, classification accuracy was improved over the corresponding Experiments 2, 4 and 7. The all-texture five-feature combinations of Experiments 4 and 5 resulted in 78.6% and 80.7% accuracy respectively, compared to the no-texture five-feature combinations of Experiments 2 and 3 with 86.0% and 86.4% accuracy respectively. The five-feature combinations of Experiments 7 and 8, which included one infrared entropy feature, performed best of any five-feature combination, with classification accuracies of 87.2% and 88.1% re-

spectively. Experiment 9 illustrated that even with the addition of an infrared entropy feature, if no information was available from the visual picture, classification results fell below 80% for five-feature combinations. Experiment 6 illustrated that, for the five-feature combinations tried, combinations of 3 texture and 2 non-texture features performed worse than all-texture features, all non-texture features, and combinations of 1 texture and 4 non-texture features.

The experiments of Table 34 illustrated that even with the addition of several potentially good discriminating features to the combinations tried in the experiments reported in Table 33, no increase in classification accuracy was achieved. Experiment 2 of Table 34 added the infrared range feature 314 to the best combination in Table 33 (Experiment 8). No improvement resulted. Experiment 1 added the visual range feature 115 to the standard five-feature combination of Experiment 1, Table 33. A slight improvement in classification of cirrus and cumulonimbus resulted in a change in total classification accuracy from 86.0% to 87.2%. Classification results for the other six-feature combinations of Experiments 3-6, Table 34, ranged from 85.2% to 86.4%. With a particular seven-feature combination (Experiment 2, Table 35) of two infrared entropy texture features, two visual brightness features, and three infrared temperature features, classification accuracy rose to 89.7%. Accuracy greater

than 90% was achieved only by changing from a single-level classifier (Figure 5) to a two-level decision tree (Figure 6).

The experiments in Table 36 show that a 2% increase in classification accuracy resulted from separating those samples that were classified as low cloud on the first pass of the maximum likelihood four-class classifier into low and mix samples by using on a second pass quadrant features combined with a maximum likelihood classifier trained on all the low samples and all the mix samples. Had the maximum likelihood classifier for the second stage of the decision process been trained only on mix samples in which the amount of low cloud predominated within the sample, or had the a priori probabilities been adjusted to reflect the uneven proportion of low clouds and mix clouds arriving at the second stage of the decision tree, classification results would probably have improved. Thus, results in Table 36 represent the minimal amount of classification accuracy achievable via this two-stage design to eliminate confusion between low and mix samples.

The mix and low samples which traveled down the left branch of decision tree 3 (see Figure 7) were easily separated by either the standard feature set or the quadrant features, as can be seen from the confusion matrices for Experiments 1-3 of Table 37. Also there was no confusion at decision node 2.2 between the cirrus and cumulonimbus samples which arrived at that node in

either of Experiments 1, 2, or 3. However, none of the feature combinations tried for decision tree 3 could solve the problem that, at level 1, several mix clouds were classified into the cirrus-cumulonimbus group and also many cirrus and cumulonimbus clouds were classified into the low-mix group.

In decision tree 4 (Figure 8), an attempt was made to separate mix clouds from the others at the top of the tree. The quadrant features which were designed to separate mix from low clouds were notadequate to separate mix from the combined set of low, cirrus, and cumulonimbus samples, since quadrant features such as maximum standard deviation of temperature are high for cirrus and cumulonimbus as well as for mix. The total classification accuracy (Experiment 2, Table 38) was only 76% for decision tree 4 with quadrant features at level 1 of the classification process. Classification accuracies for Experiments 1 and 3, Table 38, in which no quadrant features were used, were 84.0% and 81.5% respectively, with the major source of error being the classification design at level 1.

For decision tree 5 (Figure 9), quadrant features performed better at level 1 (see Experiment 3, Table 39) for separation of low from the combined set of mix, cirrus, and cumulonimbus clouds. The percentage of correctly classified samples was 85.2%. Non-quadrant features performed almost as well (see Experiments 1 and

2, Table 39) at level 1 with resultant total classification accuracies of approximately 84%.

The multi-level binary tree skeleton which offered consistently superior performance for various feature combinations was tree 6 (Figure 10). The overlap between low and mix classes was approached at the last stage of the decision process and the problem for the first stage of the decision process was the relatively easy separation of cumulonimbus clouds from the combined set of mix, low, and cirrus clouds. The first stage resulted in confusion only between mix and cumulonimbus clouds (see the confusion matrices for Experiments 1-3, Table 40). With quadrant features at the last stage of the decision tree (Experiments 2 and 3), classification accuracies were approximately 86%.

The problem of identification of mix clouds was completely disregarded for the set of experiments in Table 41. Separation of the three remaining cloud types with a single-stage maximum likelihood classifier (Figure 11) was achieved by several two-feature non-texture combinations (one visual and one infrared) with 98% classification accuracy (see Experiments 3 and 4, Table 41). Infrared features which performed well were temperature ranges, temperature standard deviation, and coldest temperature values. Visual features which performed well were highest (brightest) gray level value and ranges of visual brightness values.

The feature dimensionality for the three-class problem was reduced from 2 to 1 by changing from the single-stage decision process of Figure 11 to the multi-stage decision process outlined in Figure 12. The three-class problem was resolved into separation of low clouds from cirrus and cumulonimbus clouds at level 1 and separation of cirrus and cumulonimbus clouds at level 2. A total classification accuracy of 98.7% (Experiment 1, Table 42) was achieved by using feature 302, standard deviation of temperature, at level 1 and feature 113, brightest visible gray level value, at level 2.

5. Conclusions and Plans for Further Research

5.1 Conclusions

Features characterizing density distributions of infrared gray level values, visual gray level values, pairs of infrared gray level values separated by a specified displacement vector, and pairs of visual gray level values separated by a specified displacement vector can successfully discriminate selected categories of sample areas of tropical cloud patterns presently used for derivation of wind velocity vectors. Areas which can be differentiated are areas uniformly covered by low clouds, areas uniformly covered by cirrus clouds, and areas partially or completely covered by cumulonimbus clouds. Either single-stage classifiers with at least two appropriately selected features, one from the infrared temperature histogram and one from the visible brightness histogram, or a hierarchical classification system (in which at the first stage low clouds are separated from cirrus and cumulonimbus by one or more infrared features such as standard deviation of temperature, and at the second stage cirrus is separated from cumulonimbus by one or more visual features such as the brightest visual gray level value) can be used. The hierarchical system is to be preferred because of the reduction achievable in feature dimensionality and because of computational efficiency.

Features based on integrations over the entire

sample area of cloud patterns cannot successfully distinguish "mixed" areas which are either partially covered by cirrus with lower clouds or partially covered by cirrus clouds and partially covered by low clouds from the three categories mentioned above. For both single-stage and multistage classification systems, a minimum of five features was needed for classification accuracy of 88% on the training set. Accuracy could only be improved by the addition of quadrant features (features which compared different quadrants of the sample area instead of features based on frequency distributions) applied at a second stage to decrease the confusion between low and mix samples. Binary hierarchical classification systems failed to improve the classification accuracy or to reduce the feature dimensionality beyond that achievable by maximum likelihood single-stage classification for the four-class problem. However, if an approach based on the application of image segmentation techniques could be developed which could separate "mixed" clouds from the other three categories at the first stage of the system, then the second and third stages could separate low clouds and cirrus from cumulonimbus respectively as above. This type of (as yet unrealized) hierarchical system would definitely be preferable to a conventional single-stage system.

5.2 Plans for Further Research

The next problem which will be investigated is the

application of image segmentation and scene analysis techniques to the problem of obtaining a meaningful description (relevant to the problem of wind velocity estimation) of "mixed" cloud areas. The description should result in the delineation of areas or points from which more than one wind velocity vector can be derived, and in the derivation of one or more numerical features which can be used to identify "mixed" cloud areas. The scene analysis problem will be approached at three successive levels depending on whether or not a successful solution to the problem is attained on a lower level. First, the scene analysis approach will investigate the problem using information available from a single pair of visual and infrared image sample areas. If sufficient information is not available from analysis of only one image pair (in the time sequence of pairs of images used by meteorologists as an aid to labelling of "mixed" cloud areas), then the analysis will be extended to make use of two pairs of infrared and visual images separated in time by approximately half an hour. If problems are still encountered, the regular partitioning of sample areas will be abandoned, and context information from neighboring samples will be added.

References

[1] K. Miyakoda, "Numerical Weather Prediction", American Scientist, vol. 62, no. 5, pp. 564-574, September-October 1974.

[2] J. Parikh, "Automatic Wind Velocity Estimation from Multispectral Geosynchronous Satellite Data: A Proposal", Computer Science Center, University of Maryland, College Park, Technical Report TR-328, September 1974.

[3] R. Anderson et al., "Application of Meteorological Satellite Data in Analysis and Forecasting", U. S. Department of Commerce, Washington, D. C., ESSA Technical Report NESC 51, March 1974.

[4] C. L. Bristor, "Central Processing and Analysis of Geostationary Satellite Data", U. S. Department of Commerce, Washington, D. C., NOAA Technical Memorandum NESS 64, March 1975.

[5] L. F. Hubert, "The Effect of Sensor Resolution on Infrared Measurements", National Environmental Satellite Service Internal Report, 1975.

[6] J. J. Fortuna and L. N. Hambrick, "The Operation of the NOAA Polar Satellite System", U. S. Department of Commerce, Washington, D. C., NOAA Technical Memorandum NESS 60, November 1974.

[7] A. Schwalb, "Modified Version of the Improved TIROS Operational Satellite (ITOS D-G)", U. S. Department of Commerce, Washington, D. C., NOAA Technical Memorandum NESS 35, April, 1972.

[8] E. F. Conlan, "Operational Products from ITOS Scanning Radiometer Data", U. S. Department of Commerce, Washington, D. C., NOAA Technical Memorandum NESS 52, October 1973.

[9] A. L. Booth, "Objective Cloud Type Classification Using Visual and Infrared Satellite Data", Institute for Fluid Dynamics and Applied Mathematics, University of Maryland, College Park, Technical Note BN 768, March 1973.

[10] R. M. Haralick, K. Shanmugam, and I. Dinstein, "Textural Features for Image Classification", IEEE Transactions on Systems, Man, and Cybernetics, vol. SMC-3, no. 6, pp. 610-621, November 1973.

[11] W. Bleeker, ed., International Cloud Atlas. Geneva:

World Meteorological Organization, 1956.

[12] E. M. Darling, Jr. and R. D. Joseph, "Pattern Recognition from Satellite Altitudes", IEEE Transactions on Systems Science and Cybernetics, vol. SSC-4, no. 1, pp. 38-47, March 1968.

[13] J. K. Aggarwal and R. O. Duda, "Computer Analysis of Moving Polygonal Images", IEEE Transactions on Computers, vol. C-24, no. 10, pp. 966-976, October 1975.

[14] J. S. Weszka and A. Rosenfeld, "A Comparative Study of Texture Measures for Terrain Classification", Computer Science Center, University of Maryland, College Park, Technical Report TR-361, March 1975.

[15] K. Fukunaga, Introduction to Statistical Pattern Recognition. New York: Academic Press, 1972.

[16] L. N. Kanal, "Patterns in Pattern Recognition: 1968-1974", IEEE Transactions on Information Theory, vol. IT-20, no. 6, pp. 697-722, November 1974.

[17] G. Stockman and A. Kulkarni, "Maryland Interactive Pattern Analysis and Classification System, Part II: User's Documentation", Computer Science Department, University of Maryland, College Park, Technical Report in preparation, February 1976.

[18] C. Wu, D. Landgrebe, and P. Swain, "The Decision Tree Approach to Classification", School of Electrical Engineering, Purdue University, West Lafayette, Indiana, Technical Report TR-EE 75-17, May 1975.

[19] A. V. Kulkarni and L. N. Kanal, "An Optimization Approach to the Design of Decision Trees", Computer Science Department, University of Maryland, College Park, Technical Report TR-396, August 1975.

[20] D. H. Foley, "Considerations of Sample and Feature Size", IEEE Transactions on Information Theory, vol. IT-18, pp. 618-626, September 1972.

[21] K. G. Mehotra, "Some Further Considerations on Probability of Error in Discriminant Analysis", Unpublished Report on RADC Contract No. F30602-72-C-0281, 1973.

[22] K. Fukunaga and D. Kessell, "Application of Optimum Error-Reject Functions", IEEE Transactions on Information Theory, vol. IT-18, pp. 814-817, November 1972.

[23] K. S. Fu and P. H. Swain, "On Syntactic Pattern Recognition", Software Engineering, vol. 2, pp. 155-182, J. T. Tou, ed., New York: Academic Press, 1971.

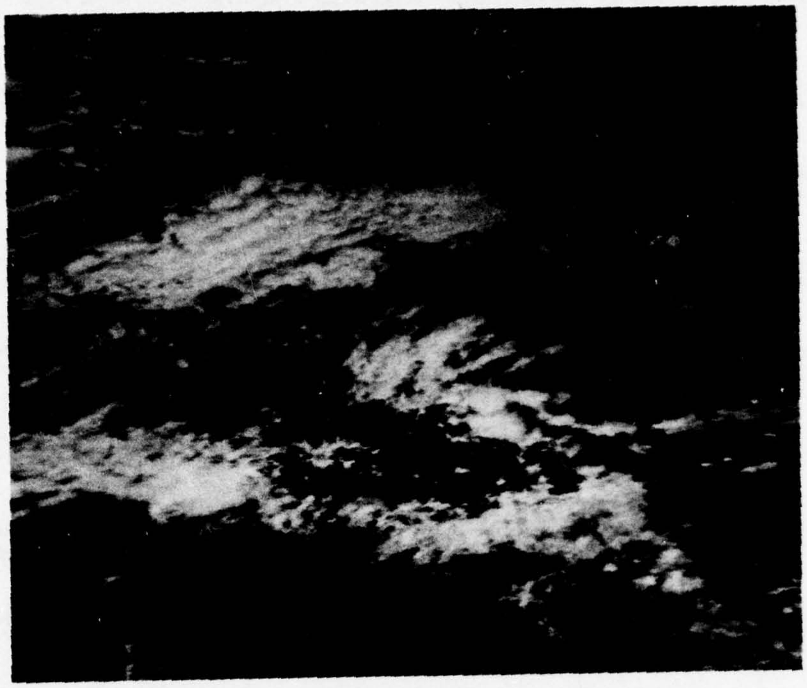

Figure 1. Visual Data for NOAA-1 Orbit 1798, May 3, 1971. Latitude limits are 26.7°N to 1.1°S.

Figure 2. Infrared Data for NOAA-1 Orbit 1798, May 3, 1971.

COLUMN NUMBERS

ROW NUMBERS	1	2	3	4	5	6	7	8	9	10	11	12	13	14	15	16	17	
1	22	22	22	22	22	22	22	22	21	12	22	11	11	11	15	55	55	5
	22	22	22	22	22	22	22	22	22	22	11	11	11	11	55	55	55	5
2	65	12	22	22	22	22	22	22	21	11	11	22	21	55	55	55	55	5
	66	66	11	22	11	22	22	22	22	22	22	12	21	55	55	55	55	5
3	66	66	66	22	22	22	22	22	22	22	23	33	11	55	15	55	55	5
	66	62	62	22	32	22	22	22	23	33	33	33	31	11	11	11	15	5
4	62	22	22	22	22	23	33	33	33	33	33	33	33	31	11	15	55	5
	22	22	22	22	23	33	33	33	33	33	33	33	13	31	51	55	55	5
5	56	66	53	33	33	33	33	33	33	33	33	36	66	65	55	55	55	5
	56	23	33	33	33	33	33	33	33	33	33	33	36	65	55	55	51	1
6	62	33	33	33	36	36	66	63	36	66	66	66	66	63	33	11	11	1
	33	33	33	36	66	66	66	66	66	55	55	56	66	33	33	31	11	3
7	33	33	66	66	66	66	66	66	65	55	55	51	53	33	33	33	33	3
	36	66	55	66	66	65	66	56	66	66	33	31	11	33	33	33	35	5
8	55	55	55	56	65	66	66	66	63	33	36	62	23	31	11	11	55	1
	55	55	55	55	55	62	26	26	63	33	66	66	63	33	31	11	51	5
9	55	55	55	65	22	22	22	23	66	66	44	44	55	55	58	55	55	5
	26	66	57	55	56	62	22	22	28	84	44	44	45	55	55	55	55	5
10	64	44	44	44	62	22	22	62	64	44	44	44	44	44	44	55	54	5
	44	44	44	44	44	44	64	44	46	22	66	44	46	64	82	76	55	5
11	44	44	44	44	44	44	62	66	22	24	44	44	64	46	66	44	46	5
	66	62	44	44	44	44	44	44	44	44	64	44	44	44	55	55	15	5
12	22	21	28	87	77	24	77	77	77	74	44	44	44	44	55	55	15	5
	22	22	22	66	65	22	66	67	77	77	44	77	74	55	54	56	66	6
13	22	22	22	22	25	62	22	57	77	77	76	68	77	46	44	66	66	5
	22	22	22	22	22	52	22	65	65	86	68	86	22	22	44	56	64	4
14	22	22	22	22	11	11	12	21	22	26	86	66	62	27	87	77	76	6
	21	22	22	22	11	11	12	22	22	22	22	26	62	22	26	77	77	7
15	11	11	22	22	22	11	11	11	11	12	22	26	62	22	68	66	26	6
	11	11	22	22	21	12	11	11	11	22	21	55	33	33	32	26	26	6

Figure 3. Cloud Category Map Prepared by Meteorologists for 32x32 Matrices. For explanation of entries (1,...,8) see text.

COLUMN NUMBERS

ROW NUMBERS	1	2	3	4	5	6	7	8	9	10	11	12	13	14	15	16	17
1	L	L	L	L	L	L	L	L	L	L	L	-	-	-	Ci	Ci	Ci
2	M	M	L	L	L	L	L	L	L	L	L	L	L	Ci	Ci	Ci	Ci
3	M	M	M	L	L	L	L	L	L	L	L	L	L	Ci	Ci	Ci	Ci
4	M	L	L	L	L	L	L	L	L	L	L	L	L	L	Ci	Ci	Ci
5	M	M	M	L	L	L	L	L	L	L	L	M	M	M	Ci	Ci	Ci
6	M	L	L	M	M	M	M	M	M	M	M	M	M	M	L	L	-
7	M	M	M	M	M	M	M	M	M	M	M	M	M	L	L	L	M
8	Ci	Ci	Ci	M	M	M	M	M	M	L	M	M	M	L	L	-	Ci
9	M	M	M	M	M	M	L	L	M	Cb	Cb	Cb	Cb	Ci	M	Ci	Ci
10	Cb	Cb	Cb	Cb	Cb	Cb	Cb	Cb	Cb	Cb	Cb	Cb	Cb	Cb	Cb	M	Cb
11	Cb	Cb	Cb	Cb	Cb	Cb	Cb	Cb	Cb	Cb	Cb	Cb	Cb	Cb	M	Cb	Cb
12	L	L	M	M	M	Cb	M	M	M	Cb	Cb	Cb	Cb	Cb	Cb	M	M
13	L	L	L	L	M	M	L	M	M	M	M	M	M	Cb	Cb	M	Cb
14	L	L	L	L	-	-	L	L	L	M	M	M	M	M	M	M	M
15	-	-	L	L	L	L	-	-	-	L	L	M	M	L	M	M	M

Figure 4. Cloud Category Map for Sample 64x64 Data Regions for Categories L (low clouds), M (mixed clouds), Ci (cirrus clouds), and Cb (cumulonimbus clouds).

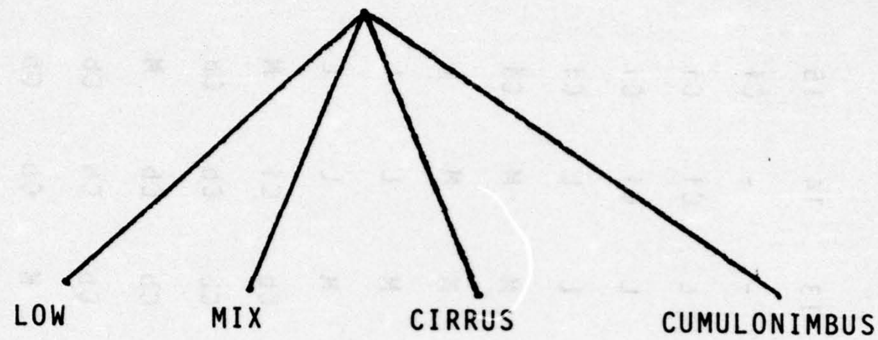

Figure 5. Decision Tree 1.

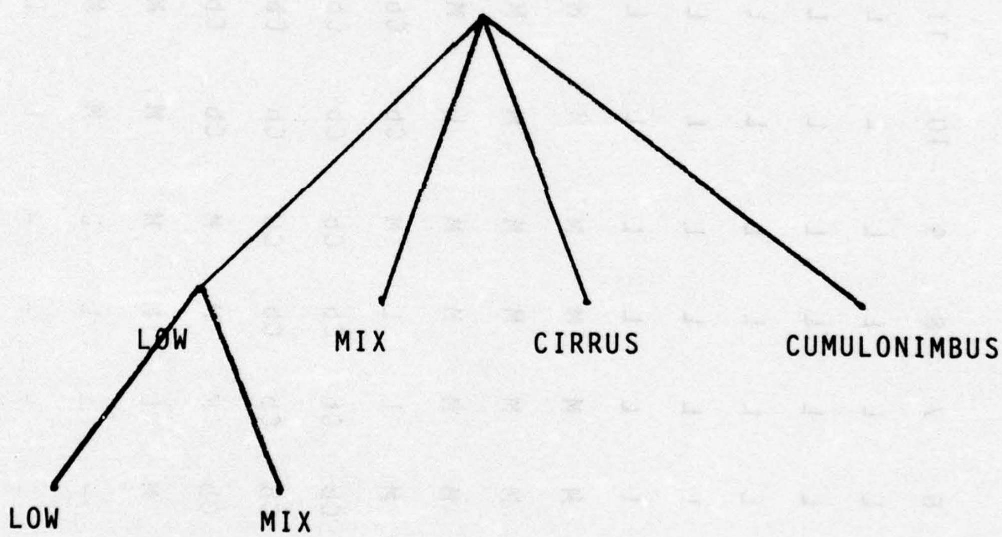

Figure 6. Decision Tree 2.

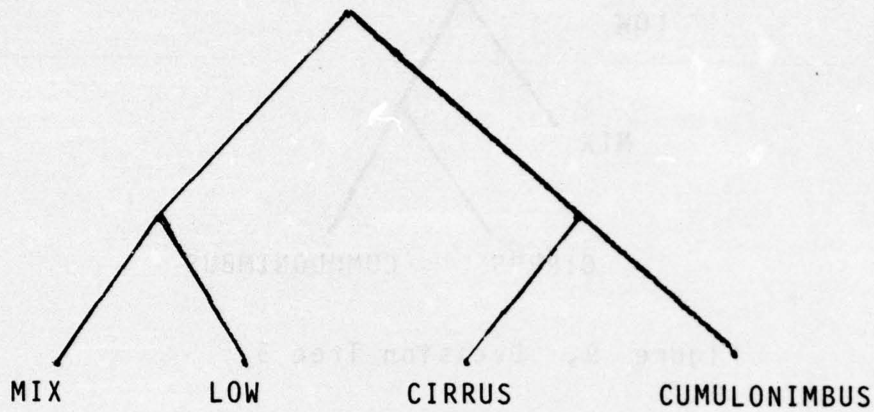

Figure 7. Decision Tree 3.

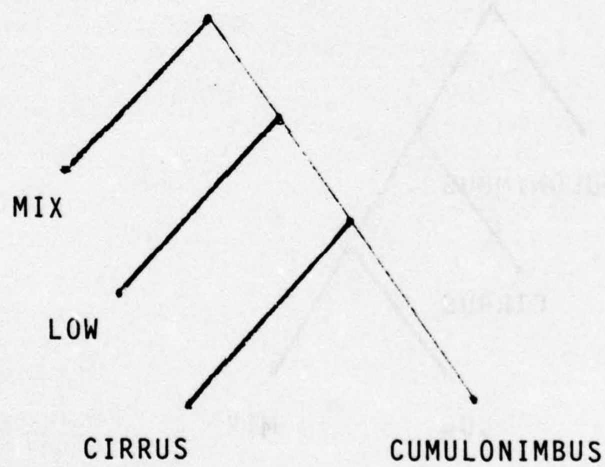

Figure 8. Decision Tree 4.

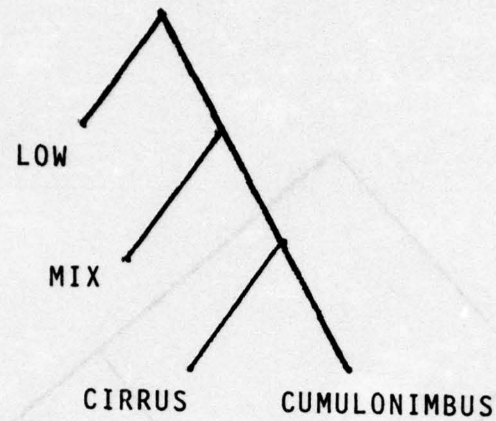

Figure 9. Decision Tree 5.

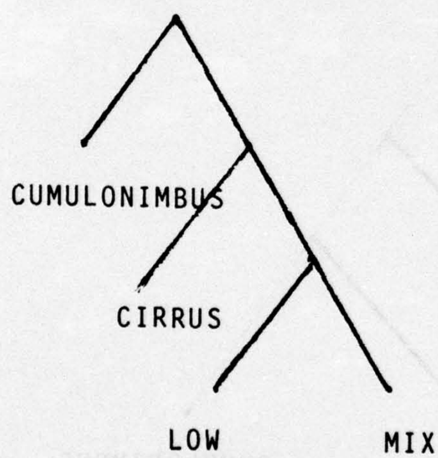

Figure 10. Decision Tree 6.

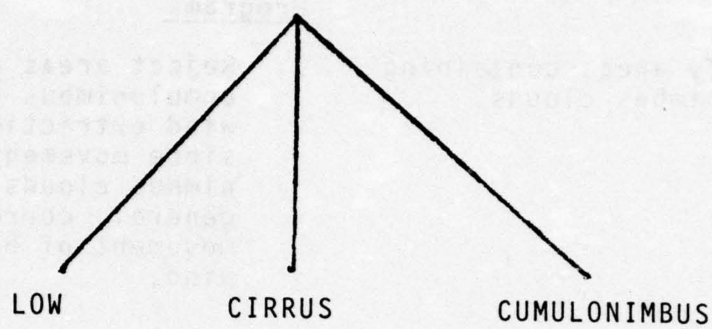

Figure 11. Decision Tree 7.

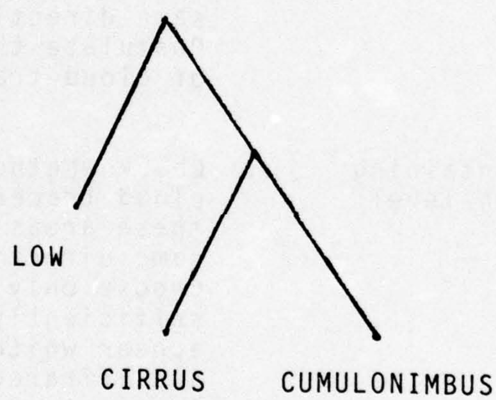

Figure 12. Decision Tree 8.

Classification Goals	Relation to Wind Extraction Programs
1. Identify areas containing cumulonimbus clouds.	1. Reject areas containing cumulonimbus clouds from wind extraction programs since movement of cumulonimbus clouds does not, in general, correspond to movement of horizontal wind.
2. Identify areas containing predominantly single-layer, low-level clouds.	2. Postulate for wind extraction program that cloud tracers located in these areas are moving in same direction and speed. Postulate that emissivity of cloud tracers is unity.
3. Identify areas containing predominantly high-level clouds.	3. Check whether or not major cloud tracers located in these areas are moving in same direction and speed. Choose only those tracers sufficiently opaque to appear white in both visible and infrared images. Postulate emissivity values between .75 and unity.
4. Identify areas containing predominantly multi-layered clouds.	4. Postulate that cloud tracers may be moving at different speeds and in different directions. Identify low cloud tracers and high cloud tracers, specifying emissivity values for high tracers depending on opacity.

Table 1. Relation of Classification Goals to Automatic Wind Velocity Extraction.

TABLES 2-17

Feature Statistics

Table	Histogram type	Cloud type
2	Visual brightness	Low
3	Visual brightness	Mix
4	Visual brightness	Ci
5	Visual brightness	Cb
6	Infrared temperature	Low
7	Infrared temperature	Mix
8	Infrared Temperature	Ci
9	Infrared temperature	Cb
10	Visual difference	Low
11	Visual difference	Mix
12	Visual difference	Ci
13	Visual difference	Cb
14	Infrared difference	Low
15	Infrared difference	Mix
16	Infrared difference	Ci
17	Infrared difference	Cb

STATISTICS FOR FEATURES EXTRACTED FROM "LOW" CLOUD VISUAL BRIGHTNESS HISTOGRAMS

FEATURE	FEATURE STATISTICS					
(Number, Name)	Mean	Standard Deviation	Minimum	Maximum	Median	Range
(101, Mean)	65.02	23.59	37.51	128.10	59.95	90.59
(102, StDev)	14.68	6.76	3.49	34.07	15.29	30.58
(103, CF0)	40.94	13.49	25.00	77.00	37.00	52.00
(104, CF10)	50.84	18.95	32.25	109.47	43.51	77.22
(105, CF20)	53.81	20.93	33.39	115.46	46.25	82.07
(106, CF30)	56.64	22.60	34.07	121.67	48.01	87.60
(107, CF40)	59.46	23.84	34.59	126.70	50.74	92.11
(108, CF50)	62.17	24.86	36.12	130.08	54.33	93.96
(109, CF60)	65.68	26.05	36.64	135.42	59.61	98.78
(110, CF70)	69.93	27.28	37.27	140.26	63.55	102.99
(111, CF80)	75.75	28.70	39.16	145.76	72.80	106.61
(112, CF90)	85.70	29.86	42.77	153.08	88.71	110.31
(113, CF100)	120.03	30.25	62.00	166.00	127.50	104.00
(114, R0-100)	79.09	26.25	24.00	127.00	82.00	103.00
(115, R10-90)	34.85	18.73	6.90	85.37	32.14	78.47
(116, R0-50)	21.23	14.82	7.61	72.71	14.45	65.10
(117, R50-100)	57.86	27.03	16.10	114.90	61.05	98.80
(118, R20-80)	21.94	14.44	4.70	65.89	19.12	61.19
(119, R30-70)	13.29	9.94	3.20	50.16	10.14	46.96
(120, R40-60)	6.22	4.99	1.14	24.10	4.66	22.96

STATISTICS FOR FEATURES EXTRACTED FROM "MIX" CLOUD VISUAL BRIGHTNESS HISTOGRAMS

FEATURE	FEATURE STATISTICS					
(Number, Name)	Mean	Standard Deviation	Minimum	Maximum	Median	Range
(101, Mean)	72.41	20.89	40.46	141.34	69.04	100.88
(102, StDev)	17.84	6.71	3.84	32.61	17.87	28.77
(103, CF0)	41.46	12.73	27.00	100.00	27.00	73.00
(104, CF10)	53.00	16.36	33.22	124.68	49.97	91.46
(105, CF20)	57.28	18.27	34.28	130.89	53.19	96.62
(106, CF30)	61.29	19.86	36.17	136.25	57.99	100.08
(107, CF40)	65.36	21.25	37.18	140.37	61.60	103.18
(108, CF50)	69.66	22.37	39.60	143.86	66.62	104.26
(109, CF60)	74.73	23.58	40.82	146.75	71.84	105.93
(110, CF70)	80.52	24.77	43.17	149.70	76.51	106.52
(111, CF80)	87.76	25.76	44.99	152.41	85.32	107.41
(112, CF90)	98.20	26.75	48.59	155.79	97.20	107.20
(113, CF100)	128.66	27.30	55.00	178.00	134.00	123.00
(114, R0-100)	87.20	24.22	22.00	144.00	91.00	122.00
(115, R10-90)	45.20	18.54	9.47	86.07	45.01	76.60
(116, R0-50)	28.20	15.09	9.00	72.92	23.81	63.92
(117, R50-100)	58.99	21.48	11.61	108.54	62.92	96.93
(118, R20-80)	30.48	14.37	5.59	65.98	28.37	60.39
(119, R30-70)	19.22	10.05	3.72	46.62	18.77	42.89
(120, R40-60)	9.37	5.16	1.26	25.04	8.95	23.78

STATISTICS FOR FEATURES EXTRACTED FROM "CIRRUS" CLOUD VISUAL BRIGHTNESS HISTOGRAMS

FEATURE	FEATURE STATISTICS					
(Number, Name)	Mean	Standard Deviation	Minimum	Maximum	Median	Range
(101, Mean)	59.84	12.20	43.59	81.31	57.46	37.72
(102, StDev)	10.84	4.17	2.84	18.03	10.30	15.18
(103, CF0)	41.29	8.52	30.00	58.00	37.00	28.00
(104, CF10)	48.65	9.51	36.29	65.49	43.77	29.20
(105, CF20)	50.88	10.01	37.53	67.18	47.33	29.65
(106, CF30)	53.28	10.45	39.60	71.12	52.50	31.52
(107, CF40)	56.07	10.85	40.89	74.20	56.53	33.31
(108, CF50)	58.52	11.50	42.80	76.45	59.19	33.65
(109, CF60)	61.07	12.36	43.49	80.23	61.10	36.74
(110, CF70)	64.51	13.69	44.22	88.31	63.33	44.09
(111, CF80)	68.67	15.70	46.19	98.92	66.07	52.73
(112, CF90)	75.11	17.91	52.23	110.46	71.61	58.23
(113, CF100)	99.46	23.74	64.00	141.00	99.50	77.00
(114, R0-100)	58.17	19.50	17.00	91.00	60.50	74.00
(115, R10-90)	26.46	11.51	7.09	46.76	23.97	39.67
(116, R0-50)	17.23	6.37	8.30	28.52	16.95	20.23
(117, R50-100)	40.94	15.64	8.70	65.32	41.36	56.62
(118, R20-80)	17.79	8.85	4.71	32.37	17.76	27.66
(119, R30-70)	11.23	5.93	3.37	22.07	11.34	18.70
(120, R40-60)	5.00	3.05	1.14	14.20	4.90	13.06

STATISTICS FOR FEATURES EXTRACTED FROM "CUMULONIMBUS" CLOUD VISUAL BRIGHTNESS HISTOGRAMS

FEATURE	FEATURE STATISTICS					
(Number, Name)	Mean	Standard Deviation	Minimum	Maximum	Median	Range
(101, Mean)	92.94	24.55	48.94	154.94	95.47	106.00
(102, StDev)	28.58	7.08	15.69	50.24	29.52	34.56
(103, CF0)	38.74	10.84	24.00	66.00	36.00	42.00
(104, CF10)	58.60	21.61	33.89	130.77	53.39	96.88
(105, CF20)	67.19	25.38	36.93	144.02	61.01	107.09
(106, CF30)	75.24	27.94	39.63	150.40	67.93	110.77
(107, CF40)	84.02	29.44	42.43	156.29	80.79	113.85
(108, CF50	91.69	30.19	44.93	160.93	93.72	115.99
(109, CF60)	99.17	30.47	48.03	165.39	105.61	117.36
(110, CF70)	108.11	29.85	52.15	169.06	113.93	116.91
(111, CF80)	118.36	28.20	57.84	172.34	124.48	114.49
(112, CF90)	131.53	24.90	65.01	176.76	138.68	111.75
(113, CF100)	172.13	13.97	145.00	196.00	172.00	51.00
(114, R0-100)	133.39	19.33	91.00	172.00	134.00	81.00
(115, R10-90)	72.92	20.74	20.96	126.30	75.51	105.34
(116, R0-50)	52.95	24.05	13.96	99.93	52.82	85.97
(117, R50-100)	80.44	30.20	29.52	135.35	81.25	105.82
(118, R20-80)	51.17	19.81	12.33	114.00	50.56	101.66
(119, R30-70)	32.86	16.32	7.19	89.35	28.09	82.16
(120, R40-60)	15.15	8.30	3.93	46.97	12.30	43.04

STATISTICS FOR FEATURES EXTRACTED FROM "LOW" CLOUD INFRARED TEMPERATURE HISTOGRAMS

FEATURE	FEATURE STATISTICS					
(Number, Name)	Mean	Standard Deviation	Minimum	Maximum	Median	Range
(301, Mean)	129.94	3.91	122.88	137.06	129.31	14.18
(302, StDev)	2.66	1.15	1.01	5.51	2.30	4.49
(303, CF0)	120.81	6.83	93.00	133.00	120.00	40.00
(304, CF10)	126.95	4.87	117.85	135.29	125.65	17.43
(305, CF20)	128.17	4.63	119.65	136.55	127.01	16.90
(306, CF30)	129.12	4.36	121.05	137.15	128.44	16.09
(307, CF40)	129.92	4.16	122.45	137.54	129.60	15.09
(308, CF50)	130.67	3.98	123.42	137.92	130.54	14.51
(309, CF60)	131.36	3.81	124.50	138.28	131.53	13.77
(310, CF70)	132.03	3.66	125.47	138.62	132.16	13.15
(311, CF80)	132.76	3.51	125.90	138.96	132.84	13.06
(312, CF90)	133.62	3.35	126.57	139.57	133.54	13.00
(313, CF100)	136.35	3.38	128.00	150.00	136.00	22.00
(314, R0-100)	15.53	5.73	6.00	44.00	15.00	38.00
(315, R10-90)	6.67	2.98	2.63	12.48	5.36	9.85
(316, R0-50)	9.86	4.85	3.61	37.69	9.01	34.07
(317, R50-100)	5.68	2.72	2.08	19.83	4.75	17.76
(318, R20-80)	4.58	2.42	1.60	10.55	3.25	8.95
(319, R30-70)	2.91	1.77	.89	8.59	1.89	7.70
(320, R40-60)	1.45	1.02	.42	6.59	.91	6.16

STATISTICS FOR FEATURES EXTRACTED FROM "MIX" CLOUD INFRARED TEMPERATURE HISTOGRAMS

FEATURE	FEATURE STATISTICS					
(Number, Name)	Mean	Standard Deviation	Minimum	Maximum	Median	Range
(301, Mean)	121.71	8.88	97.10	135.76	121.74	38.67
(302, StDev)	9.63	4.73	1.39	20.09	9.73	18.70
(303, CF0)	86.11	21.07	46.00	130.00	86.00	84.00
(304, CF10)	108.69	15.30	77.39	134.42	107.31	57.04
(305, CF20)	114.89	13.07	83.70	135.24	113.74	51.54
(306, CF30)	118.78	11.40	88.45	135.64	119.71	47.19
(307, CF40)	121.77	10.06	92.25	136.13	123.36	43.88
(308, CF50)	124.32	8.86	97.79	136.61	125.46	38.82
(309, CF60)	126.60	7.85	101.92	137.08	127.68	35.15
(310, CF70)	128.55	6.87	106.57	137.49	129.52	30.92
(311, CF80)	130.34	6.00	111.43	138.13	130.93	26.70
(312, CF90)	132.28	4.92	116.53	138.91	133.44	22.38
(313, CF100)	136.16	3.27	126.00	141.00	137.00	15.00
(314, R0-100)	50.05	20.15	10.00	93.00	50.00	83.00
(315, R10-90)	23.59	12.95	3.43	53.85	24.25	50.42
(316, R0-50)	38.20	16.60	6.36	85.68	38.30	79.32
(317, R50-100)	11.84	7.02	2.39	34.21	10.56	31.82
(318, R20-80)	15.44	9.51	1.89	42.52	15.40	40.63
(319, R30-70)	9.77	6.59	1.11	28.08	8.59	26.98
(320, R40-60)	4.83	3.48	.46	13.78	4.09	13.32

STATISTICS FOR FEATURES EXTRACTED FROM "CIRRUS" CLOUD INFRARED TEMPERATURE HISTOGRAMS

FEATURE	FEATURE STATISTICS					
(Number, Name)	Mean	Standard Deviation	Minimum	Maximum	Median	Range
(301, Mean)	126.09	13.62	98.89	146.03	128.70	47.14
(302, StDev)	13.37	5.39	2.08	25.77	13.10	23.69
(303, CF0)	82.88	20.81	42.00	127.00	81.50	85.00
(304, CF10)	108.40	19.80	72.44	133.01	114.31	60.57
(305, CF20)	115.63	18.40	78.52	137.11	121.03	58.60
(306, CF30)	120.77	16.67	86.06	141.54	125.64	55.48
(307, CF40)	125.13	15.22	91.94	146.88	129.96	54.94
(308, CF50)	128.91	13.99	96.73	150.53	132.36	53.79
(309, CF60)	131.93	13.06	101.67	152.33	133.95	50.66
(310, CF70)	134.91	12.32	107.72	153.75	136.25	46.03
(311, CF80)	138.15	11.45	113.96	155.03	137.59	41.08
(312, CF90)	142.11	10.99	120.70	156.63	139.45	35.93
(313, CF100)	147.83	10.[illegible]	133.00	160.00	149.00	27.00
(314, R0-100)	64.96	17.90	14.00	96.00	66.50	82.00
(315, R10-90)	33.70	15.14	5.30	63.12	30.97	57.82
(316, R0-50)	46.03	15.10	9.29	73.22	49.43	63.93
(317, R50-100)	18.92	9.79	4.71	36.27	18.32	31.56
(318, R20-80)	22.52	12.86	3.52	55.01	19.71	51.49
(319, R30-70)	14.14	9.35	2.15	45.36	13.31	43.22
(320, R40-60)	6.80	5.54	.98	27.16	6.75	26.18

STATISTICS FOR FEATURES EXTRACTED FROM "CUMULONIMBUS" CLOUD INFRARED TEMPERATURE HISTOGRAMS

FEATURE (Number, Name)	FEATURE STATISTICS Mean	Standard Deviation	Minimum	Maximum	Median	Range
(301, Mean)	102.37	17.19	66.26	130.87	102.98	64.60
(302, StDev)	18.19	6.02	7.93	38.36	17.07	30.43
(303, CF0)	45.98	18.60	6.00	91.00	45.50	85.00
(304, CF10)	77.72	21.35	38.50	121.36	76.83	82.86
(305, CF20)	86.92	21.98	46.56	128.11	84.42	81.54
(306, CF30)	94.12	21.59	58.56	130.74	90.95	72.18
(307, CF40)	100.38	20.66	61.66	132.91	97.19	71.25
(308, CF50)	105.55	20.04	64.57	134.31	105.79	69.74
(309, CF60)	110.06	19.09	67.12	135.35	109.29	68.23
(310, CF70)	114.49	17.86	71.34	135.95	115.22	64.61
(311, CF80)	119.21	15.63	75.27	136.59	121.62	61.32
(312, CF90)	124.14	12.45	85.30	137.39	127.75	52.09
(313, CF100)	133.33	6.12	113.00	140.00	135.00	27.00
(314, R0-100)	87.35	18.24	46.00	128.00	86.00	82.00
(315, R10-90)	46.42	17.44	16.03	96.74	43.44	80.71
(316, R0-50)	59.57	18.47	28.00	97.19	56.71	69.19
(317, R50-100)	27.78	16.44	4.69	66.70	26.41	62.01
(318, R20-80)	32.29	15.25	8.48	86.44	30.39	77.96
(319, R30-70)	20.37	11.12	5.21	66.40	17.97	61.19
(320, R40-60)	9.68	5.17	2.44	25.41	8.55	22.97

STATISTICS FOR FEATURES EXTRACTED FROM "LOW" CLOUD VISUAL DIFFERENCE HISTOGRAMS

FEATURE	FEATURE STATISTICS					
(Number, Name)	Mean	Standard Deviation	Minimum	Maximum	Median	Range
(121, MeanHor)	.0063	.0022	.0026	.0121	.0061	.0095
(122, MeanVer)	.0260	.0097	.0091	.0519	.0254	.0428
(123, Mean1D)	.0268	.0102	.0092	.0536	.0261	.0444
(124, Mean2D)	.0259	.0095	.0092	.0518	.0257	.0425
(125, MeanM)	.0213	.0078	.0075	.0422	.0207	.0346
(126, Mean S)	.0087	.0035	.0028	.0178	.0085	.0150
(127, MeanN)	.0063	.0022	.0026	.0121	.0061	.0095
(128, MeanX)	.0271	.0102	.0092	.0536	.0263	.0444
(129, MeanR)	.0208	.0084	.0066	.0423	.0203	.0357
(130, ConHor)	6.9066	4.0276	1.2669	18.5060	6.1838	17.2391
(131, ConVer)	108.6881	73.8639	9.9189	356.0322	100.9239	346.1133
(132, Con1D)	115.0176	78.2809	10.0210	376.0434	103.9480	366.0225
(133, Con2D)	107.5753	73.3934	10.0486	353.8919	98.5310	343.8433
(134, ConM)	84.5469	57.0142	7.8374	275.9211	79.1069	268.0837
(135, ConS)	45.1942	31.1545	3.7942	149.3245	42.0039	145.5303
(136, ConN)	6.9066	4.0276	1.2669	18.5060	6.1838	17.2391
(137, ConX)	117.5099	79.4796	10.1152	376.0434	104.9135	365.9282
(138, ConR)	110.6034	76.0111	8.8483	358.3267	100.3161	349.4783
(139, ASMHor)	.2560	.0755	.1308	.4314	.2452	.3006
(140, ASMVer)	.0832	.0302	.0369	.1652	.0761	.1283
(141, ASM1D)	.0814	.0303	.0362	.1637	.0747	.1275
(142, ASM2D)	.0829	.0292	.0381	.1638	.0757	.1257
(143, ASMM)	.1259	.0380	.0631	.2232	.1202	.1601
(144, ASMS)	.0752	.0254	.0336	.1425	.0698	.1089
(145, ASMN)	.0806	.0300	.0362	.1637	.0742	.1275
(146, ASMX)	.2560	.0755	.1308	.4314	.2452	.3006
(147, ASMR)	.1754	.0585	.0797	.3301	.1630	.2504
(148, EntHor)	1.6622	.2729	1.1030	2.2415	1.6810	1.1385
(149, EntVer)	2.8315	.3873	1.9695	3.5912	2.8936	1.6217
(150, Ent1D)	2.8586	.3962	1.9766	3.6171	2.9206	1.6405
(151, Ent2D)	2.8326	.3799	1.9767	3.5823	2.8937	1.6056
(152, EntM)	2.5462	.3514	1.7576	3.2477	2.6016	1.4900
(153, EntS)	.5109	.0870	.3336	.7261	.5255	.3925
(154, EntN)	1.6622	.2729	1.1031	2.2415	1.6811	1.1385
(155, EntX)	2.8683	.3956	1.9767	3.6171	2.9365	1.6404
(156, EntR)	1.2062	.2036	.7771	1.6993	1.2477	.9221

STATISTICS FOR FEATURES EXTRACTED FROM "MIX" CLOUD VISUAL DIFFERENCE HISTOGRAMS

FEATURE (Number, Name)	FEATURE STATISTICS Mean	Standard Deviation	Minimum	Maximum	Median	Range
(121, MeanHor)	.0070	.0025	.0023	.0148	.0065	.0125
(122, MeanVer)	.0284	.0092	.0104	.0535	.0279	.0431
(123, Mean1D)	.0298	.0099	.0107	.0587	.0295	.0481
(124, Mean2D)	.0280	.0088	.0106	.0500	.0273	.0394
(125, MeanM)	.0233	.0075	.0088	.0443	.0230	.0355
(126, MeanS)	.0095	.0032	.0031	.0173	.0092	.0142
(127, MeanN)	.0070	.0025	.0023	.0148	.0065	.0125
(128, MeanX)	.0299	.0099	.0107	.0587	.0297	.0481
(129, MeanR)	.0229	.0080	.0072	.0439	.0228	.0367
(130, ConHor)	8.0410	4.6927	1.1052	25.8447	7.5769	24.7396
(131, ConVer)	110.3566	65.1584	11.9455	319.8956	98.1109	307.9521
(132, Con1D)	121.1856	73.6917	12.3815	379.2457	108.7752	366.8642
(133, Con2D)	106.8746	61.7774	12.3431	285.7921	99.7225	273.4490
(134, ConM)	86.6144	50.8984	9.6416	252.6945	77.7142	243.0529
(135, ConS)	45.9638	27.5823	4.4739	135.1735	41.0863	130.6996
(136, ConN)	8.0410	4.6927	1.1052	25.8447	7.5769	24.7396
(137, ConX)	122.1076	73.4494	12.3815	379.2457	108.7752	366.8642
(138, ConR)	114.0667	69.3968	10.4832	353.4010	103.0545	342.9178
(139, ASMHor)	.2435	.0761	.1085	.4405	.2361	.3320
(140, ASMVer)	.0708	.0252	.0335	.1448	.0645	.1113
(141, ASM1D)	.0683	.0253	.0309	.1434	.0614	.1125
(142, ASM2D)	.0710	.0246	.0357	.1428	.0653	.1071
(143, ASMM)	.1134	.0340	.0521	.2161	.1092	.1640
(144, ASMS)	.0751	.0276	.0310	.1381	.0684	.1071
(145, ASMN)	.0679	.0251	.0309	.1426	.0614	.1118
(146, ASMX)	.2435	.0761	.1085	.4405	.2361	.3320
(147, ASMR)	.1755	.0634	.0724	.3206	.1594	.2482
(148, EntHor)	1.7354	.2734	1.0406	2.4081	1.7109	1.3675
(149, EntVer)	2.9417	.3363	2.0638	3.5989	2.9799	1.5351
(150, Ent1D)	2.9849	.3476	2.0752	3.6793	3.0147	1.6041
(151, Ent2D)	2.9348	.3303	2.0775	3.5390	2.9702	1.4615
(152, EntM)	2.6492	.3113	1.8290	3.3063	2.6738	1.4773
(153, EntS)	.5284	.0831	.3471	.7433	.5217	.3962
(154, EntN)	1.7354	.2724	1.0406	2.4081	1.7109	1.3675
(155, EntX)	2.9892	.3469	2.0775	3.6793	3.0445	1.6018
(156, EntR)	1.2537	.1915	.8069	1.7521	1.2406	.9452

STATISTICS FOR FEATURES EXTRACTED FROM "CIRRUS" CLOUD VISUAL DIFFERENCE HISTOGRAMS

FEATURE (Number, Name)	FEATURE STATISTICS Mean	Standard Deviation	Minimum	Maximum	Median	Range
(121, MeanHor)	.0043	.0013	.0021	.0072	.0040	.0050
(122, MeanVer)	.0187	.0068	.0089	.0333	.0166	.0244
(123, Mean1D)	.0194	.0073	.0089	.0342	.0170	.0253
(124, Mean2D)	.0187	.0064	.0090	.0327	.0171	.0237
(125, MeanM)	.0153	.0054	.0072	.0265	.0138	.0193
(126, MeanS)	.0064	.0025	.0029	.0119	.0057	.0090
(127, MeanN)	.0043	.0013	.0021	.0072	.0040	.0050
(128, MeanX)	.0196	.0073	.0090	.0342	.0174	.0252
(129, MeanR)	.0153	.0061	.0069	.0283	.0134	.0214
(130, ConHor)	3.9565	2.4720	.9985	11.2009	3.0828	10.2024
(131, ConVer)	52.3015	42.9426	8.4330	170.3105	39.7870	161.8775
(132, Con1D)	56.5163	47.7054	8.5259	176.2468	41.1580	167.7209
(133, Con2D)	51.5795	40.3802	8.6820	167.0911	40.1779	158.4091
(134, ConM)	41.0884	33.2014	6.6598	130.0438	31.2842	123.3840
(135, ConS)	21.6300	18.2178	3.2698	71.3714	16.2272	68.1016
(136, ConN)	3.9565	2.4720	.9985	11.2009	3.0828	10.2024
(137, ConX)	57.4602	47.3605	8.6820	176.2468	43.5827	167.5647
(138, ConR)	53.5037	45.3219	7.6835	169.6635	40.1816	161.9800
(139, ASMHor)	.3388	.0566	.2535	.4640	.3339	.2105
(140, ASMVer)	.1017	.0293	.0592	.1695	.0991	.1104
(141, ASM1D)	.0995	.0298	.0574	.1687	.0982	.1113
(142, ASM2D)	.1014	.0282	.0605	.1665	.0983	.1060
(143, ASMM)	.1603	.0339	.1103	.2422	.1589	.1319
(144, ASMS)	.1030	.0168	.0721	.1309	.1022	.0168
(145, ASMN)	.0986	.0294	.0574	.1665	.0961	.1091
(146, ASMX)	.3388	.0566	.2535	.4640	.3339	.2105
(147, ASMR)	.2402	.0387	.1696	.3047	.2393	.1351
(148, EntHor)	1.4100	.2002	.9946	1.7459	1.3917	.7512
(149, EntVer)	2.5492	.3308	1.8981	3.1342	2.5033	1.2361
(150, Ent1D)	2.5810	.3477	1.9044	3.1837	2.5206	1.2793
(151, Ent2D)	2.5551	.3226	1.9150	3.1355	2.5282	1.2205
(152, EntM)	2.2738	.2960	1.6780	2.7823	2.2443	1.1043
(153, EntS)	.4992	.0753	.3828	.6391	.5022	.2563
(154, EntN)	1.4100	.2002	.9946	1.7459	1.3917	.7512
(155, EntX)	2.5928	.3422	1.9150	3.1837	2.5419	1.2687
(156, EntR)	1.1828	.1791	.9083	1.5077	1.1823	.5994

STATISTICS FOR FEATURES EXTRACTED FROM "CUMULONIMBUS" CLOUD VISUAL DIFFERENCE HISTOGRAMS

FEATURE (Number, Name)	FEATURE STATISTICS Mean	Standard Deviation	Minimum	Maximum	Median	Range
(121, MeanHor)	.0099	.0031	.0047	.0161	.0093	.0114
(122, MeanVer)	.0432	.0118	.0260	.0762	.0402	.0502
(123, Mean1D)	.0446	.0123	.0261	.0791	.0412	.0530
(124, Mean2D)	.0430	.0117	.0257	.0750	.0416	.0493
(125, MeanM)	.0352	.0097	.0211	.0616	.0328	.0405
(126, MeanS)	.0146	.0040	.0087	.0263	.0137	.0176
(127, MeanN)	.0099	.0031	.0047	.0161	.0093	.0114
(128, MeanX)	.0448	.0122	.0272	.0791	.0418	.0519
(129, MeanR)	.0349	.0094	.0209	.0630	.0331	.0421
(130, ConHor)	15.3248	7.7089	5.6786	35.0888	12.7961	29.4102
(131, ConVer)	251.0684	146.4238	81.6492	702.4363	207.4032	620.7872
(132, Con1D)	266.5795	153.6783	91.1449	734.3464	219.6042	643.2016
(133, Con2D)	249.0973	143.8298	77.4245	689.0490	201.8305	611.6245
(134, ConM)	195.5175	112.5765	63.9743	539.5772	162.0230	475.6030
(135, ConS)	104.5348	60.9717	34.0218	293.2364	85.7422	259.2146
(136, ConN)	15.3248	7.7089	5.6786	35.0888	12.7961	29.4102
(137, ConX)	269.2467	153.0081	91.1449	734.3464	222.8781	643.2016
(138, ConR)	253.9218	145.8004	85.4663	701.8693	208.1011	616.4029
(139, ASMHor)	.1889	.0720	.1014	.3604	.1713	.2590
(140, ASMVer)	.0461	.0125	.0241	.0785	.0460	.0544
(141, ASM1D)	.0445	.0123	.0230	.0782	.0437	.0552
(142, ASM2D)	.0461	.0122	.0248	.0771	.0452	.0523
(143, ASMM)	.0814	.0256	.0433	.1480	.0779	.1047
(144, ASMS)	.0621	.0275	.0316	.1259	.0532	.0943
(145, ASMN)	.0443	.0122	.0230	.0771	.0436	.0541
(146, ASMX)	.1889	.0720	.1014	.3604	.1713	.0052
(147, ASMR)	.1446	.0637	.0743	.2920	.1238	.2177
(148, EntHor)	2.0321	.2802	1.4637	2.5093	2.0211	1.0456
(149, EntVer)	3.3568	.2625	2.8588	3.9421	3.3319	1.0833
(150, Ent1D)	3.3939	.2617	2.8669	3.9787	3.3488	1.1117
(151, Ent2D)	3.3564	.2590	2.8699	3.9299	3.3571	1.0600
(152, EntM)	3.0348	.2601	2.5303	3.5890	2.9971	1.0587
(153, EntS)	.5793	.0537	.5013	.7313	.5731	.2300
(154, EntN)	2.0321	.2802	1.4637	2.5093	2.0211	1.0456
(155, EntX)	3.3979	.2607	2.8904	3.9787	3.3683	1.0883
(156, EntR)	1.3658	.1267	1.1816	1.7426	1.3556	.5609

STATISTICS FOR FEATURES EXTRACTED FROM "LOW" CLOUD INFRARED DIFFERENCE HISTOGRAMS

FEATURE (Number, Name)	FEATURE STATISTICS Mean	Standard Deviation	Minimum	Maximum	Median	Range
(321, MeanHor)	.0021	.0005	.0009	.0030	.0022	.0021
(322, MeanVer)	.0066	.0015	.0039	.0111	.0065	.0071
(323, Mean1D)	.0067	.0015	.0039	.0110	.0066	.0071
(324, Mean2D)	.0067	.0015	.0040	.0115	.0066	.0075
(325, MeanM)	.0055	.0012	.0032	.0089	.0055	.0057
(326, MeanS)	.0020	.0005	.0010	.0039	.0019	.0029
(327, MeanN)	.0021	.0005	.0009	.0030	.0022	.0021
(328, MeanX)	.0068	.0015	.0040	.0115	.0067	.0075
(329, MeanR)	.0047	.0013	.0023	.0094	.0044	.0070
(330, ConHor)	.7234	.2026	.2589	1.1488	.7547	.8899
(331, ConVer)	5.2462	2.4087	1.8180	13.7671	4.7049	11.9491
(332, Con1D)	5.3284	2.3852	1.8449	13.8469	4.8062	12.0020
(333, Con2D)	5.3569	2.5665	1.8402	14.9099	4.7716	13.0696
(334, ConM)	4.1637	1.8713	1.4417	10.9054	3.7711	9.4637
(335, ConS)	1.9915	1.0043	.5981	5.6804	1.7120	5.0824
(336, ConN)	.7234	.2026	.2589	1.1488	.7547	.8899
(337, ConX)	5.4877	2.5928	1.8495	14.9099	4.8062	13.0604
(338, ConR)	4.7643	2.4541	1.4036	13.8122	4.0093	12.4086
(339, ASMHor)	.4609	.0567	.3779	.6521	.4389	.2743
(340, ASMVer)	.2311	.0409	.1448	.3360	.2289	.1912
(341, ASM1D)	.2294	.0405	.1469	.3295	.2264	.1825
(342, ASM2D)	.2291	.0414	.1395	.3363	.2265	.1968
(343, ASMM)	.2876	.0416	.2272	.4111	.2775	.1839
(344, ASMS)	.1000	.0181	.0729	.1445	.0970	.0716
(345, ASMN)	.2268	.0411	.1395	.3282	.2239	.1887
(346, ASMX)	.4609	.0567	.3779	.6521	.4389	.2743
(347, ASMR)	.2341	.0418	.1698	.3379	.2255	.1681
(348, EntHor)	.8968	.1061	.5788	1.0759	.9303	.4971
(349, EntVer)	1.6357	.1907	1.2300	2.1063	1.6287	.8763
(350, Ent1D)	1.6449	.1892	1.2383	2.1050	1.6404	.8668
(351, Ent2D)	1.6436	.1947	1.2331	2.1486	1.6375	.9155
(352, EntM)	1.4553	.1653	1.0729	1.8404	1.4654	.7674
(353, EntS)	.3226	.0539	.2065	.4846	.3087	.2781
(354, EntN)	.8968	.1061	.5788	1.0759	.9303	.4971
(355, EntX)	1.6547	.1951	1.2499	2.1486	1.6432	.8987
(356, EntR)	.7578	.1277	.4810	1.1471	.7267	.6661

STATISTICS FOR FEATURES EXTRACTED FROM "MIX" CLOUD INFRARED DIFFERENCE HISTOGRAMS

FEATURE	FEATURE STATISTICS					
(Number, Name)	Mean	Standard Deviation	Minimum	Maximum	Median	Range
(321, MeanHor)	.0036	.0015	.0013	.0088	.0036	.0075
(322, MeanVer)	.0133	.0056	.0045	.0281	.0136	.0237
(323, Mean1D)	.0139	.0060	.0046	.0296	.0137	.0250
(324, Mean2D)	.0134	.0056	.0045	.0287	.0133	.0242
(325, MeanM)	.0111	.0046	.0038	.0238	.0112	.0200
(326, MeanS)	.0043	.0019	.0012	.0092	.0040	.0081
(327, MeanN)	.0036	.0015	.0013	.0088	.0036	.0075
(328, MeanX)	.0140	.0061	.0046	.0296	.0142	.0250
(329, MeanR)	.0104	.0047	.0027	.0223	.0100	.0196
(330, ConHor)	2.4059	1.6594	.4256	8.9018	2.1190	8.4762
(331, ConVer)	26.5945	20.0807	2.8967	85.8574	24.0761	82.9607
(332, Con1D)	28.9451	22.3222	2.9048	95.6528	25.2924	92.7481
(333, Con2D)	26.5990	20.1175	2.9621	86.2284	23.5110	83.2662
(334, ConM)	21.1361	15.9426	2.3376	69.1601	19.1203	66.8225
(335, ConS)	10.9536	8.4222	1.0111	35.3656	9.7480	34.3545
(336, ConN)	2.4059	1.6594	.4256	8.9018	2.1190	8.4762
(337, ConX)	29.6789	22.7500	2.9621	95.6528	25.5689	92.6907
(338, ConR)	27.2730	21.1855	2.3753	86.7800	23.7390	84.4047
(339, ASMHor)	.3607	.0889	.1675	.5736	.3649	.4061
(340, ASMVer)	.1488	.0578	.0604	.2964	.1291	.2359
(341, ASM1D)	.1449	.0581	.0575	.2965	.1234	.2390
(342, ASM2D)	.1480	.0573	.0602	.2986	.1310	.2383
(343, ASMM)	.2006	.0627	.0864	.3430	.1812	.2566
(344, ASMS)	.0925	.0233	.0468	.1485	.0912	.1017
(345, ASMN)	.1436	.0580	.0575	.2964	.1234	.2388
(346, ASMX)	.3607	.0889	.1675	.5736	.3649	.4061
(347, ASMR)	.2171	.0533	.1099	.3478	.2115	.2379
(348, EntHor)	1.2531	.2708	.7262	1.9342	1.2732	1.2080
(349, EntVer)	2.2203	.4009	1.3948	2.9719	2.3208	1.5771
(350, Ent1D)	2.2534	.4120	1.3966	3.0262	2.3428	1.6296
(351, Ent2D)	2.2243	.3996	1.3899	2.9739	2.3135	1.5840
(352, EntM)	1.9878	.3664	1.2545	2.7266	2.0608	1.4721
(353, EntS)	.4248	.0788	.2413	.6030	.4315	.3617
(354, EntN)	1.2531	.2708	.7262	1.9342	1.2732	1.2080
(355, EntX)	2.2630	.4150	1.3966	3.0262	2.3531	1.6296
(356, EntR)	1.0100	.1890	.5601	1.4502	1.0224	.8901

STATISTICS FOR FEATURES EXTRACTED FROM "CIRRUS" CLOUD INFRARED DIFFERENCE HISTOGRAMS

Feature	FEATURE STATISTICS					
(Number, Name)	Mean	Standard Deviation	Minimum	Maximum	Median	Range
(321, MeanHor)	.0040	.0017	.0014	.0076	.0034	.0062
(322, MeanVer)	.0175	.0080	.0062	.0334	.0160	.0272
(323, Mean1D)	.0185	.0088	.0063	.0364	.0170	.0302
(324, Mean2D)	.0173	.0078	.0061	.0336	.0157	.0275
(325, MeanM)	.0143	.0065	.0050	.0269	.0129	.0219
(326, MeanS)	.0060	.0029	.0021	.0121	.0058	.0100
(327, MeanN)	.0040	.0017	.0014	.0076	.0034	.0062
(328, MeanX)	.0187	.0088	.0063	.0364	.0170	.0302
(329, MeanR)	.0147	.0072	.0048	.0302	.0136	.0254
(330, ConHor)	3.6453	2.8759	.4831	10.8750	2.5077	10.3919
(331, ConVer)	45.7854	34.6651	4.0186	125.3548	36.4902	121.3362
(332, Con1D)	51.8696	40.4881	4.1444	148.9047	41.3799	144.7604
(333, Con2D)	44.2357	33.6062	3.9913	125.8136	36.4726	121.8223
(334, ConM)	36.3840	27.6404	3.1594	98.4842	28.4801	95.3248
(335, ConS)	19.3376	14.8916	1.5462	54.4215	15.4191	52.8753
(336, ConN)	3.6453	2.8759	.4831	10.8750	2.5077	10.3919
(337, ConX)	52.8396	40.9260	4.1444	148.9047	41.3799	144.7604
(338, ConR)	49.1944	38.3875	3.6613	141.9603	39.2968	138.2990
(339, ASMHor)	.3624	.0719	.2500	.5433	.3563	.2933
(340, ASMVer)	.1238	.0544	.0535	.2431	.1133	.1896
(341, ASM1D)	.1192	.0551	.0482	.2389	.1084	.1907
(342, ASM2D)	.1230	.0528	.0521	.2424	.1153	.1903
(343, ASMM)	.1821	.0569	.1092	.3169	.1811	.2077
(344, ASMS)	.1042	.0154	.0728	.1307	.1007	.0579
(345, ASMN)	.1174	.0533	.0482	.2389	.1082	.1907
(346, ASMX)	.3624	.0719	.2500	.5433	.3563	.2933
(347, ASMR)	.2451	.0362	.1706	.3045	.2378	.1338
(348, EntHor)	1.3423	.2560	.7728	1.7786	1.2887	1.0058
(349, EntVer)	2.4468	.4384	1.5512	3.1303	2.4766	1.5792
(350, Ent1D)	2.4995	.4567	1.5680	3.2193	2.5343	1.6513
(351, Ent2D)	2.4474	.4268	1.5529	3.1529	2.4608	1.6000
(352, EntM)	2.1840	.3901	1.3612	2.7787	2.1732	1.4175
(353, EntS)	.4874	.0944	.3296	.6425	.5071	.3129
(354, EntN)	1.3423	.2560	.7728	1.7786	1.2887	1.0058
(355, EntX)	2.5144	.4460	1.5680	3.2193	2.5343	1.6513
(356, EntR)	1.1721	.2212	.7952	1.5517	1.2180	.7565

STATISTICS FOR FEATURES EXTRACTED FROM "CUMULONIMBUS" CLOUD INFRARED DIFFERENCE HISTOGRAMS

FEATURE	FEATURE STATISTICS					
(Number, Name)	Mean	Standard Deviation	Minimum	Maximum	Median	Range
(321, MeanHor)	.0056	.0017	.0030	.0091	.0055	.0061
(322, MeanVer)	.0239	.0071	.0127	.0435	.0223	.0307
(323, Mean1D)	.0244	.0072	.0131	.0442	.0227	.0312
(324, Mean2D)	.0241	.0072	.0126	.0435	.0226	.0309
(325, MeanM)	.0195	.0058	.0105	.0351	.0185	.0246
(326, MeanS)	.0080	.0025	.0040	.0150	.0076	.0110
(327, MeanN)	.0056	.0017	.0030	.0091	.0055	.0061
(328, MeanX)	.0246	.0073	.0131	.0442	.0230	.0312
(329, MeanR)	.0190	.0058	.0095	.0351	.0180	.0256
(330, ConHor)	4.9576	2.2476	1.8363	9.9891	4.3795	8.1528
(331, ConVer)	75.3973	39.8238	20.3977	204.8049	60.6668	184.4072
(332, Con1D)	78.3034	41.5432	21.1183	213.3563	64.4480	192.2381
(333, Con2D)	76.8679	40.3489	20.6677	205.5980	62.5704	184.9303
(334, ConM)	58.8815	30.8504	16.0050	158.4350	47.3185	142.4300
(335, ConS)	31.2519	16.6725	8.1843	85.7752	25.3095	77.5909
(336, ConN)	4.9576	2.2476	1.8363	9.9891	4.3795	8.1528
(337, ConX)	80.0929	41.7595	21.1183	213.3563	65.4265	192.2381
(338, ConR)	75.1354	39.7127	19.2820	203.3757	61.8618	184.0937
(339, ASMHor)	.2653	.0702	.1599	.4089	.2565	.2491
(340, ASMVer)	.0827	.0262	.0411	.1412	.0780	.1000
(341, ASM1D)	.0811	.0256	.0401	.1387	.0783	.0986
(342, ASM2D)	.0817	.0261	.0401	.1410	.0786	.1009
(343, ASMM)	.1277	.0352	.0703	.1976	.1270	.1273
(344, ASMS)	.0795	.0223	.0479	.1375	.0750	.0897
(345, ASMN)	.0802	.0255	.0401	.1387	.0781	.0986
(346, ASMX)	.2653	.0702	.1599	.4089	.2565	.2491
(347, ASMR)	.1851	.0517	.1111	.3190	.1746	.2080
(348, EntHor)	1.5914	.2210	1.2069	1.9889	1.5970	.7819
(349, EntVer)	2.7871	.2757	2.2502	3.3794	2.7681	1.1291
(350, Ent1D)	2.8076	.2746	2.2751	3.4069	2.7800	1.1317
(351, Ent2D)	2.8009	.2753	2.2492	3.3935	2.7802	1.1443
(352, EntM)	2.4968	.2583	2.0100	3.0418	2.4965	1.0318
(353, EntS)	.5229	.0461	.4300	.6384	.5251	.2084
(354, EntN)	1.5914	.2210	1.2069	1.9889	1.5970	.7819
(355, EntX)	2.8174	.2752	2.2751	3.4069	2.7911	1.1317
(356, EntR)	1.2260	.1068	1.0097	1.4901	1.2271	.4804

TABLES 18-27

Fisher Distances

Table	Histogram type	Distance
18	Visual brightness	-
19	Infrared temperature	-
20	Visual difference	1
21	Visual difference	2
22	Visual difference	4
23	Visual difference	8
24	Infrared difference	1
25	Infrared difference	2
26	Infrared difference	4
27	Infrared difference	8

FISHER DISTANCE BETWEEN PAIRS OF CLASSES FOR SINGLE FEATURES EXTRACTED FROM VISUAL BRIGHTNESS HISTOGRAMS

FEATURE	FISHER DISTANCE BETWEEN CLASSES					
(Number, Name)	Low, Mix	Low, Ci	Low, Cb	Mix, Ci	Mix, Cb	Ci, Cb
(101, Mean)	.17	.14	.58	.38	.45	.90
(102, StDev)	.23	.35	1.00	.64	.78	1.58
(103, CF0)	.02	.02	.09	.01	.12	.13
(104, CF10)	.06	.08	.19	.17	.15	.32
(105, CF20)	.09	.09	.29	.23	.23	.46
(106, CF30)	.11	.10	.37	.26	.29	.57
(107, CF40)	.13	.10	.46	.29	.37	.69
(108, CF50)	.16	.10	.54	.33	.42	.80
(109, CF60)	.19	.12	.59	.38	.45	.89
(110, CF70)	.20	.13	.67	.42	.51	1.00
(111, CF80)	.22	.16	.75	.46	.57	1.13
(112, CF90)	.22	.22	.84	.52	.65	1.32
(113, CF100)	.15	.38	1.18	.57	1.05	1.93
(114, R0-100)	.16	.46	1.19	.66	1.06	1.94
(115, R10-90)	.28	.28	.96	.62	.71	1.44
(116, R0-50)	.23	.19	.82	.51	.63	1.17
(117, R50-100)	.02	.40	.39	.49	.42	.86
(118, R20-80)	.30	.18	.85	.55	.61	1.17
(119, R30-70)	.30	.13	.75	.50	.52	.97
(120, R40-60)	.31	.15	.67	.53	.43	.89

FISHER DISTANCE BETWEEN PAIRS OF CLASSES FOR SINGLE FEATURES EXTRACTED FROM INFRARED TEMPERATURE HISTOGRAMS

FEATURE	FISHER DISTANCE BETWEEN CLASSES					
(Number, Name)	Low, Mix	Low, Ci	Low, Cb	Mix, Ci	Mix, Cb	Ci, Cb
(301, Mean)	.64	.22	1.31	.19	.74	.77
(302, StDev)	1.19	1.64	2.17	.37	.80	.42
(303, CF0)	1.24	1.37	2.94	.08	1.01	.94
(304, CF10)	.91	.75	1.88	.01	.84	.75
(305, CF20)	.75	.54	1.55	.02	.80	.71
(306, CF30)	.66	.40	1.35	.07	.75	.70
(307, CF40)	.57	.25	1.19	.13	.70	.69
(308, CF50)	.49	.10	1.05	.20	.65	.69
(309, CF60)	.41	.03	.93	.25	.61	.68
(310, CF70)	.33	.18	.81	.33	.57	.68
(311, CF80)	.25	.36	.71	.45	.51	.70
(312, CF90)	.16	.59	.60	.62	.47	.77
(313, CF100)	.03	.83	.32	.85	.30	.87
(314, R0-100)	1.33	2.09	3.00	.39	.97	.62
(315, R10-90)	1.06	1.49	1.95	.36	.75	.39
(316, R0-50)	1.32	1.81	2.13	.25	.61	.40
(317, R50-100)	.63	1.06	1.15	.42	.68	.34
(318, R20-80)	.91	1.17	1.57	.32	.68	.35
(319, R30-70)	.82	1.01	1.35	.27	.60	.30
(320, R40-60)	.75	.82	1.33	.22	.56	.27
(465, MaxR10-90)	1.23	1.89	2.25	.39	.73	.38
(466, RanR10-90)	1.04	1.45	1.52	.19	.43	.28
(467, MinCF0)	1.24	1.37	2.94	.08	1.01	.94
(468, RanCF0)	1.02	1.33	1.31	.13	.34	.24
(469, MaxStDev)	1.27	1.91	2.36	.38	.76	.41
(470, RanStDev)	1.06	1.31	1.52	.13	.42	.31

FISHER DISTANCE BETWEEN PAIRS OF CLASSES FOR SINGLE FEATURES EXTRACTED FROM VISUAL DIFFERENCE HISTOGRAMS, DISTANCE 1

FEATURE	FISHER DISTANCE BETWEEN CLASSES					
(Number, Name)	Low, Mix	Low, Ci	Low, Cb	Mix, Ci	Mix, Cb	Ci, Cb
(121, MeanHor)	.14	.57	.67	.70	.52	1.26
(122, MeanVer)	.13	.44	.80	.61	.70	1.31
(123, Mean1D)	.15	.42	.79	.60	.67	1.28
(124, Mean2D)	.12	.45	.81	.61	.73	1.34
(125, MeanM)	.13	.45	.80	.62	.69	1.32
(126, MeanS)	.12	.39	.80	.54	.71	1.28
(127, MeanN)	.14	.57	.67	.70	.52	1.26
(128, MeanX)	.14	.43	.79	.60	.67	1.29
(129, MeanR)	.13	.38	.79	.54	.69	1.26
(130, ConHor)	.13	.45	.72	.57	.59	1.12
(131, ConVer)	.01	.48	.65	.54	.67	1.05
(132, Con1D)	.04	.46	.65	.53	.64	1.04
(133, Con2D)	.01	.49	.65	.54	.69	1.07
(134, ConM)	.02	.48	.65	.54	.67	1.06
(135, ConS)	.01	.48	.64	.53	.66	1.05
(136, ConN)	.13	.45	.72	.57	.59	1.12
(137, ConX)	.03	.47	.65	.54	.65	1.06
(138, ConR)	.02	.47	.65	.53	.65	1.05
(139, ASMHor)	.08	.63	.46	.72	.37	1.17
(140, ASMVer)	.22	.31	.87	.57	.65	1.33
(141, ASM1D)	.24	.30	.87	.57	.63	1.31
(142, ASM2D)	.22	.32	.89	.58	.68	1.37
(143, ASMM)	.17	.48	.70	.69	.54	1.33
(144, ASMS)	.00	.66	.25	.63	.24	.92
(145, ASMN)	.23	.30	.86	.56	.63	1.31
(146, ASMX)	.08	.63	.46	.72	.37	1.17
(147, ASMR)	.00	.67	.25	.63	.24	.93
(148, EntHor)	.13	.53	.67	.69	.54	1.29
(149, EntVer)	.15	.39	.81	.59	.69	1.36
(150, Ent1D)	.17	.37	.81	.58	.67	1.33
(151, Ent2D)	.14	.39	.82	.58	.72	1.38
(152, EntM)	.16	.42	.80	.62	.67	1.37
(153, EntS)	.10	.07	.49	.18	.37	.62
(154, EntN)	.13	.53	.67	.69	.54	1.29
(155, EntX)	.16	.37	.81	.58	.67	1.34
(156, EntR)	.12	.06	.48	.19	.35	.60

FISHER DISTANCE BETWEEN PAIRS OF CLASSES FOR SINGLE FEATURES EXTRACTED FROM VISUAL DIFFERENCES HISTOGRAMS, DISTANCE 2

FEATURE	FISHER DISTANCE BETWEEN CLASSES					
(Number, Name)	Low, Mix	Low, Ci	Low, Cb	Mix, Ci	Mix, Cb	Ci, Cb
(157, MeanHor2)	.16	.50	.72	.67	.54	1.26
(158, MeanVer2)	.14	.40	.83	.58	.73	1.35
(159, Mean1D2)	.16	.38	.83	.57	.69	1.32
(160, Mean2D2)	.12	.41	.84	.58	.76	1.37
(161, MeanM2)	.14	.41	.83	.60	.72	1.36
(162, MeanS2)	.12	.34	.81	.51	.74	1.29
(163, MeanN2)	.16	.50	.72	.67	.54	1.26
(164, MeanX2)	.15	.39	.83	.58	.70	1.35
(165, MeanR2)	.13	.34	.81	.50	.71	1.29
(166, ConHor2)	.11	.56	.66	.62	.55	1.12
(167, ConVer2)	.02	.46	.71	.53	.72	1.16
(168, Con1D2)	.05	.44	.71	.52	.68	1.15
(169, Con2D2)	.00	.47	.71	.53	.76	1.18
(170, ConM2)	.03	.46	.72	.53	.72	1.17
(171, ConS2)	.02	.44	.71	.51	.72	1.16
(172, ConN2)	.11	.56	.66	.62	.55	1.12
(173, ConX2)	.04	.45	.72	.53	.70	1.18
(174, ConR2)	.04	.43	.71	.51	.71	1.17
(175, ASMHor2)	.19	.43	.73	.64	.52	1.29
(176, ASMVer2)	.26	.29	.89	.55	.63	1.23
(177, ASM1D2)	.27	.27	.87	.55	.61	1.20
(178, ASM2D2)	.24	.29	.89	.55	.65	1.27
(179, ASMM2)	.24	.34	.85	.60	.61	1.29
(180, ASMS2)	.07	.45	.43	.55	.36	1.03
(181, ASMN2)	.26	.27	.87	.54	.61	1.21
(182, ASMX2)	.19	.43	.73	.64	.52	1.29
(183, ASMR2)	.07	.47	.45	.57	.38	1.07
(184, EntHor2)	.16	.47	.72	.66	.56	1.31
(185, EntVer2)	.18	.35	.85	.57	.71	1.35
(186, Ent1D2)	.19	.33	.84	.56	.67	1.31
(187, Ent2D2)	.16	.36	.86	.56	.74	1.37
(188, EntM2)	.18	.38	.84	.59	.69	1.36
(189, EntS2)	.11	.05	.44	.16	.35	.53
(190, EntN2)	.16	.47	.72	.66	.56	1.31
(191, EntX2)	.19	.33	.84	.56	.68	1.33
(192, EntR2)	.12	.03	.44	.16	.32	.51

FISHER DISTANCE BETWEEN PAIRS OF CLASSES FOR SINGLE FEATURES EXTRACTED FROM VISUAL DIFFERENCE HISTOGRAMS, DISTANCE 4

FEATURE	FISHER DISTANCE BETWEEN CLASSES					
(Number, Name)	Low, Mix	Low, Ci	Low, Cb	Mix, Ci	Mix, Cb	Ci, Cb
(193, MeanHor4)	.19	.45	.76	.65	.56	1.26
(194, MeanVer4)	.18	.38	.91	.59	.75	1.44
(195, Mean1D4)	.17	.36	.86	.56	.70	1.35
(196, Mean2D4)	.13	.39	.88	.58	.79	1.42
(197, MeanM4)	.17	.39	.89	.60	.74	1.42
(198, MeanS4)	.13	.29	.79	.46	.69	1.24
(199, MeanN4)	.19	.45	.76	.65	.56	1.26
(200, MeanX4)	.17	.38	.91	.59	.75	1.44
(201, MeanR4)	.14	.30	.81	.47	.70	1.26
(202, ConHor4)	.12	.52	.68	.61	.55	1.12
(203, ConVer4)	.09	.46	.84	.58	.78	1.36
(204, Con1D4)	.08	.43	.79	.53	.72	1.26
(205, Con2D4)	.03	.46	.78	.55	.81	1.28
(206, ConM4)	.07	.46	.81	.57	.77	1.32
(207, ConS4)	.06	.42	.80	.52	.77	1.30
(208, ConN4)	.12	.52	.68	.61	.55	1.12
(209, ConX4)	.08	.46	.84	.58	.78	1.36
(210, ConR4)	.07	.43	.82	.54	.78	1.33
(211, ASMHor4)	.24	.33	.79	.59	.53	1.20
(212, ASMVer4)	.27	.22	.86	.50	.59	1.15
(213, ASM1D4)	.27	.24	.86	.53	.59	1.16
(214, ASM2D4)	.25	.25	.88	.51	.63	1.18
(215, ASMM4)	.26	.27	.87	.55	.60	1.21
(216, ASMS4)	.06	.29	.32	.38	.26	.71
(217, ASMN4)	.27	.22	.86	.50	.60	1.16
(218, ASMX4)	.24	.33	.79	.59	.53	1.20
(219, ASMR4)	.06	.30	.33	.39	.27	.73
(220, EntHor4)	.20	.40	.77	.63	.57	1.29
(221, EntVer4)	.21	.31	.90	.55	.71	1.36
(222, Ent1D4)	.21	.31	.87	.55	.68	1.31
(223, Ent2D4)	.18	.32	.89	.54	.75	1.36
(224, EntM4)	.20	.34	.88	.58	.70	1.37
(225, EntS4)	.09	.01	.37	.11	.30	.42
(226, EntN4)	.20	.40	.77	.63	.57	1.29
(227, EntX4)	.21	.31	.90	.55	.71	1.37
(228, EntR4)	.10	.01	.39	.12	.30	.44

FISHER DISTANCE BETWEEN PAIRS OF CLASSES FOR SINGLE FEATURES EXTRACTED FROM VISUAL DIFFERENCE HISTOGRAMS, DISTANCE 8

FEATURE	FISHER DISTANCE BETWEEN CLASSES					
(Number, Name)	Low, Mix	Low, Ci	Low, Cb	Mix, Ci	Mix, Cb	Ci, Cb
(229, MeanHor8)	.25	.31	.86	.58	.61	1.25
(230, MeanVer8)	.25	.32	.99	.61	.73	1.43
(231, Mean1D8)	.21	.34	.89	.59	.70	1.38
(232, Mean2D8)	.22	.32	.97	.62	.76	1.47
(233, MeanM8)	.24	.35	.98	.62	.74	1.47
(234, MeanS8)	.16	.26	.70	.45	.56	1.03
(235, MeanN8)	.24	.32	.86	.59	.61	1.26
(236, MeanX8)	.24	.32	.96	.59	.73	1.40
(237, MeanR8)	.17	.24	.71	.44	.55	1.01
(238, ConHor8)	.16	.41	.76	.57	.60	1.14
(239, ConVer8)	.19	.41	.97	.62	.78	1.41
(240, Con1D8)	.14	.43	.87	.59	.74	1.35
(241, Con2D8)	.15	.47	.93	.64	.80	1.41
(242, ConM8)	.17	.45	.94	.63	.79	1.42
(243, ConS8)	.15	.37	.83	.55	.70	1.23
(244, ConN8)	.16	.41	.76	.57	.61	1.14
(245, ConX8)	.18	.42	.95	.61	.78	1.39
(246, ConR8)	.16	.36	.84	.54	.70	1.22
(247, ASMHor8)	.32	.16	.91	.50	.55	1.13
(248, ASMVer8)	.29	.16	.85	.46	.55	1.04
(249, ASM1D8)	.28	.18	.81	.48	.53	1.03
(250, ASM2D8)	.28	.17	.86	.46	.58	1.10
(251, ASMM8)	.30	.17	.88	.49	.57	1.11
(252, ASMS8)	.15	.07	.40	.24	.24	.51
(253, ASMN8)	.28	.15	.83	.44	.55	1.02
(254, ASMX8)	.32	.17	.91	.55	.55	1.14
(255, ASMR8)	.15	.08	.39	.25	.24	.53
(256, EntHor8)	.26	.26	.88	.55	.61	1.26
(257, EntVer8)	.26	.26	.96	.55	.70	1.37
(258, Ent1D8)	.23	.27	.89	.54	.67	1.32
(259, Ent2D8)	.23	.28	.94	.55	.72	1.39
(260, EntM8)	.25	.27	.95	.56	.70	1.38
(261, EntS8)	.05	.08	.26	.14	.23	.37
(262, EntN8)	.26	.26	.88	.55	.61	1.27
(263, EntX8)	.25	.25	.94	.53	.70	1.34
(264, EntR8)	.05	.07	.27	.14	.23	.37

FISHER DISTANCE BETWEEN PAIRS OF CLASSES FOR SINGLE FEATURES EXTRACTED FROM INFRARED DIFFERENCE HISTOGRAMS, DISTANCE 1

FEATURE	FISHER DISTANCE BETWEEN CLASSES					
(Number, Name)	Low, Mix	Low, Ci	Low, Cb	Mix, Ci	Mix, Cb	Ci, Cb
(321, MeanHor)	.78	.91	1.67	.13	.63	.48
(322, MeanVer)	.94	1.14	2.00	.31	.83	.42
(323, Mean1D)	.96	1.15	2.03	.32	.79	.36
(324, Mean2D)	.93	1.14	2.00	.29	.84	.46
(325, MeanM)	.95	1.14	2.01	.30	.81	.42
(326, MeanS)	.93	1.16	2.00	.35	.85	.38
(327, MeanN)	.78	.91	1.67	.13	.63	.48
(328, MeanX)	.95	1.16	2.02	.32	.79	.37
(329, MeanR)	.94	1.17	2.01	.36	.81	.33
(330, ConHor)	.90	.95	1.73	.27	.65	.26
(331, ConVer)	.95	1.09	1.66	.35	.81	.40
(332, Con1D)	.96	1.09	1.66	.37	.77	.32
(333, Con2D)	.94	1.07	1.67	.33	.83	.44
(334, ConM)	.95	1.09	1.67	.35	.81	.38
(335, ConS)	.95	1.09	1.66	.36	.81	.38
(336, ConN)	.90	.95	1.73	.27	.65	.26
(337, ConX)	.95	1.09	1.68	.36	.78	.33
(338, ConR)	.95	1.09	1.67	.37	.79	.33
(339, ASMHor)	.69	.77	1.54	.01	.60	.68
(340, ASMVer)	.83	1.13	2.21	.22	.79	.51
(341, ASM1D)	.86	1.15	2.25	.23	.76	.47
(342, ASM2D)	.82	1.13	2.19	.23	.80	.52
(343, ASMM)	.83	1.07	2.08	.15	.75	.59
(344, ASMS)	.18	.12	.51	.30	.29	.65
(345, ASMN)	.84	1.16	2.20	.24	.76	.47
(346, ASMX)	.69	.77	1.54	.01	.60	.68
(347, ASMR)	.18	.14	.52	.31	.30	.68
(348, EntHor)	.95	1.23	2.12	.17	.69	.52
(349, EntVer)	.99	1.29	2.47	.27	.84	.48
(350, Ent1D)	1.01	1.32	2.51	.28	.81	.42
(351, Ent2D)	.98	1.29	2.46	.27	.85	.50
(352, EntM)	1.00	1.31	2.46	.26	.81	.48
(353, EntS)	.77	1.11	2.00	.36	.79	.25
(354, EntN)	.95	1.23	2.12	.17	.69	.52
(355, EntX)	1.00	1.34	2.47	.29	.80	.42
(356, EntR)	.80	1.19	2.00	.40	.73	.16

FISHER DISTANCE BETWEEN PAIRS OF CLASSES FOR SINGLE FEATURES EXTRACTED FROM INFRARED DIFFERENCE HISTOGRAMS, DISTANCE 2

FEATURE	FISHER DISTANCE BETWEEN CLASSES					
(Number, Name)	Low, Mix	Low, Ci	Low, Cb	Mix, Ci	Mix, Cb	Ci, Cb
(357, MeanHor2)	.84	1.00	1.77	.16	.64	.45
(358, MeanVer2)	.96	1.16	1.96	.33	.75	.30
(359, Mean1D2)	.98	1.15	1.99	.33	.71	.24
(360, Mean2D2)	.94	1.15	1.96	.32	.78	.36
(361, MeanM2)	.96	1.16	1.99	.32	.75	.31
(362, MeanS2)	.93	1.15	1.86	.38	.74	.22
(363, MeanN2)	.84	1.00	1.77	.16	.64	.45
(364, MeanX2)	.97	1.17	1.98	.34	.71	.25
(365, MeanR2)	.94	1.16	1.86	.38	.70	.18
(366, ConHor2)	.85	.99	1.58	.17	.60	.41
(367, ConVer2)	.94	1.04	1.52	.37	.72	.27
(368, Con1D2)	.94	1.02	1.51	.37	.67	.20
(369, Con2D2)	.93	1.03	1.52	.35	.75	.33
(370, ConM2)	.94	1.03	1.53	.36	.72	.27
(371, ConS2)	.94	1.03	1.49	.39	.70	.23
(372, ConN2)	.85	.99	1.58	.17	.60	.41
(373, ConX2)	.94	1.03	1.53	.37	.68	.22
(374, ConR2)	.93	1.02	1.50	.38	.68	.20
(375, ASMHor2)	.80	1.03	1.96	.17	.68	.49
(376, ASMVer2)	.83	1.12	2.09	.23	.74	.46
(377, ASM1D2)	.85	1.14	2.12	.22	.71	.43
(378, ASM2D2)	.81	1.12	2.10	.23	.76	.48
(379, ASMM2)	.85	1.14	2.16	.21	.73	.48
(380, ASMS2)	.09	.07	.44	.02	.37	.41
(381, ASMN2)	.83	1.16	2.09	.24	.71	.43
(382, ASMX2)	.80	1.03	1.96	.17	.68	.49
(383, ASMR2)	.09	.06	.47	.03	.41	.45
(384, EntHor2)	.92	1.19	2.14	.18	.68	.48
(385, EntVer2)	.99	1.30	2.41	.29	.79	.39
(386, Ent1D2)	1.02	1.32	2.44	.28	.75	.35
(387, Ent2D2)	.97	1.30	2.42	.29	.81	.44
(388, EntM2)	1.00	1.32	2.45	.27	.77	.42
(389, EntS2)	.74	1.07	1.48	.37	.56	.08
(390, EntN2)	.92	1.19	2.14	.18	.68	.48
(391, EntX2)	1.01	1.36	2.41	.30	.75	.35
(392, EntR2)	.77	1.14	1.49	.39	.51	.01

FISHER DISTANCE BETWEEN PAIRS OF CLASSES FOR SINGLE FEATURES EXTRACTED FROM INFRARED DIFFERENCE HISTOGRAMS, DISTANCE 4

FEATURE	FISHER DISTANCE BETWEEN CLASSES					
(Number, Name)	Low, Mix	Low, Ci	Low, Cb	Mix, Ci	Mix, Cb	Ci, Cb
(393, MeanHor4)	.91	1.10	1.91	.20	.64	.40
(394, MeanVer4)	.98	1.22	1.95	.33	.70	.28
(395, Mean1D4)	.98	1.15	1.94	.32	.67	.23
(396, Mean2D4)	.95	1.20	1.95	.33	.76	.33
(397, MeanM4)	.99	1.20	1.99	.32	.71	.30
(398, MeanS4)	.91	1.16	1.70	.39	.66	.17
(399, MeanN4)	.92	1.12	1.92	.20	.64	.40
(400, MeanX4)	.98	1.22	1.95	.33	.70	.28
(401, MeanR4)	.91	1.17	1.71	.38	.67	.20
(402, ConHor4)	.88	1.01	1.64	.19	.59	.36
(403, ConVer4)	.94	1.05	1.47	.36	.68	.26
(404, Con1D4)	.93	1.00	1.46	.36	.64	.19
(405, Con2D4)	.93	1.03	1.49	.35	.73	.31
(406, ConM4)	.95	1.04	1.51	.35	.69	.26
(407, ConS4)	.91	1.03	1.40	.39	.66	.22
(408, ConN4)	.88	1.01	1.64	.19	.59	.36
(409, ConX4)	.94	1.06	1.47	.36	.68	.26
(410, ConR4)	.91	1.04	1.40	.38	.67	.24
(411, ASMHor4)	.81	1.09	1.98	.20	.68	.46
(412, ASMVer4)	.83	1.14	1.96	.23	.68	.42
(413, ASM1D4)	.85	1.11	2.01	.20	.68	.43
(414, ASM2D4)	.82	1.18	2.05	.26	.73	.45
(415, ASMM4)	.85	1.16	2.08	.22	.71	.45
(416, ASMS4)	.12	.16	.07	.04	.25	.32
(417, ASMN4)	.82	1.13	1.98	.23	.68	.42
(418, ASMX4)	.83	1.11	2.02	.20	.68	.46
(419, ASMR4)	.12	.14	.02	.02	.27	.31
(420, EntHor4)	.97	1.30	2.29	.21	.68	.44
(421, EntVer4)	1.02	1.37	2.36	.29	.74	.38
(422, Ent1D4)	1.03	1.31	2.38	.27	.72	.35
(423, Ent2D4)	.98	1.36	2.39	.30	.79	.42
(424, EntM4)	1.02	1.37	2.44	.27	.75	.40
(425, EntS4)	.70	1.00	1.27	.34	.47	.06
(426, EntN4)	.99	1.31	2.31	.21	.68	.44
(427, EntX4)	1.02	1.37	2.37	.29	.74	.37
(428, EntR4)	.71	.97	1.29	.32	.48	.08

FISHER DISTANCE BETWEEN PAIRS OF CLASSES FOR SINGLE FEATURES EXTRACTED FROM INFRARED DIFFERENCE HISTOGRAMS, DISTANCE 8

FEATURE	FISHER DISTANCE BETWEEN CLASSES					
(Number, Name)	Low, Mix	Low, Ci	Low, Cb	Mix, Ci	Mix, Cb	Ci, Cb
(429, MeanHor8)	1.03	1.29	2.14	.27	.62	.28
(430, MeanVer8)	.99	1.27	1.95	.32	.70	.32
(431, Mean1D8)	.99	1.22	1.93	.31	.66	.26
(432, Mean2D8)	.99	1.31	1.94	.33	.74	.35
(433, MeanM8)	1.02	1.31	2.03	.32	.71	.32
(434, MeanS8)	.81	1.03	1.50	.32	.62	.24
(435, MeanN8)	1.04	1.27	2.13	.26	.62	.28
(436, MeanX8)	.99	1.29	1.94	.34	.71	.30
(437, MeanR8)	.80	1.02	1.48	.33	.64	.25
(438, ConHor8)	.93	1.05	1.72	.25	.57	.24
(439, ConVer8)	.93	1.08	1.47	.33	.68	.32
(440, Con1D8)	.91	1.03	1.44	.33	.63	.25
(441, Con2D8)	.95	1.10	1.46	.34	.71	.35
(442, ConM8)	.95	1.11	1.53	.34	.69	.31
(443, ConS8)	.84	1.00	1.30	.35	.66	.29
(444, ConN8)	.93	1.03	1.72	.25	.57	.24
(445, ConX8)	.93	1.10	1.47	.36	.69	.30
(446, ConR8)	.84	1.01	1.29	.36	.67	.29
(447, ASMHor8)	.96	1.41	2.31	.27	.66	.37
(448, ASMVer8)	.80	1.08	1.81	.21	.65	.42
(449, ASM1D8)	.84	1.12	1.84	.21	.62	.39
(450, ASM2D8)	.81	1.15	1.92	.24	.68	.42
(451, ASMM8)	.86	1.21	2.01	.24	.66	.41
(452, ASMS8)	.11	.23	.34	.17	.32	.13
(453, ASMN8)	.81	1.10	1.85	.22	.65	.41
(454, ASMX8)	.96	1.40	2.29	.26	.66	.38
(455, ASMR8)	.13	.26	.36	.18	.32	.11
(456, EntHor8)	1.13	1.59	2.69	.28	.67	.35
(457, EntVer8)	1.03	1.39	2.38	.27	.74	.41
(458, Ent1D8)	1.05	1.38	2.32	.27	.70	.36
(459, Ent2D8)	1.01	1.43	2.38	.30	.76	.41
(460, EntM8)	1.07	1.47	2.49	.28	.73	.40
(461, EntS8)	.49	.58	.91	.16	.41	.17
(462, EntN8)	1.13	1.56	2.66	.27	.67	.36
(463, EntX8)	1.04	1.42	2.41	.29	.74	.39
(464, EntR8)	.49	.58	.92	.16	.42	.18

AD-A033 037 MARYLAND UNIV COLLEGE PARK COMPUTER SCIENCE CENTER F/G 4/2
CLOUD PATTERN CLASSIFICATION FROM VISIBLE AND INFRARED DATA.(U)
FEB 76 J PARIKH F44620-72-C-0062
UNCLASSIFIED TR-442 AFOSR-TR-76-1137 NL

2 OF 2
AD
A033037

END
DATE
FILMED
1-77

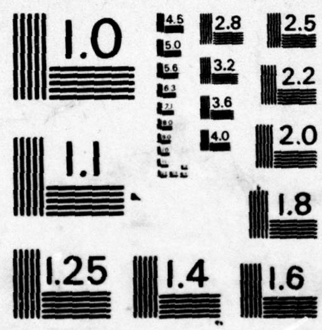

MICROCOPY RESOLUTION TEST CHART
NATIONAL BUREAU OF STANDARDS-1963-A

EXPERIMENT NUMBER	FEATURE SELECTION Level	Feature (Number, Name)	PERCENTAGE OF SAMPLES CORRECTLY CLASSIFIED Low	Mix	Ci	Cb	Total
1	1	(108, CF50)	55.8	57.5	0.0	47.8	49.4
2	1	(113, CF100)	39.5	64.4	0.0	84.8	53.1
3	1	(114, R0-100)	41.9	66.7	0.0	73.9	52.7
4	1	(115, R10-90)	62.8	54.0	0.0	58.7	52.7
5	1	(116, R0-50)	72.1	37.9	0.0	50.0	48.6
6	1	(117, R50-100)	40.7	71.3	0.0	37.0	46.9
7	1	(118, R20-80)	68.6	50.6	0.0	50.0	51.9

DECISION LOGIC

STRUCTURE: Tree 1

LEVEL 1:

CLASSIFIER: Maximum Likelihood
TRAINING SETS: Low, Mix, Cirrus, Cumulonimbus

Table 28. Maximum Likelihood Single-Level Classification for Single Features Extracted from Visual Brightness Histograms.

EXPERIMENT NUMBER	FEATURE SELECTION Level	Feature (Number, Name)	PERCENTAGE OF SAMPLES CORRECTLY CLASSIFIED Low	Mix	Ci	Cb	Total
1	1	(121, MeanHor)	68.6	31.0	0.0	41.3	43.2
2	1	(122, MeanVer)	45.4	55.2	0.0	47.8	44.9
3	1	(123, Mean1D)	53.5	49.4	0.0	47.8	45.7
4	1	(124, Mean2D)	43.0	58.6	0.0	54.4	46.5
5	1	(139, ASMHor)	37.2	43.7	29.2	41.3	39.5
6	1	(140, ASMVer)	38.4	46.0	4.2	78.3	45.3
7	1	(141, ASM1D)	39.5	47.1	4.2	80.4	46.5
8	1	(142, ASM2D)	38.4	44.8	4.2	76.1	44.4
9	1	(148, EntHor)	51.2	46.0	0.0	45.7	43.2
10	1	(149, EntVer)	36.1	59.8	0.0	63.0	46.1
11	1	(150, Ent1D)	39.5	54.0	0.0	63.0	45.3
12	1	(151, Ent2D)	37.2	59.8	0.0	63.0	46.5

DECISION LOGIC

STRUCTURE: Tree 1

LEVEL 1:

CLASSIFIER: Maximum Likelihood
TRAINING SETS: Low, Mix, Cirrus, Cumulonimbus

Table 29. Maximum Likelihood Single-Level Classification for Single Features Extracted from Visual Difference Histograms.

EXPERIMENT NUMBER	FEATURE SELECTION Level	Feature (Number, Name)	PERCENTAGE OF SAMPLES CORRECTLY CLASSIFIED Low	Mix	Ci	Cb	Total
1	1	(302, StDev)	95.4	72.4	0.0	58.7	70.8
2	1	(303, CF0)	95.4	71.3	0.0	73.9	73.3
3	1	(308, CF50)	87.2	41.4	12.5	54.4	57.2
4	1	(314, R0-100)	95.4	70.1	0.0	76.1	73.3
5	1	(315, R10-90)	97.7	66.7	0.0	58.7	69.6
6	1	(316, R0-50)	96.5	77.0	0.0	45.7	70.4
7	1	(317, R50-100)	89.5	51.7	0.0	52.2	60.1
8	1	(318, R20-80)	94.2	62.1	0.0	50.0	65.0
9	1	(465, MaxR10-90)	95.4	69.0	0.0	56.5	69.1
10	1	(466, RanR10-90)	95.4	65.5	0.0	28.3	62.6
11	1	(467, MinCF0)	95.4	71.3	0.0	73.9	73.3
12	1	(468, RanCF0)	95.4	70.1	0.0	30.4	64.6
13	1	(469, MaxStDev)	95.4	72.4	0.0	58.7	70.8
14	1	(470, RanStDev)	95.4	65.5	0.0	32.6	63.4

DECISION LOGIC

STRUCTURE: Tree 1

LEVEL 1:

CLASSIFIER: Maximum Likelihood
TRAINING SETS: Low, Mix, Cirrus, Cumulonimbus

Table 30. Maximum Likelihood Single-Level Classification for Single Features Extracted from Infrared Temperature Histograms.

EXPERIMENT NUMBER	FEATURE SELECTION Level	Feature (Number, Name)	PERCENTAGE OF SAMPLES CORRECTLY CLASSIFIED Low	Mix	Ci	Cb	Total
1	1	(321, MeanHor)	96.5	56.3	0.0	52.2	64.2
2	1	(322, MeanVer)	94.2	59.8	0.0	56.5	65.4
3	1	(323, Mean1D)	95.4	59.8	0.0	56.5	65.8
4	1	(324, Mean2D)	93.0	58.6	0.0	54.4	64.2
5	1	(339, ASMHor)	94.2	46.0	0.0	63.0	61.7
6	1	(340, ASMVer)	87.2	47.1	0.0	78.3	62.6
7	1	(341, ASM1D)	89.5	49.4	0.0	80.4	64.2
8	1	(342, ASM2D)	87.2	47.1	0.0	80.4	63.0
9	1	(348, EntHor)	96.5	54.0	0.0	60.9	65.0
10	1	(349, EntVer)	93.0	59.8	0.0	73.9	68.3
11	1	(350, Ent1D)	93.0	59.8	0.0	73.9	68.3
12	1	(351, Ent2D)	91.9	59.8	0.0	73.9	67.9

DECISION LOGIC

STRUCTURE: Tree 1

LEVEL 1:

CLASSIFIER: Maximum Likelihood
TRAINING SETS: Low, Mix, Cirrus, Cumulonimbus

Table 31. Maximum Likelihood Single-Level Classification for Single Features Extracted from Infrared Difference Histograms.

EXPERIMENT NUMBER	Level	FEATURE SELECTION Features (Number, Name)	PERCENTAGE OF SAMPLES CORRECTLY CLASSIFIED Low	Mix	Ci	Cb	TOTAL
1	1	(114, R0-100), (314, R0-100) (315, R10-90)	94.2	77.0	70.8	84.8	84.0
2	1	(114, R0-100), (314, R0-100) (350, EntlD)	95.4	74.7	75.0	84.8	84.0
3	1	(302, StDev), (303, CF0), (314, R0-100), (315, R10-90),	95.4	74.7	54.2	71.7	79.4
4	1	(114, R0-100), (303, CF0), (314, R0-100), (315, R10-90)	94.2	80.5	75.0	87.0	86.0
5	1	(114, R0-100), (302, StDev), (314, R0-100), (315, R10-90)	95.4	79.3	66.7	84.8	84.8
6	1	(114, R0-100), (302, StDev) (303, CF0), (315, R10-90)	96.5	79.3	75.0	87.0	86.4
7	1	(114, R0-100), (302, StDev), (303, CF0), (314, R0-100)	94.2	79.3	75.0	87.0	85.6

DECISION LOGIC

STRUCTURE: Tree 1

LEVEL 1:

CLASSIFIER: Maximum Likelihood
TRAINING SETS: Low, Mix, Cirrus, Cumulonimbus

Table 32. Maximum Likelihood Single-Level Classification for Selected Combinations of Three and Four Features.

EXPERIMENT NUMBER	FEATURE SELECTION Level	Features (Number, Name)	PERCENTAGE OF SAMPLES CORRECTLY CLASSIFIED Low	Mix	Ci	Cb	Total
1	1	(114, R0-100), (302, StDev), (303, CF0), (314, R0-100), (315, R10-90)	94.2	82.8	66.7	87.0	86.0
2	1	(114, R0-100), (303, CF0), (314, R0-100), (315, R10-90), (469, MaxStDev)	94.2	80.5	70.8	89.1	86.0
3	1	(113, CF100), (114, R0-100), (303, CF0), (314, R0-100), (315, R10-90)	94.2	79.3	79.2	89.1	86.4
4	1	(142, ASM2D), (323, Mean1D) (341, ASM1D), (350, Ent1D), (351, Ent2D)	96.5	65.5	54.2	82.6	78.6
5	1	(141, ASM1D), (151, Ent2D), (324, Mean2D), (342, ASM2D), (351, Ent2D)	98.8	65.5	62.5	84.8	80.7
6	1	(114, R0-100), (314, R0-100), (323, Mean1D), (341, ASM1D), (350, Ent1D)	95.4	78.2	70.8	4.4	69.6
7	1	(114, R0-100), (302, CF0), (314, R0-100), (315, R10-90), (350, Ent1D)	96.5	80.5	66.7	93.5	87.2
8	1	(113, CF100), (114, R0-100), (303, CF0), (315, R10-90), (350, Ent1D)	98.8	79.3	83.3	87.0	88.1
9	1	(302, StDev), (303, CF0), (314, R0-100), (315, R10-90), (350, Ent1D)	96.5	73.6	54.2	73.9	79.8

DECISION LOGIC

STRUCTURE: Tree 1

LEVEL 1:

CLASSIFIER: Maximum Likelihood
TRAINING SETS: Low, Mix, Cirrus, Cumulonimbus

Table 33. Maximum Likelihood Single-Level Classification for Selected Combinations of Five Features.

EXPERIMENT NUMBER	FEATURE SELECTION Level	Features (Number, Name)	PERCENTAGE OF SAMPLES CORRECTLY CLASSIFIED Low	Mix	Ci	Cb	Total
1	1	(114, R0-100), (115, R10-90), (302, StDev), (303, CF0), (314, R0-100), (315, R10-90)	94.2	81.6	79.2	89.1	87.2
2	1	(113, R0-100), (114, R0-100), (303, CF0), (314, R0-100), (315, R10-90), (350, Ent1D)	97.7	79.3	75.0	93.5	88.1
3	1	(114, R0-100), (302, StDev), (303, CF0), (314, R0-100), (315, R10-90), (35D, Ent1D)	95.4	81.6	66.7	89.1	86.4
4	1	(114, R0-100), (302, StDev) (303, CF0), (314, R0-100), (315, R10-90), (324, Mean2D)	94.2	81.6	66.7	84.8	85.2
5	1	(114, R0-100), (302, StDev), (303, CF0), (314, R0-100), (315, R10-90), (317, R50-100)	95.4	80.5	79.2	84.8	86.4
6	1	(114, R0-100), (302, StDev), (303, CF0), (314, R0-100), (315, R10-90), (469, MaxStDev)	94.2	81.6	70.8	84.8	85.6

DECISION LOGIC

STRUCTURE: Tree 1

LEVEL 1:

CLASSIFIER: Maximum Likelihood
TRAINING SETS: Low, Mix, Cirrus, Cumulonimbus

Table 34. Maximum Likelihood Single-Level Classification for Selected Combinations of Six Features.

EXPERIMENT NUMBER	FEATURE SELECTION Level	Features (Number, Name)	PERCENTAGE OF SAMPLES CORRECTLY CLASSIFIED Low	Mix	Ci	Cb	Total
1	1	(114, R0-100), (115, R10-90), (302, StDev), (303, CF0), (314, R0-100), (315, R10-90), (350, Ent1D)	94.2	83.9	79.2	93.5	88.9
2	1	(113, CF0), (114, R0-100), (303, CF0), (314, R0-100), (315, R10-90), (350, Ent1D), (351, Ent2D)	97.7	82.8	79.2	93.5	89.7
3	1	(114, R0-100), (115, R10-90), (302, StDev), (303, CF0), (314, R0-100), (315, R10-90), (317, R50-100)	94.2	82.8	79.2	87.0	87.2

DECISION LOGIC

STRUCTURE: Tree 1

LEVEL 1:

CLASSIFIER: Maximum Likelihood
TRAINING SETS: Low, Mix, Cirrus, Cumulonimbus

Table 35. Maximum Likelihood Single-Level Classification for Selected Combinations of Seven Features.

EXPERIMENT NUMBER	FEATURE SELECTION Level	Features (Number, Name)	PERCENTAGE OF SAMPLES CORRECTLY CLASSIFIED Low	Mix	Ci	Cb	Total
1	1	(114, R0-100), (115, R10-90), (302, StDev), (303, CF0), (314, R0-100), (315, R10-90), (350, Ent1D)	94.2	90.8	79.2	93.5	91.4
	2	(302, StDev), (465, MaxR10-90) (466, RanR10-90), (467, MinCF0), (468, RanCF0), (469, MaxStDev)					
2	1	(114, R0-100), (115, R10-90), (302, StDev), (303, CF0), (314, R0-100), (315, R10-90), (350, Ent1D)	94.2	89.7	79.2	93.5	91.0
	2	(303, R0-100) (315, R10-90), (317, R50-100), (467, MinCF0), (468, RanCF0), (469, MaxStDev)					
3	1	(114, R0-100), (115, R10-90), (302, StDev), (303, CF0), (314, R0-100), (315, R10-90), (350, Ent1D)	94.2	85.1	79.2	93.5	89.3
	2	(114, R0-100), (115, R10-90), (302, StDev), (303, CF0), (314, R0-100), (315, R10-90), (317, R50-100)					
4	1	(114, R0-100), (302, StDev), (303, CF0), (314, R0-100), (315, R10-90)	94.2	89.7	66.7	87.0	88.5
	2	(302, StDev), (465, MaxR10-90), (466, RanR10-90), (467, MinCF0), (468, RanCF0), (469, MaxStDev)					

DECISION LOGIC

STRUCTURE: TREE 2

LEVEL 1:

CLASSIFIER: Maximum Likelihood
TRAINING SETS: Low, Mix, Cirrus, Cumulonimbus

LEVEL 2:

CLASSIFIER: Maximum Likelihood
TRAINING SETS: Low, Mix

Table 36. Maximum Likelihood Two-Level Classification Designed to Reduce Confusion of Mix With Low Samples.

EXPERIMENT NUMBER	FEATURE SELECTION Level	Features (Number, Name)	PERCENTAGE OF SAMPLES CORRECTLY CLASSIFIED Low	Mix	Ci	Cb	Total
1	1	(114, R0-100), (302, StDev), (303, CF0), (314, R0-100), (315, R10-90)	94.2	69.0	75.0	82.6	81.1
	2.1	(114, R0-100), (302, StDev), (303, CF0), (314, R0-100), (315, R10-90)					
	2.2	(114, R0-100), (302, StDev), (303, CF0), (314, R0-100), (315, R10-90)					
2	1	(113, CF100), (114, R0-100), (314, R0-100), (315, R10-90), (350, Ent1D)	94.2	64.4	62.5	87.0	79.0
	2.1	(302, StDev), (465, MaxR10-90), (466, RanR10-90), (467, MinCF0), (468, RanCF0), (469, MaxStDev)					
	2.2	(113, CF100), (114, R0-100)					
3	1	(114, R0-100), (115, R10-90), (302, StDev), (303, CF0), (314, R0-100), (315, R10-90), (351, Ent2D)	94.2	71.3	75.0	87.0	82.7
	2.1	(302, StDev), (465, MaxR10-90), (466, RanR10-90), (467, MinCF0), (468, RanCF0), (469, MaxStDev)					
	2.2	(113, CF100)					

DECISION LOGIC

STRUCTURE: Tree 3

LEVEL 1:

CLASSIFIER: Maximum Likelihood
TRAINING SETS: Set of Mix and Low Samples, Set of Cirrus and Cumulonimbus Samples

LEVEL 2.1:

CLASSIFIER: Maximum Likelihood
TRAINING SETS: Mix, Low

LEVEL 2.2:

CLASSIFIER: Maximum Likelihood
TRAINING SETS: Cirrus, Cumulonimbus

Table 37. Maximum Likelihood Two-Level Classification Grouping Mix and Low Samples into One Class and Cirrus and Cumulonimbus Samples into a Second Class.

EXPERIMENT NUMBER	Level	FEATURE SELECTION Features (Number, Name)	PERCENTAGE OF SAMPLES CORRECTLY CLASSIFIED Low	Mix	Ci	Cb	Total
1	1	(114, R0-100), (302, StDev), (303, CF0), (314, R0-100), (315, R10-90)	95.4	73.6	66.7	91.3	84.0
	2	(114, R0-100), (302, StDev), (303, CF0), (314, R0-100), (315, R10-90)					
	3	(114, R0-100), (302, StDev), (303, CF0), (314, R0-100), (315, R10-90)					
2	1	(302, StDev), (465, MaxR10-90), (466, RanR10-90), (467, MinCF0), (468, RanCF0), (469, MaxStDev)	94.2	58.6	66.7	80.4	76.1
	2	(302, StDev), (314, R0-100),					
	3	(113, CF100), (114, R0-100)					
3	1	(114, R0-100), (115, R10-90), (302, StDev), (303, CF0), (314, R0-100), (315, R10-90), (350, Ent1D)	76.7	83.9	66.7	93.5	81.5
	2	(302, StDev), (314, R0-100),					
	3	(113, CF100), (114, R0-100)					

DECISION LOGIC

STRUCTURE: Tree 4

LEVEL 1:

CLASSIFIER: Maximum Likelihood
TRAINING SETS: Mix, Set of Cirrus, Cumulonimbus, and Low Samples

LEVEL 2:

CLASSIFIER: Maximum Likelihood
TRAINING SETS: Low, Set of Cirrus and Cumulonimbus Samples

LEVEL 3:

CLASSIFIER: Maximum Likelihood
TRAINING SETS: Cirrus, Cumulonimbus

Table 38. Maximum Likelihood Three-Level Classificcation Designed to Separate Mix Samples at Level 1 of the Decision Tree.

EXPERIMENT NUMBER	Level	FEATURE SELECTION Features (Number, Name)	PERCENTAGE OF SAMPLES CORRECTLY CLASSIFIED Low	Mix	Ci	Cb	Total
1	1	(114, R0-100), (302, StDev), (303, CF0), (314, R0-100), (315, R10-90)	96.5	77.0	66.7	82.6	84.0
	2	(114, R0-100), (302, StDev), (303, CF0), (314, R0-100), (315, R10-90)					
	3	(114, R0-100), (302, StDev), (303, CF0), (314, R0-100), (315, R10-90)					
2	1	(113, CF100), (114, R0-100), (302, StDev), (303, CF0), (314, R0-100), (315, R10-90), (351, Ent2D)	96.5	75.9	70.8	84.8	84.4
	2	(113, CF100), (114, R0-100), (302, StDev), (303, CF0), (314, R0-100), (315, R10-90), (351, Ent1D)					
	3	(113, CF100), (114, R0-100)					
3	1	(302, StDev), (465, MaxR10-90), (466, RanR10-90), (467, MinCF0), (468, RanCF0), (469, MaxStDev)	94.2	80.5	66.7	87.0	85.2
	2	(114, R0-100), (115, R10-90), (302, StDev), (303, CF0), (314, R0-100), (315, R10-90), (351, Ent1D)					
	3	(113, CF100), (114, R0-100)					

DECISION LOGIC

STRUCTURE: Tree 5

LEVEL 1:

CLASSIFIER: Maximum Likelihood
TRAINING SETS: Low, Set of Mix, Cirrus, and Cumulonimbus Samples

LEVEL 2:

CLASSIFIER: Maximum Likelihood
TRAINING SETS: Mix, Set of Cirrus and Cumulonimbus Samples

LEVEL 3:

CLASSIFIER: Maximum Likelihood
TRAINING SETS: Cirrus, Cumulonimbus

Table 39. Maximum Likelihood Three-Level Classification Designed to Separate Mix Samples at Level 2 of the Decision Tree.

EXPERIMENT NUMBER	Level	FEATURE SELECTION Features (Number, Name)		PERCENTAGE OF SAMPLES CORRECTLY CLASSIFIED Low	Mix	Ci	Cb	Total
1	1	(114, R0-100), (303, CF0), (315, R10-90)	(302, StDev), (314, R0-100),	94.2	75.9	75.0	89.1	84.8
	2	(114, R0-100), (303, CF0), (315, R10-90)	(302, StDev), (314, R0-100),					
	3	(114, R0-100), (303, CF0), (315, R10-90)	(302, StDev), (314, R0-100),					
2	1	(114, R0-100), (303, CF0), (315, R10-90)	(302, StDev), (314, R0-100),	94.2	80.5	75.0	89.1	86.4
	2	(114, R0-100), (303, CF0), (315, R10-90)	(302, StDev), (314, R0-100),					
	3	(302, StDev), (466, RanR10-90), (468, RanCF0),	(465, MaxR10-90), (467, MinCF0), (469, MaxStDev)					
3	1	(114, R0-100), (303, CF0), (315, R10-90)	(302, StDev), (314, R0-100),	94.2	81.6	75.0	89.1	86.8
	2	(114, R0-100), (303, CF0), (350, EntlD)	(142, ASM2D), (314, R0-100),					
	3	(302, StDev), (466, RanR10-90), (468, RanCF0),	(465, MaxR10-90), (467, MinCF0), (469, MaxStDev)					

DECISION LOGIC

STRUCTURE: Tree 6

LEVEL 1:

CLASSIFIER: Maximum Likelihood
TRAINING SETS: Cumulonimbus, Set of Low, Mix, and Cirrus Samples

LEVEL 2:

CLASSIFIER: Maximum Likelihood
TRAINING SETS: Cirrus, Set of Low and Mix Samples

LEVEL 3:

CLASSIFIER: Maimum Likelihood
TRAINING SETS: Low, Mix

Table 40. Maximum Likelihood Three-Level Classification Designed to Separate Mix Samples at Level 3 of the Decision Tree.

EXPERIMENT NUMBER	Level	FEATURE SELECTION Features (Number, Name)	PERCENTAGE OF SAMPLES CORRECTLY CLASSIFIED Low	Ci	Cb	Total
1	1	(114, RO-100)	89.5	0.0	87.0	75.0
2	1	(314, RO-100)	98.8	50.0	89.1	88.5
3	1	(114, RO-100), (314, RO-100)	98.8	95.8	100.0	98.7
4	1	(113, CF100), (302, StDev)	100.0	91.7	100.0	98.7
5	1	(114, RO-100), (302, StDev), (303, CF0), (314, RO-100), (315, R10-90)	97.7	95.8	100.0	98.1

DECISION LOGIC

STRUCTURE: Tree 7

LEVEL 1:

CLASSIFIER: Maximum Likelihood
TRAINING SETS: Low, Cirrus, Cumulonimbus

Table 41. Maximum Likelihood Single-Level Classification for the Three-Class Problem.

EXPERIMENT NUMBER	FEATURE SELECTION Level	Features (Number, Name)		PERCENTAGE OF SAMPLES CORRECTLY CLASSIFIED Low	Ci	Cb	Total
1	1	(302, StDev)		100.0	91.7	100.0	98.7
	2	(113, CF100)					
2	1	(314, R0-100)		98.8	95.8	97.8	98.1
	2	(114, R0-100)					
3	1	(302, StDev)	(314, R0-100)	98.8	95.8	100.0	98.7
	2	(113, CF100),	(114, R0-100)				
4	1	(114, R0-100),	(302, StDev),	97.7	95.8	100.0	98.1
		(303, CF0),	(314, R0-100),				
		(315, R10-90)					
	2	(114, R0-100),	(302, StDev),				
		(303, CF0),	(314, R0-100)				
		(315, R10-90)					

DECISION LOGIC

STRUCTURE: Tree 8

LEVEL 1:

CLASSIFIER: Maximum Likelihood
TRAINING SETS: Low, Set of Cirrus and Cumulonimbus Samples

LEVEL 2:

CLASSIFIER: Maximum Likelihood
TRAINING SETS: Cirrus, Cumulonimbus

Table 42. Maximum Likelihood Two-Level Classification for the Three Class Problem.

EXPERIMENT NUMBER	DECISION LOGIC Structure	Level	Classifier	Training Sets	PERCENTAGE OF SAMPLES CORRECTLY CLASSIFIED Low	Mix	Ci	Cb	Total
1	Tree 1	1	Multiclass Voting	Low, Mix, Ci, Cb	97.7	60.9	87.5	91.3	82.3
2	Tree 6	1	Multiclass Voting	Cb, Ci + Low + Mix	97.7	46.0	100.0	95.7	79.0
		2	Multiclass Voting	Ci, Low + Mix					
		3	Multiclass Voting	Low, Mix					
3	Tree 7	1	Multiclass Voting	Low, Ci, Cb	98.8		95.8	97.8	98.1
4	Tree 8	1	Multiclass Voting	Low, Ci + Cb	98.8		95.8	95.7	97.4
		2	Multiclass Voting	Ci, Cb					
5	Tree 1	1	Multiclass One vs. Rest	Low, Mix, Ci, Cb	1.2	19.5	79.2	67.4	28.0
6	Tree 7	1	Multiclass One vs. Rest	Low, Ci, Cb	95.4		91.7	93.5	94.2
7	Tree 6	1	Fisher (Sample $P(w_i)$)	Cb, Ci + Low + Mix	97.7	73.6	62.5	87.0	83.5
		2	Fisher (Sample $P(w_i)$)	Ci, Low + Mix					
		3	Fisher (Sample $P(w_i)$)	Low, Mix					
8	Tree 8	1	Fisher (Sample $P(w_i)$)	Low, Ci + Cb	98.8		91.7	95.7	96.8
		2	Fisher (Sample $P(w_i)$)	Ci, Cb					

FEATURE SELECTION
LEVEL 1: (114, R0-100), (302, StDev), (303, CF0), (314, R0-100), (315, R10-90)
LEVEL 2: (114, R0-100), (302, StDev), (303, CF0), (314, R0-100), (315, R10-90)
LEVEL 3: (114, R0-100), (302, StDev), (303, CF0), (314, R0-100), (315, R10-90)

Table 43. Performance of Various Classifiers other than Maximum Likelihood on Selected Decision Trees Using a Standard Five-Feature Combination.

Appendix A

Feature Definitions

DEFINITIONS OF HISTOGRAMS CALCULATED FOR EACH SAMPLE AREA

I. Histograms of Reflectivity and Radiation Measurements

a) Visual Brightness Histogram (VB)

The visual brightness histogram represents the frequency distribution of reflected solar radiation measurements from the visual (.5 - .7μm) channel, coded in a 0-255 value range.

b) Infrared Temperature Histogram (IT)

The infrared temperature histogram represents the frequency distribution of long-wave radiation measurements from the infrared (10.5 - 12.5μm) channel converted to temperature values in the 160° Kelvin - 330° Kelvin range (assuming emissivity values of 1.0) and then shifted by -160° to a range of 0 - 170.

II. Histograms of Visual and Infrared Difference Measurements

a) Visual Difference Histogram for Direction "θ" and Distance "ρ" (VDθρ)

A visual difference histogram for direction "θ" and distance "ρ" represents the frequency distribution of absolute values of differences between pairs of brightness measurements from the visual observation array separated by "ρ" steps along an array line in the direction "θ". Directional values "θ" range over the set {Hor, Ver, 1D, 2D} where Hor (or "horizontal") denotes the East-West direction, Ver (or "vertical") the North-South direction, 1D (or "first diagonal") the Northwest-Southeast direction, and 2D (or "second

diagonal") the Northeast-Southwest direction. Distance values "ρ" range over the set {1, 2, 4, 8} with a distance of "1" specifying adjacent pairs of measurements, a distance of "2" specifying pairs of measurements separated by a single measurement, etc. A total of 16 visual difference histograms were calculated, for each of the 4x4 (direction, distance) pairs.

b) <u>Infrared Difference Histograms for Direction "θ" and Distance "ρ" (ID$\theta\rho$)</u>

An infrared difference histogram for direction "θ" and distance "ρ" represents the frequency distribution of absolute values of differences between pairs of rescaled temperature measurements from the infrared observation array separated by "ρ" steps along a line in the direction "θ". A total of 16 infrared difference histograms were calculated, just as for the visual differences.

Difference histograms for the simple illustrative examples of Figure A.1 are given in Table A.1. The difference histograms were used to derive texture features, as described in Section 3.1. The feature definitions are presented in Table A.2, and the feature numbering used is defined in Tables A.3-4.

Simplified Visual Observation

0	0	0	0	0	0	0	0	0	0
0	0	0	0	0	0	0	0	0	0
1	1	1	1	1	1	1	1	1	1
1	1	1	1	1	1	1	1	1	1
2	2	2	2	2	2	2	2	2	2
2	2	2	2	2	2	2	2	2	2
3	3	3	3	3	3	3	3	3	3
3	3	3	3	3	3	3	3	3	3
0	0	1	0	0	2	0	0	3	0
1	0	0	2	0	0	3	0	0	0

Simplified Infrared Observation

3	3	3	3	3	3	3	3	3	3
3	3	3	3	3	3	3	3	3	3
2	2	2	2	2	2	2	2	2	2
2	2	2	2	2	2	2	2	2	2
1	1	1	1	1	1	1	1	1	1
1	1	1	1	1	1	1	1	1	1
0	0	0	0	0	0	0	0	0	0
0	0	0	0	0	0	0	0	0	0
3	3	0	3	3	1	3	3	2	2
0	3	3	1	3	3	2	3	3	2

Figure A.1. Simplified Visual and Infrared Observation Matrices Used to Illustrate the Calculation of Sample Histograms.

Visual Histograms					Infrared Histograms				
Histogram (Name)	Frequency Distribution 0	1	2	3	Histogram (Name)	Frequency Distribution 0	1	2	3
VB	34	22	22	22	IT	22	22	24	32
VDHor1*	79	3	4	4	IDHor1*	80	3	4	3
VDVer1	45	33	3	9	IDVer1	45	33	4	8
VD1D1	43	30	1	7	ID1D1	44	30	2	5
VD2D1	41	29	3	8	ID2D1	39	31	3	8
VDHor2	70	3	4	3	IDHor2	68	5	4	3
VDVer2	2	62	2	14	IDVer2	2	62	4	12
VD1D2	2	50	1	11	ID1D2	1	50	4	9
VD2D2	1	50	2	11	ID2D2	2	50	1	11
VDHor4	53	2	3	2	IDHor4	52	4	2	2
VDVer4	2	4	54	0	IDVer4	2	6	52	0
VD1D4	1	2	33	0	ID1D4	1	4	31	0
VD2D4	2	2	32	0	ID2D4	2	2	32	0
VDHor8	18	1	0	1	IDHor8	16	3	0	1
VDVer8	14	2	2	2	IDVer8	12	4	2	2
VD1D8	3	0	0	1	ID1D8	1	3	0	0
VD2D8	3	1	0	0	ID2D8	3	0	0	1

*VDHor1 denotes a visual difference (VD) histogram for the "horizontal" direction and a distance of "1". IDHor1 denotes an infrared difference (ID) histogram for "horizontal" direction and a distance of "1". The other histogram names are interpreted similarly.

Table A.1. Sample Histograms Calculated from Simplified Visual and Infrared Observation Matrices of Figure A.1.

Feature Name: Abbreviation	Feature Name: Descriptive Name	Formula*
Mean	Mean Value of Data Measurements	$\text{Mean} = \dfrac{\sum_{i=0}^{255} i\, f(i)}{\sum_{i=0}^{255} f(i)}$
StDev	Standard Deviation of Data Measurements	$\text{StDev} = \sqrt{\dfrac{\sum_{i=0}^{255} f(i)\,(\text{Mean}-i)^2}{\sum_{i=0}^{255} f(i) - 1}}$
CF(α)	Interpolated Data Measurement for which Cumulative Frequency Percentage is (α)% where (α) = "0", "10", "20", "30", "40", "50", "60", "70", "80", "90", "100"	$CF(\alpha) = k + \dfrac{\dfrac{(\alpha)}{100} - \dfrac{\sum_{i=0}^{k} f(i)}{\sum_{i=0}^{255} f(i)}}{\dfrac{\sum_{i=0}^{h} f(k)}{\sum_{i=0}^{255} f(i)} - \dfrac{\sum_{i=0}^{k} f(i)}{\sum_{i=0}^{255} f(i)}}$ where $k = \underset{i\,\varepsilon\,[0,255]}{\text{Max}}\,[i]$ such that $100\,\dfrac{\sum_{i=0}^{k} f(i)}{\sum_{i=0}^{255} f(i)} < (\alpha)$ and $h = \underset{i\,\varepsilon\,[0,255]}{\text{Min}}\,[i]$ such that $f(h) \neq 0$ and $h > k$

*Frequency counts f(i) for value i appearing in the formulas correspond to frequency counts appearing in the histogram associated with a given feature number. See Table for corresponding feature numbers and feature histograms.

Table A.2. FEATURE DEFINITIONS

Abbreviation	Name	Formula
$R(\beta)-(\gamma)$	Range of Data Measurements between the Data Value with Cumulative Frequency Percentage (β)% and the Data Value with Cumulative Frequency Percentage (γ)% where (β)-(γ) = "0-100", "10-90", "0-50", "50-100", "20-80", "30-70", "40-60"	$R(\beta) - (\gamma) = CF(\gamma) - CF(\beta)$
$\text{Mean}(\theta)(\rho)$	Mean Difference Feature for Direction (θ) and Distance (ρ) where (θ) = "Hor", "Ver", "1D", "2D" and (ρ) = " ", "2", "4", "8"**	$\text{Mean }(\theta)(\rho) = \dfrac{\sum_{i=0}^{255} \dfrac{f(i)}{\sum_{i=0}^{255} f(i)}\, i}{256}$
$\text{Con}(\theta)(\rho)$	Contrast Difference Feature for Direction (θ) and Distance (ρ) where (θ) = "Hor", "Ver", "1D", "2D", and (ρ) = " ", "2", "4", "8"	$\text{Con}(\theta)(\rho) = \sum_{i=0}^{255} \dfrac{f(i)}{\sum_{i=0}^{255} f(i)}\, i^2$
$\text{ASM}(\theta)(\rho)$	Angular Second Moment Feature for Direction (θ) and Distance (ρ) where (θ) = "Hor", "Ver", "1D", "2D" and (ρ) = " ", "2", "4", "8"	$\text{ASM}(\theta)(\rho) = \sum_{i=0}^{255} \left(\dfrac{f(i)}{\sum_{i=0}^{255} f(i)} \right)^2$

**For textural features, the directions calculated for (θ) are horizontal, vertical, first diagonal, and second diagonal and the distances calculated for (ρ) are 1, 2, 4, and 8. For distances of 1 (or adjacent points), the number "1" is dropped or left blank. For example, the acronym MeanHor denotes a mean texture feature calculated for the horizontal direction and for a distance of 1.

Table A.2. FEATURE DEFINITIONS (CONTINUED)

Abbreviation	Name	Formula
$Ent(\theta)(\rho)$	Entropy Difference Feature for Direction (θ) and Distance (ρ) where (θ) = "Hor", "Ver", "1D", "2D", and (ρ) = " ", "2", "4", "8"	$Ent(\theta)(\rho) = -\sum_{i=0}^{255} \frac{f(i)}{\sum_{i=0}^{255} f(i)} \log_e \frac{f(i)}{\sum_{i=0}^{255} f(i)}$
$(\delta)\ M(\rho)$	Mean Value of the (δ) Difference Feature Averaged Over all Four Directions for a Given Distance (ρ) where (δ) = "Mean", "Con", "ASM", "Ent" and (ρ) = " ", "2", "4", "8"	$(\delta)\ M(\rho) = \frac{(\delta)Hor(\rho)+(\delta)Ver(\rho)+(\delta)1D(\rho)+(\delta)2D(\rho)}{4}$
$(\delta)S(\rho)$	Standard Deviation Value of the (δ) Difference Feature over all Four Directions for a Given Distance (ρ) where (δ) = "Mean", "Con", "ASM", "Ent" and (ρ) = " ", "2", "4", "8"	$(\delta)S(\rho) = \sqrt{\frac{\sum_{(\theta)\varepsilon(Hor,Ver,1D,2D)} ((\delta)(\theta)(\rho)-(\delta)M(\rho))^2}{4}}$
$(\delta)N(\rho)$	Minimum Value of the (δ) Difference Feature over all Four Directions for a Given Distance (ρ) where (δ) = "Mean", "Con", "ASM", "Ent" and (δ) = " ", "2", "4", "8"	$(\delta)N(\rho) = \underset{(\theta)}{Min}\ [(\delta)(\theta)(\rho)]$ where $(\theta)\ \varepsilon\ \{Hor,Ver,1D,2D\}$
$(\delta)X(\rho)$	Maximum Value of the (δ) Difference Feature over all Four Directions for a Given Distance (ρ) where (δ) = "Mean", "Con", "ASM", "Ent" and (ρ) = " ", "2", "4", "8"	$(\delta)X(\rho) = \underset{(\theta)}{Max}\ [(\delta)(\theta)(\rho)]$ where $(\theta)\ \varepsilon\ \{Hor,Ver,1D,2D\}$

Table A.2. FEATURE DEFINITIONS (CONTINUED)

Abbreviation	Name	Formula
$(\delta)R(\rho)$	Range of the (δ) Difference Value Features for all Four Directions and for a Given Distance (ρ) where (δ) = "Mean", "Con", "ASM", "Ent", and (ρ) = " ", "2", "4", "8"	$(\delta)R(\rho) = (\sigma)X(\rho) - (\sigma)N(\rho)$
MaxR10-90	Quadrant Feature Representing the Maximum of the Range from CF10 to CF90 over all Four Quadrants of a Given Infrared Sample Observation	$\mathrm{MaxR10\text{-}90} = \mathrm{Maximum}\,[\mathrm{R10\text{-}90}_{(\mathrm{Quadrant\ 1})} + \mathrm{R10\text{-}90}_{(\mathrm{Quadrant\ 2})} + \mathrm{R10\text{-}90}_{(\mathrm{Quadrant\ 3})} + \mathrm{R10\text{-}90}_{(\mathrm{Quadrant\ 4})}]$
RanR10-90	Quadrant Feature Representing the Range of the R10-90 Feature over all Four Quadrants of a Given Infrared Sample Observation	$\mathrm{RanR10\text{-}90} = \mathrm{MaxR10\text{-}90} - \mathrm{Minimum}\,[\mathrm{R10\text{-}90}_{(\mathrm{Quadrant\ 1})} + \mathrm{R10\text{-}90}_{(\mathrm{Quadrant\ 2})} + \mathrm{R10\text{-}90}_{(\mathrm{Quadrant\ 3})} + \mathrm{R10\text{-}90}_{(\mathrm{Quadrant\ 4})}]$
MinCFO	Quadrant Feature Representing the Minimum Measurement Value of a Given Infrared Sample Observation	MinCFO = CFO
RanCFO	Quadrant Feature Representing the Range of the MinCFO Feature over all Four Quadrants of a Given Infrared Sample Observation	$\mathrm{RanCFO} = \mathrm{Maximum}\,[\mathrm{MinCFO}_{(\mathrm{Quadrant\ 1})} + \mathrm{MinCFO}_{(\mathrm{Quadrant\ 2})} + \mathrm{MinCFO}_{(\mathrm{Quadrant\ 3})} + \mathrm{MinCFO}_{(\mathrm{Quadrant\ 4})}]$

Table A.2. FEATURE DEFINITIONS (CONTINUED)

Abbreviation	Name	Formula
MaxStDev	Quadrant Feature Representing the Maximum Value of the Quadrant Standard Deviations	$MaxStDev = Maximum\ [StDev_{(Quadrant\ 1)} + StDev_{(Quadrant\ 2)} + StDev_{(Quadrant\ 3)} + StDev_{(Quadrant\ 4)}]$
RanStDev	Quadrant Feature Representing the Range of the MaxStDev Feature over all Four Quadrants of a Given Infrared Sample Observation	$RanStDev = MaxStDev - Minimum\ [StDev_{(Quadrant\ 1)} + StDev_{(Quadrant\ 2)} + StDev_{(Quadrant\ 3)} + StDev_{(Quadrant\ 4)}]$

Table A.2. FEATURE DEFINITIONS (CONTINUED)

Table A.3

VISUAL FEATURES

Feature Number	Feature Histogram(s)	Feature Name
101	VB	Mean
102	VB	StDev
103	VB	CF0
104	VB	CF10
105	VB	CF20
106	VB	CF30
107	VB	CF40
108	VB	CF50
109	VB	CF60
110	VB	CF70
111	VB	CF80
112	VB	CF90
113	VB	CF100
114	VB	R0-100
115	VB	R10-90
116	VB	R0-50
117	VB	R50-100
118	VB	R20-80
119	VB	R30-70
120	VB	R40-60
121	VDHor1	MeanHor
122	VDVer1	MeanVer
123	VD1D1	Mean1D
124	VD2D1	Mean2D
125	VDHor1, VDVer1, VD1D1, VD2D1	MeanM
126	VDHor1, VDVer1, VD1D1, VD2D1	MeanS
127	VDHor1, VDVer1, VD1D1, VD2D1	MeanN
128	VDHor1, VDVer1, VD1D1, VD2D1	MeanX
129	VDHor1, VDVer1, VD1D1, VD2D1	MeanR
130	VDHor1	ConHor

VISUAL FEATURES (page 2)

Feature Number	Feature Histogram(s)	Feature Name
131	VDVer1	ConVer
132	VD1D1	Con1D
133	VD2D1	Con2D
134	VDHor1, VDVer1, VD1D1, VD2D1	ConM
135	VDHor1, VDVer1, VD1D1, VD2D1	ConS
136	VDHor1, VDVer1, VD1D1, VD2D1	ConN
137	VDHor1, VDVer1, VD1D1, VD2D1	ConX
138	VDHor1, VDVer1, VD1D1, VD2D1	ConR
139	VDHor1	ASMHor
140	VDVer1	ASMVer
141	VD1D1	ASM1D
142	VD2D1	ASM2D
143	VDHor1, VDVer1, VD1D1, VD2D1	ASMM
144	VDHor1, VDVer1, VD1D1, VD2D1	ASMS
145	VDHor1, VDVer1, VD1D1, VD2D1	ASMN
146	VDHor1, VDVer1, VD1D1, VD2D1	ASMX
147	VDHor1, VDVer1, VD1D1, VD2D1	ASMR
148	VDHor1	EntHor
149	VDVer1	EntVer
150	VD1D1	Ent1D
151	VD2D1	Ent2D
152	VDHor1, VDVer1, VD1D1, VD2D1	EntM
153	VDHor1, VDVer1, VD1D1, VD2D1	EntS
154	VDHor1, VDVer1, VD1D1, VD2D1	EntN
155	VDHor1, VDVer1, VD1D1, VD2D1	EntX
156	VDHor1, VDVer1, VD1D1, VD2D1	EntR
157	VDHor2	MeanHor2
158	VDVer2	MeanVer2
159	VD1D2	Mean1D2
160	VD2D2	Mean2D2

VISUAL FEATURES (page 3)

Feature Number	Feature Histogram(s)	Feature Name
161	VDHor2, VDVer2, VD1D2, VD2D2	MeanM2
162	VDHor2, VDVer2, VD1D2, VD2D2	MeanS2
163	VDHor2, VDVer2, VD1D2, VD2D2	MeanN2
164	VDHor2, VDVer2, VD1D2, VD2D2	MeanX2
165	VDHor2, VDVer2, VD1D2, VD2D2	MeanR2
166	VDHor2	ConHor2
167	VDVer2	ConVer2
168	VD1D2	Con1D2
169	VD2D2	Con2D2
170	VDHor2, VDVer2, VD1D2, VD2D2	ConM2
171	VDHor2, VDVer2, VD1D2, VD2D2	ConS2
172	VDHor2, VDVer2, VD1D2, VD2D2	ConN2
173	VDHor2, VDVer2, VD1D2, VD2D2	ConX2
174	VDHor2, VDVer2, VD1D2, VD2D2	ConR2
175	VDHor2	ASMHor2
176	VDVer2	ASMVer2
177	VD1D2	ASM1D2
178	VD2D2	ASM2D2
179	VDHor2, VDVer2, VD1D2, VD2D2	ASMM2
180	VDHor2, VDVer2, VD1D2, VD2D2	ASMS2
181	VDHor2, VDVer2, VD1D2, VD2D2	ASMN2
182	VDHor2, VDVer2, VD1D2, VD2D2	ASMX2
183	VDHor2, VDVer2, VD1D2, VD2D2	ASMR2
184	VDHor2	EntHor2
185	VDVer2	EntVer2
186	VD1D2	Ent1D2
187	VD2D2	Ent2D2
188	VDHor2, VDVer2, VD1D2, VD2D2	EntM2
189	VDHor2, VDVer2, VD1D2, VD2D2	EntS2
190	VDHor2, VDVer2, VD1D2, VD2D2	EntN2

VISUAL FEATURES (page 4)

Feature Number	Feature Histogram(s)	Feature Name
191	VDHor2, VDVer2, VD1D2, VD2D2	EntX2
192	VDHor2, VDVer2, VD1D2, VD2D2	EntR2
193	VDHor4	MeanHor4
194	VDVer4	MeanVer4
195	VD1D4	Mean1D4
196	VD2D4	Mean2D4
197	VDHor4, VDVer4, VD1D4, VD2D4	MeanM4
198	VDHor4, VDVer4, VD1D4, VD2D4	MeanS4
199	VDHor4, VDVer4, VD1D4, VD2D4	MeanN4
200	VDHor4, VDVer4, VD1D4, VD2D4	MeanX4
201	VDHor4, VDVer4, VD1D4, VD2D4	MeanR4
202	VDHor4	ConHor4
203	VDVer4	ConVer4
204	VD1D4	Con1D4
205	VD2D4	Con2D4
206	VDHor4, VDVer4, VD1D4, VD2D4	ConM4
207	VDHor4, VDVer4, VD1D4, VD2D4	ConS4
208	VDHor4, VDVer4, VD1D4, VD2D4	ConN4
209	VDHor4, VDVer4, VD1D4, VD2D4	ConX4
210	VDHor4, VDVer4, VD1D4, VD2D4	ConR4
211	VDHor4	ASMHor4
212	VDVer4	ASMVer4
213	VD1D4	ASM1D4
214	VD2D4	ASM2D4
215	VDHor4, VDVer4, VD1D4, VD2D4	ASMM4
216	VDHor4, VDVer4, VD1D4, VD2D4	ASMS4
217	VDHor4, VDVer4, VD1D4, VD2D4	ASMN4
218	VDHor4, VDVer4, VD1D4, VD2D4	ASMX4
219	VDHor4, VDVer4, VD1D4, VD2D4	ASMR4
220	VDHor4	EntHor4

VISUAL FEATURES (page 5)

Feature Number	Feature Histogram(s)	Feature Name
221	VDVer4	EntVer4
222	VD1D4	Ent1D4
223	VD2D4	Ent2D4
224	VDHor4, VDVer4, VD1D4, VD2D4	EntM4
225	VDHor4, VDVer4, VD1D4, VD2D4	EntS4
226	VDHor4, VDVer4, VD1D4, VD2D4	EntN4
227	VDHor4, VDVer4, VD1D4, VD2D4	EntX4
228	VDHor4, VDVer4, VD1D4, VD2D4	EntR4
229	VDHor8	MeanHor8
230	VDVer8	MeanVer8
231	VD1D8	Mean1D8
232	VD2D8	Mean2D8
233	VDHor8, VDVer8, VD1D8, VD2D8	MeanM8
234	VDHor8, VDVer8, VD1D8, VD2D8	MeanS8
235	VDHor8, VDVer8, VD1D8, VD2D8	MeanN8
236	VDHor8, VDVer8, VD1D8, VD2D8	MeanX8
237	VDHor8, VDVer8, VD1D8, VD2D8	MeanR8
238	VDHor8	ConHor8
239	VDVer8	ConVer8
240	VD1D8	Con1D8
241	VD2D8	Con2D8
242	VDHor8, VDVer8, VD1D8, VD2D8	ConM8
243	VDHor8, VDVer8, VD1D8, VD2D8	ConS8
244	VDHor8, VDVer8, VD1D8, VD2D8	ConN8
245	VDHor8, VDVer8, VD1D8, VD2D8	ConX8
246	VDHor8, VDVer8, VD1D8, VD2D8	ConR8
247	VDHor8	ASMHor8
248	VDVer8	ASMVer8
249	VD1D8	ASM1D8
250	VD2D8	ASM2D8

VISUAL FEATURES (page 6)

Feature Number	Feature Histogram(s)	Feature Name
251	VDHor8, VDVer8, VD1D8, VD2D8	ASMM8
252	VDHor8, VDVer8, VD1D8, VD2D8	ASMS8
253	VDHor8, VDVer8, VD1D8, VD2D8	ASMN8
254	VDHor8, VDVer8, VD1D8, VD2D8	ASMX8
255	VDHor8, VDVer8, VD1D8, VD2D8	ASMR8
256	VDHor8	EntHor8
257	VDVer8	EntVer8
258	VD1D8	Ent1D8
259	VD2D8	Ent2D8
260	VDHor8, VDVer8, VD1D8, VD2D8	EntM8
261	VDHor8, VDVer8, VD1D8, VD2D8	EntS8
262	VDHor8, VDVer8, VD1D8, VD2D8	EntN8
263	VDHor8, VDVer8, VD1D8, VD2D8	EntX8
264	VDHor8, VDVer8, VD1D8, VD2D8	EntR8

Table A.4

INFRARED FEATURES

Feature Number	Feature Histogram(s)	Feature Name
301	IT	Mean
302	IT	StDev
303	IT	CF0
304	IT	CF10
305	IT	CF20
306	IT	CF30
307	IT	CF40
308	IT	CF50
309	IT	CF60
310	IT	CF70
311	IT	CF80
312	IT	CF90
313	IT	CF100
314	IT	R0-100
315	IT	R10-90
316	IT	R0-50
317	IT	R50-100
318	IT	R20-80
319	IT	R30-70
320	IT	R40-60
321	IDHor1	MeanHor
322	IDVer1	MeanVer
323	ID1D1	Mean1D
324	ID2D1	Mean2D
325	IDHor1, IDVer1, ID1D1, ID2D1	MeanM
326	IDHor1, IDVer1, ID1D1, ID2D1	MeanS
327	IDHor1, IDVer1, ID1D1, ID2D1	MeanN
328	IDHor1, IDVer1, ID1D1, ID2D1	MeanX
329	IDHor1, IDVer1, ID1D1, ID2D1	MeanR
330	IDHor1	ConHor

INFRARED FEATURES (page 2)

Feature Number	Feature Histogram(s)	Feature Name
331	IDVer1	ConVer
332	ID1D1	Con1D
333	ID2D1	Con2D
334	IDHor1, IDVer1, ID1D1, ID2D1	ConM
335	IDHor1, IDVer1, ID1D1, ID2D1	ConS
336	IDHor1, IDVer1, ID1D1, ID2D1	ConN
337	IDHor1, IDVer1, ID1D1, ID2D1	ConX
338	IDHor1, IDVer1, ID1D1, ID2D1	ConR
339	IDHor1	ASMHor
340	IDVer1	ASMVer
341	ID1D1	ASM1D
342	ID2D1	ASM2D
343	IDHor1, IDVer1, ID1D1, ID2D1	ASMM
344	IDHor1, IDVer1, ID1D1, ID2D1	ASMS
345	IDHor1, IDVer1, ID1D1, ID2D1	ASMN
346	IDHor1, IDVer1, ID1D1, ID2D1	ASMX
347	IDHor1, IDVer1, ID1D1, ID2D1	ASMR
348	IDHor1	EntHor
349	IDVer1	EntVer
350	ID1D1	Ent1D
351	ID2D1	Ent2D
352	IDHor1, IDVer1, ID1D1, ID2D1	EntM
353	IDHor1, IDVer1, ID1D1, ID2D1	EntS
354	IDHor1, IDVer1, ID1D1, ID2D1	EntN
355	IDHor1, IDVer1, ID1D1, ID2D1	EntX
356	IDHor1, IDVer1, ID1D1, ID2D1	EntR
357	IDHor2	MeanHor2
358	IDVer2	MeanVer2
359	ID1D2	Mean1D2
360	ID2D2	Mean2D2

INFRARED FEATURES (page 3)

Feature Number	Feature Histogram(s)	Feature Name
361	IDHor2, IDVer2, ID1D2, ID2D2	MeanM2
362	IDHor2, IDVer2, ID1D2, ID2D2	MeanS2
363	IDHor2, IDVer2, ID1D2, ID2D2	MeanN2
364	IDHor2, IDVer2, ID1D2, ID2D2	MeanX2
365	IDHor2, IDVer2, ID1D2, ID2D2	MeanR2
366	IDHor2	ConHor2
367	IDVer2	ConVer2
368	ID1D2	Con1D2
369	ID2D2	Con2D2
370	IDHor2, IDVer2, ID1D2, ID2D2	ConM2
371	IDHor2, IDVer2, ID1D2, ID2D2	ConS2
372	IDHor2, IDVer2, ID1D2, ID2D2	ConN2
373	IDHor2, IDVer2, ID1D2, ID2D2	ConX2
374	IDHor2, IDVer2, ID1D2, ID2D2	ConR2
375	IDHor2	ASMHor2
376	IDVer2	ASMVer2
377	ID1D2	ASM1D2
378	ID2D2	ASM2D2
379	IDHor2, IDVer2, ID1D2, ID2D2	ASMM2
380	IDHor2, IDVer2, ID1D2, ID2D2	ASMS2
381	IDHor2, IDVer2, ID1D2, ID2D2	ASMN2
382	IDHor2, IDVer2, ID1D2, ID2D2	ASMX2
383	IDHor2, IDVer2, ID1D2, ID2D2	ASMR2
384	IDHor2	EntHor2
385	IDVer2	EntVer2
386	ID1D2	Ent1D2
387	ID2D2	Ent2D2
388	IDHor2, IDVer2, ID1D2, ID2D2	EntM2
389	IDHor2, IDVer2, ID1D2, ID2D2	EntS2
390	IDHor2, IDVer2, ID1D2, ID2D2	EntN2

INFRARED FEATURES (page 4)

Feature Number	Feature Histogram(s)	Feature Name
391	IDHor2, IDVer2, ID1D2, ID2D2	ENTX2
392	IDHor2, IDVer2, ID1D2, ID2D2	ENTR2
393	IDHor4	MeanHor4
394	IDVer4	MeanVer4
395	ID1D4	Mean1D4
396	ID2D4	Mean2D4
397	IDHor4, IDVer4, ID1D4, ID2D4	MeanM4
398	IDHor4, IDVer4, ID1D4, ID2D4	MeanS4
399	IDHor4, IDVer4, ID1D4, ID2D4	MeanN4
400	IDHor4, IDVer4, ID1D4, ID2D4	MeanX4
401	IDHor4, IDVer4, ID1D4, ID2D4	MeanR4
402	IDHor4	ConHor4
403	IDVer4	ConVer4
404	ID1D4	Con1D4
405	ID2D4	Con2D4
406	IDHor4, IDVer4, ID1D4, ID2D4	ConM4
407	IDHor4, IDVer4, ID1D4, ID2D4	ConS4
408	IDHor4, IDVer4, ID1D4, ID2D4	ConN4
409	IDHor4, IDVer4, ID1D4, ID2D4	ConX4
410	IDHor4, IDVer4, ID1D4, ID2D4	ConR4
411	IDHor4	ASMHor4
412	IDVer4	ASMVer4
413	ID1D4	ASM1D4
414	ID2D4	ASM2D4
415	IDHor4, IDVer4, ID1D4, ID2D4	ASMM4
416	IDHor4, IDVer4, ID1D4, ID2D4	ASMS4
417	IDHor4, IDVer4, ID1D4, ID2D4	ASMN4
418	IDHor4, IDVer4, ID1D4, ID2D4	ASMX4
419	IDHor4, IDVer4, ID1D4, ID2D4	ASMR4
420	IDHor4	EntHor4

INFRARED FEATURES (page 5)

Feature Number	Feature Histogram(s)	Feature Name
421	IDVer4	EntVer4
422	ID1D4	Ent1D4
423	ID2D4	Ent2D4
424	IDHor4, IDVer4, ID1D4, ID2D4	EntM4
425	IDHor4, IDVer4, ID1D4, ID2D4	EntS4
426	IDHor4, IDVer4, ID1D4, ID2D4	EntN4
427	IDHor4, IDVer4, ID1D4, ID2D4	EntX4
428	IDHor4, IDVer4, ID1D4, ID2D4	EntR4
429	IDHor8	MeanHor8
430	IDVer8	MeanVer8
431	ID1D8	Mean1D8
432	ID2D8	Mean2D8
433	IDHor8, IDVer8, ID1D8, ID2D8	MeanM8
434	IDHor8, IDVer8, ID1D8, ID2D8	MeanS8
435	IDHor8, IDVer8, ID1D8, ID2D8	MeanN8
436	IDHor8, IDVer8, ID1D8, ID2D8	MeanX8
437	IDHor8, IDVer8, ID1D8, ID2D8	MeanR8
438	IDHor8	ConHor8
439	IDVer8	ConVer8
440	ID1D8	Con1D8
441	ID2D8	Con2D8
442	IDHor8, IDVer8, ID1D8, ID2D8	ConM8
443	IDHor8, IDVer8, ID1D8, ID2D8	ConS8
444	IDHor8, IDVer8, ID1D8, ID2D8	ConN8
445	IDHor8, IDVer8, ID1D8, ID2D8	ConX8
446	IDHor8, IDVer8, ID1D8, ID2D8	ConR8
447	IDHor8	ASMHor8
448	IDVer8	ASMVer8
449	ID1D8	ASM1D8
450	ID2D8	ASM2D8

INFRARED FEATURES (page 6)

Feature Number	Feature Histogram(s)	Feature Name
452	IDHor8, IDVer8, ID1D8, ID2D8	ASMS8
453	IDHor8, IDVer8, ID1D8, ID2D8	ASMN8
454	IDHor8, IDVer8, ID1D8, ID2D8	ASMX8
455	IDHor8, IDVer8, ID1D8, ID2D8	ASMR8
456	IDHor8	EntHor8
457	IDVer8	EntVer8
458	ID1D8	Ent1D8
459	ID2D8	Ent2D8
460	IDHor8, IDVer8, ID1D8, ID2D8	EntM8
461	IDHor8, IDVer8, ID1D8, ID2D8	EntS8
462	IDHor8, IDVer8, ID1D8, ID2D8	EntN8
463	IDHor8, IDVer8, ID1D8, ID2D8	EntX8
464	IDHor8, IDVer8, ID1D8, ID2D8	EntR8
465	$IT_{(QUADRANT\ 1)}$, $IT_{(QUADRANT\ 2)}$, $IT_{(QUADRANT\ 3)}$, $IT_{(QUADRANT\ 4)}$	MaxR10-90
466	$IT_{(QUADRANT\ 1)}$, $IT_{(QUADRANT\ 2)}$, $IT_{(QUADRANT\ 3)}$, $IT_{(QUADRANT\ 4)}$	RanR10-90
467	$IT_{(QUADRANT\ 1)}$, $IT_{(QUADRANT\ 2)}$, $IT_{(QUADRANT\ 3)}$, $IT_{(QUADRANT\ 4)}$	MinCF0
468	$IT_{(QUADRANT\ 1)}$, $IT_{(QUADRANT\ 2)}$, $IT_{(QUADRANT\ 3)}$, $IT_{(QUADRANT\ 4)}$	RanCF0
469	$IT_{(QUADRANT\ 1)}$, $IT_{(QUADRANT\ 2)}$, $IT_{(QUADRANT\ 3)}$, $IT_{(QUADRANT\ 4)}$	MaxStDev
470	$IT_{(QUADRANT\ 1)}$, $IT_{(QUADRANT\ 2)}$, $IT_{(QUADRANT\ 3)}$, $IT_{(QUADRANT\ 4)}$	RanStDev

Appendix B

Classifiers and Feature Selection Criterion

I. Maximum Likelihood Classifier

The maximum likelihood classifier for a k-class problem (classes $w_1,\ldots,w_k$) assigns a sample observation with feature vector $\vec{X}$ to class w_j iff

(1) $\ln P(w_j/\vec{X}) > \ln P(w_i/\vec{X})$ for all $i \neq j$, $i=1,\ldots,k$

where $P(w_j/\vec{X})$ is the a posteriori probability that the observation with feature vector $\vec{X}$ belongs to class w_j. According to Bayes' Rule, the a posteriori probability $P(w_j/\vec{X})$ is related to the conditional probability $p(\vec{X}/w_j)$ as follows:

(2) $$P(w_j/\vec{X}) = \frac{p(\vec{X}/w_j)P(w_j)}{\sum_{i=1}^{k} p(\vec{X}/w_i)P(w_i)}$$

where the a priori probability $P(w_j)$ is given by

(3) $$P(w_j) = \frac{n_j}{\sum_{i=1}^{k} n_i}$$

where n_i = number of samples in class w_i, $i=1,\ldots,k$.

Since the denominator in the expression for $P(w_j/\vec{X})$ is common to all classes, the decision rule can be rephrased as:

Assign an observation with feature vector $\vec{X}$ to class w_j iff

(4) $\ln p(\vec{X}/w_j)P(w_j) > \ln p(\vec{X}/w_i)P(w_i)$ for all $i \neq j$,
$i=1,\ldots,k$

Assuming that the class conditional densities can be modeled by multivariate normal densities,

$$(5)\quad p(X/w_j) = \frac{1}{(2\Pi)^{d/2}|\Sigma_j|^{1/2}} \exp[-\tfrac{1}{2}(\vec{X}-\vec{M}_j)^T \Sigma_j^{-1} (\vec{X}-\vec{M}_j)]$$

where d is the number of features selected at the decision node

Σ_j is the dxd covariance matrix for the class w_j

$\vec{X}$ is the d-component column vector of feature values

$\vec{M}_j$ is the d-component column vector of feature means for the class w_j.

If X_{rc} is the rth component of the feature vector $\vec{X}$ for sample c of class w_j where $c = 1,\ldots,n_j$ and m_r is the rth component of the mean vector M_j for class w_j and $\sigma_{rs} = \sigma_{sr}$ is the r-sth component of Σ_j, then

$$(6)\quad m_r = \frac{\sum_{c=1}^{n_j} X_{rc}}{n_j}$$

and

$$(7)\quad \sigma_{rs} = \frac{\sum_{c=1}^{n_j} (X_{rc}-m_r)(X_{sc}-m_s)}{n_j}$$

The next three classifiers -- multiclass one-against-the-rest, multiclass voting, and Fisher (for two-class problem) with sample $P(w_i)$ classify a simple observation with feature vector $\vec{X}$ into class w_j depending on the result of one or more two-class comparisons of the form

$$(8)\quad \ln P(w_j/\vec{X}) > \ln P(w_i/\vec{X})$$

where for each two-class comparison, the covariance matrix of both classes is assumed to be equal and is estimated by an averaged covariance matrix.

II. Multiclass One-Against-The-Rest

The multiclass one-against-the-rest classifier for a k-class problem assigns a sample observation with feature vector $\vec{X}$ to class w_j iff one and only one of the following inequalities is satisfied:

$$
(9)\qquad
\begin{aligned}
\ln p(\vec{X}/w_1) &> \ln p(\vec{X}/\text{not } w_1)\\
&\vdots\\
\ln p(\vec{X}/w_k) &> \ln p(\vec{X}/\text{not } w_k)
\end{aligned}
$$

Otherwise the sample is rejected and no classification decision is made. Sample a priori probabilities $P(w_i)$ and $P(\text{not } w_i)$ are assumed to be equal for all $i=1,\ldots,k$ and thus have been dropped from equation (4) to obtain the above inequalities. $p(\vec{X}/w_i)$ is assumed to be distributed normally with mean vector M_i and covariance matrix $\tilde{\sum}_i$ and $p(\vec{X}/\text{not } w_i)$ is assumed to be distributed normally with mean vector $\tilde{M}_i$ and the same covariance matrix $\tilde{\sum}_i$ used to characterize $p(\vec{X}/w_i)$. If the components of the mean vector $\tilde{M}_j$ are given by equation (6) and the components of the covariance matrix $\sum_j$ for $j=1,\ldots,k$ are given by equation (7), then the mean vector $\tilde{M}_i$ and the covariance matrix $\tilde{\sum}_i$ are given by

$$(10)\quad \tilde{M}_i = \frac{M_1+\cdots+M_{i-1}+M_{i+1}+\cdots+M_k}{k-1}$$

where k is the number of classes and

$$(11)\quad \tilde{\sum}_i = \frac{1}{2}\left[\sum_i + \frac{\sum_1+\cdots+\sum_{i-1}+\sum_{i+1}+\cdots+\sum_k}{k-1}\right]$$

III. Multiclass Voting

The multiclass voting classifier for a k-class problem determines, for each of the $\frac{k!}{(k-2)!2!}$ two-class combinations of k classes, which one of the two classes satisfies the inequality

(12) $\ln p(\vec{X}/w_j) > \ln p(\vec{X}/w_i),\ i \neq j$

The multiclass voting classifier then assigns a sample cloud observation with feature vector $\vec{X}$ to that class w_v such that the number of two-class inequalities of the form (12) satisfied by w_v is greater than the number satisfied by any other class w_i, $i \neq v$. If two classes are tied for the greatest number of votes, the sample is rejected. Sample a priori probabilities $P(w_i)$ and $P(w_j)$ are assumed to be equal for all $i, j = 1,\ldots,k$. $p(\vec{X}/w_i)$ is assumed to be distributed normally with mean vector M_i and covariance matrix $\sum_{ij}$ and $p(\vec{X}/w_j)$ is assumed to be distributed normally with mean vector M_j and covariance matrix $\sum_{ij}$, the averaged covariance of $\sum_i$ and $\sum_j$. Components of the mean vector M_j for $j = 1,\ldots,k$ are given by (6) and components of the covariance matrix $\sum_j$ for $j=1,\ldots,k$ are given by (7). The covariance matrix $\sum_{ij}$ is then given by

(13) $\sum_{ij} = \frac{1}{2}[\sum_i + \sum_j]$

IV. Fisher Two-Class Classifier with Sample $P(w_i)$

The Fisher classifier with sample $P(w_i)$ for a two-class problem (w_1, w_2) assigns a sample observation with feature vector $\vec{X}$ to class w_i iff

(14) $\ln p(\vec{X}/w_i)P(w_i) > \ln p(\vec{X}/w_j)P(w_j)$ for $i \neq j$, $i = 1, 2$.

A priori probabilities are computed from sample sizes by equation (3). $p(\vec{X}/w_1)$ and $p(\vec{X}/w_2)$ are assumed to be normally distributed with mean vectors M_1 and M_2 respectively and with averaged covariance matrix $\tilde{\sum}_{1\,2}$ where the components of M_j, $j = 1, 2$ are given by equation (6), and if the components of $\sum_j$ for $j = 1,2$ are given by equation (7), then the covariance matrix $\tilde{\sum}_{1\,2}$ is defined as

(15) $\tilde{\sum}_{1\,2} = P(w_1)\sum_1 + P(w_2)\sum_2$.

V. Fisher Distance Feature Selection Criterion

The Fisher Distance feature selection criterion for single combinations of features is defined as

$$(16) \quad J = \frac{|m_1 - m_2|}{\sigma_1 + \sigma_2}$$

where m_1, m_2 are the means of the selected feature for classes w_1 and w_2, respectively, and σ_1, σ_2 are the standard deviations for classes w_1 and w_2. The Fisher Distance measures the separation between two classes for the given feature.

Appendix C

Confusion Matrices

<ins>Note</ins>: In the confusion matrices for Table 36, user categories "MIX1" and "MIX2", the row headings for the confusion matrices, represent respectively the training set of labelled mixed samples used to train the classifier at level 2 and the identical training set of labelled mixed samples used to train the classifier at level 1 of Tree 2 (Figure 6). Both rows 2 and 3, therefore, repeat the same information concerning the automatic classification categories (column headings) into which the mixed samples were classified. The column heading "MIX1" denotes the terminal automatic classification bin at level 2 for mixed samples and the column heading "MIX2" denotes the terminal automatic classification bin at level 1 for mixed samples. In experiment 1 (Table 36) at level 1, 12 mixed samples were incorrectly classified as low. From these 12 samples, the entry under the column heading "MIX1" shows that 6 samples were classified at level 2 into "MIX1", making the total number of correctly classified mixed samples 73 + 6 = 79.

TABLE 28, EXPERIMENT 1

	LOW	MIX	CI	CB
LOW	48	29	0	9
MIX	28	50	0	9
CI	11	13	0	0
CB	6	18	0	22

TABLE 28, EXPERIMENT 2

	LOW	MIX	CI	CB
LOW	34	45	0	7
MIX	21	56	0	10
CI	16	8	0	0
CB	0	7	0	39

TABLE 28, EXPERIMENT 3

	LOW	MIX	CI	CB
LOW	36	46	0	4
MIX	24	58	0	5
CI	19	5	0	0
CB	0	12	0	34

TABLE 28, EXPERIMENT 4

	LOW	MIX	CI	CB
LOW	54	26	0	6
MIX	30	47	0	10
CI	19	5	0	0
CB	2	17	0	27

TABLE 28, EXPERIMENT 5

	LOW	MIX	CI	CB
LOW	62	19	0	5
MIX	45	33	0	9
CI	20	4	0	0
CB	6	17	0	23

TABLE 28, EXPERIMENT 6

	LOW	MIX	CI	CB
LOW	35	42	0	9
MIX	21	62	0	4
CI	9	15	0	0
CB	8	21	0	17

TABLE 28, EXPERIMENT 7

	LOW	MIX	CI	CB
LOW	59	22	0	5
MIX	33	44	0	10
CI	18	6	0	0
CB	4	19	0	23

TABLE 29, EXPERIMENT 1

	LOW	MIX	CI	CB
LOW	59	23	0	4
MIX	54	27	0	6
CI	24	0	0	0
CB	12	15	0	19

TABLE 29, EXPERIMENT 2

	LOW	MIX	CI	CB
LOW	39	43	0	4
MIX	32	48	0	7
CI	20	4	0	0
CB	0	24	0	22

TABLE 29, EXPERIMENT 3

	LOW	MIX	CI	CB
LOW	46	36	0	4
MIX	36	43	0	8
CI	20	4	0	0
CB	1	23	0	22

TABLE 29, EXPERIMENT 4

	LOW	MIX	CI	CB
LOW	37	45	0	4
MIX	29	51	0	7
CI	20	4	0	0
CB	0	21	0	25

TABLE 29, EXPERIMENT 5

	LOW	MIX	CI	CB
LOW	32	41	9	4
MIX	36	38	4	9
CI	17	0	7	0
CB	9	18	0	19

TABLE 29, EXPERIMENT 6

	LOW	MIX	CI	CB
LOW	33	35	1	17
MIX	18	40	0	29
CI	15	8	1	0
CB	0	10	0	36

TABLE 29, EXPERIMENT 7

	LOW	MIX	CI	CB
LOW	34	33	1	18
MIX	18	41	0	28
CI	15	8	1	0
CB	0	9	0	37

TABLE 29, EXPERIMENT 8

	LOW	MIX	CI	CB
LOW	33	36	1	16
MIX	17	39	0	31
CI	15	8	1	0
CB	0	11	0	35

TABLE 29, EXPERIMENT 9

	LOW	MIX	CI	CB
LOW	44	34	0	8
MIX	38	40	0	9
CI	22	2	0	0
CB	4	21	0	21

TABLE 29, EXPERIMENT 10

	LOW	MIX	CI	CB
LOW	31	45	0	10
MIX	21	52	0	14
CI	16	8	0	0
CB	0	17	0	29

TABLE 29, EXPERIMENT 11

	LOW	MIX	CI	CB
LOW	34	42	0	10
MIX	24	47	0	16
CI	17	7	0	0
CB	0	17	0	29

TABLE 29, EXPERIMENT 12

	LOW	MIX	CI	CB
LOW	32	44	0	10
MIX	22	52	0	13
CI	16	8	0	0
CB	0	17	0	29

TABLE 30, EXPERIMENT 1

	LOW	MIX	CI	CB
LOW	82	4	0	0
MIX	18	63	0	6
CI	1	17	0	6
CB	0	19	0	27

TABLE 30, EXPERIMENT 2

	LOW	MIX	CI	CB
LOW	82	4	0	0
MIX	15	62	0	10
CI	3	18	0	3
CB	0	12	0	34

TABLE 30, EXPERIMENT 3

	LOW	MIX	CI	CB
LOW	75	11	0	0
MIX	43	36	0	8
CI	13	5	3	3
CB	10	11	0	25

TABLE 30, EXPERIMENT 4

	LOW	MIX	CI	CB
LOW	82	4	0	0
MIX	15	61	0	11
CI	1	14	0	9
CB	0	11	0	35

TABLE 30, EXPERIMENT 5

	LOW	MIX	CI	CB
LOW	84	2	0	0
MIX	23	58	0	6
CI	1	15	0	8
CB	0	19	0	27

TABLE 30, EXPERIMENT 6

	LOW	MIX	CI	CB
LOW	83	3	0	0
MIX	12	67	0	8
CI	2	19	0	3
CB	0	25	0	21

TABLE 30, EXPERIMENT 7

	LOW	MIX	CI	CB
LOW	77	9	0	0
MIX	37	45	0	5
CI	6	10	0	8
CB	6	16	0	24

TABLE 30, EXPERIMENT 8

	LOW	MIX	CI	CB
LOW	81	5	0	0
MIX	29	54	0	4
CI	4	14	0	6
CB	1	22	0	23

TABLE 30, EXPERIMENT 9

	LOW	MIX	CI	CB
LOW	82	4	0	0
MIX	17	60	0	10
CI	1	17	0	6
CB	0	20	0	26

TABLE 30, EXPERIMENT 10

	LOW	MIX	CI	CB
LOW	82	4	0	0
MIX	19	57	0	11
CI	3	19	0	2
CB	1	32	0	13

TABLE 30, EXPERIMENT 11

	LOW	MIX	CI	CB
LOW	82	4	0	0
MIX	15	62	0	10
CI	3	18	0	3
CB	0	12	0	34

TABLE 30, EXPERIMENT 12

	LOW	MIX	CI	CB
LOW	82	4	0	0
MIX	18	61	0	8
CI	3	19	0	2
CB	2	30	0	14

TABLE 30, EXPERIMENT 13

	LOW	MIX	CI	CB
LOW	82	4	0	0
MIX	15	63	0	9
CI	1	18	0	5
CB	0	19	0	27

TABLE 30, EXPERIMENT 14

	LOW	MIX	CI	CB
LOW	82	4	0	0
MIX	20	57	0	10
CI	3	19	0	2
CB	2	29	0	15

TABLE 31, EXPERIMENT 1

	LOW	MIX	CI	CB
LOW	83	3	Ø	Ø
MIX	3Ø	49	Ø	8
CI	6	14	Ø	4
CB	Ø	22	Ø	24

TABLE 31, EXPERIMENT 2

	LOW	MIX	CI	CB
LOW	81	5	Ø	Ø
MIX	25	52	Ø	1Ø
CI	2	15	Ø	7
CB	Ø	2Ø	Ø	26

TABLE 31, EXPERIMENT 3

	LOW	MIX	CI	CB
LOW	82	4	Ø	Ø
MIX	25	52	Ø	1Ø
CI	2	14	Ø	8
CB	Ø	2Ø	Ø	26

TABLE 31, EXPERIMENT 4

	LOW	MIX	CI	CB
LOW	8Ø	6	Ø	Ø
MIX	26	51	Ø	1Ø
CI	4	13	Ø	7
CB	Ø	21	Ø	25

TABLE 31, EXPERIMENT 5

	LOW	MIX	CI	CB
LOW	81	5	Ø	Ø
MIX	31	4Ø	Ø	16
CI	9	12	Ø	3
CB	3	14	Ø	29

TABLE 31, EXPERIMENT 6

	LOW	MIX	CI	CB
LOW	75	11	0	0
MIX	23	41	0	23
CI	2	11	0	11
CB	0	10	0	36

TABLE 31, EXPERIMENT 7

	LOW	MIX	CI	CB
LOW	77	9	0	0
MIX	22	43	0	22
CI	3	11	0	10
CB	0	9	0	37

TABLE 31, EXPERIMENT 8

	LOW	MIX	CI	CB
LOW	75	11	0	0
MIX	23	41	0	23
CI	3	10	0	11
CB	0	9	0	37

TABLE 31, EXPERIMENT 9

	LOW	MIX	CI	CB
LOW	83	3	0	0
MIX	27	47	0	13
CI	2	16	0	6
CB	0	18	0	28

TABLE 31, EXPERIMENT 10

	LOW	MIX	CI	CB
LOW	80	6	0	0
MIX	22	52	0	13
CI	2	13	0	9
CB	0	12	0	34

TABLE 31, EXPERIMENT 11

	LOW	MIX	CI	CB
LOW	80	6	0	0
MIX	20	52	0	15
CI	2	13	0	9
CB	0	12	0	34

TABLE 31, EXPERIMENT 12

	LOW	MIX	CI	CB
LOW	79	7	0	0
MIX	22	52	0	13
CI	2	13	0	9
CB	0	12	0	34

TABLE 32, EXPERIMENT 1

	LOW	MIX	CI	CB
LOW	83	3	0	0
MIX	12	67	0	8
CI	2	19	0	3
CB	0	25	0	21

TABLE 32, EXPERIMENT 2

	LOW	MIX	CI	CB
LOW	82	4	0	0
MIX	13	65	5	4
CI	1	5	18	0
CB	0	7	0	39

TABLE 32, EXPERIMENT 3

	LOW	MIX	CI	CB
LOW	82	3	1	0
MIX	12	65	0	10
CI	1	8	13	2
CB	0	13	0	33

TABLE 32, EXPERIMENT 4

	LOW	MIX	CI	CB
LOW	81	4	1	0
MIX	14	70	0	3
CI	1	5	18	0
CB	0	6	0	40

TABLE 32, EXPERIMENT 5

	LOW	MIX	CI	CB
LOW	82	4	0	0
MIX	12	69	4	2
CI	1	7	16	0
CB	0	7	0	39

TABLE 32, EXPERIMENT 6

	LOW	MIX	CI	CB
LOW	83	3	Ø	Ø
MIX	14	69	1	3
CI	1	5	18	Ø
CB	Ø	6	Ø	4Ø

TABLE 32, EXPERIMENT 7

	LOW	MIX	CI	CB
LOW	81	4	1	Ø
MIX	15	69	Ø	3
CI	1	5	18	Ø
CB	Ø	6	Ø	4Ø

TABLE 33, EXPERIMENT 1

	LOW	MIX	CI	CB
LOW	81	4	1	Ø
MIX	12	72	Ø	3
CI	1	7	16	Ø
CB	Ø	6	Ø	4Ø

TABLE 33, EXPERIMENT 2

	LOW	MIX	CI	CB
LOW	81	4	1	Ø
MIX	13	7Ø	Ø	4
CI	1	6	17	Ø
CB	Ø	5	Ø	41

TABLE 33, EXPERIMENT 3

	LOW	MIX	CI	CB
LOW	81	4	1	Ø
MIX	13	69	Ø	5
CI	1	4	19	Ø
CB	Ø	5	Ø	41

TABLE 33, EXPERIMENT 4

	LOW	MIX	CI	CB
LOW	83	3	Ø	Ø
MIX	14	57	4	12
CI	1	9	13	1
CB	Ø	6	2	38

TABLE 33, EXPERIMENT 5

	LOW	MIX	CI	CB
LOW	85	1	Ø	Ø
MIX	13	57	1	16
CI	1	2	15	6
CB	Ø	6	1	39

TABLE 33, EXPERIMENT 6

	LOW	MIX	CI	CB
LOW	82	4	0	0
MIX	14	68	5	0
CI	1	6	17	0
CB	0	37	7	2

TABLE 33, EXPERIMENT 7

	LOW	MIX	CI	CB
LOW	83	2	1	0
MIX	14	70	0	3
CI	1	7	16	0
CB	0	3	0	43

TABLE 33, EXPERIMENT 8

	LOW	MIX	CI	CB
LOW	85	1	0	0
MIX	13	69	2	3
CI	1	3	20	0
CB	0	6	0	40

TABLE 33, EXPERIMENT 9

	LOW	MIX	CI	CB
LOW	83	2	1	0
MIX	13	64	0	10
CI	1	8	13	2
CB	0	12	0	34

TABLE 34, EXPERIMENT 1

	LOW	MIX	CI	CB
LOW	81	5	0	0
MIX	12	71	0	4
CI	1	4	19	0
CB	0	5	0	41

TABLE 34, EXPERIMENT 2

	LOW	MIX	CI	CB
LOW	84	1	0	0
MIX	13	69	0	5
CI	1	5	18	0
CB	0	3	0	43

TABLE 34, EXPERIMENT 3

	LOW	MIX	CI	CB
LOW	82	3	1	0
MIX	13	71	0	3
CI	1	7	16	0
CB	0	5	0	41

TABLE 34, EXPERIMENT 4

	LOW	MIX	CI	CB
LOW	81	4	1	0
MIX	10	71	1	5
CI	1	7	16	0
CB	0	7	0	39

TABLE 34, EXPERIMENT 5

	LOW	MIX	CI	CB
LOW	82	3	1	0
MIX	12	70	0	5
CI	1	4	19	0
CB	0	7	0	39

TABLE 34, EXPERIMENT 6

	LOW	MIX	CI	CB
LOW	81	5	Ø	Ø
MIX	13	71	Ø	3
CI	1	6	17	Ø
CB	Ø	7	Ø	39

TABLE 35, EXPERIMENT 1

	LOW	MIX	CI	CB
LOW	81	4	1	Ø
MIX	12	73	Ø	2
CI	1	4	19	Ø
CB	Ø	3	Ø	43

TABLE 35, EXPERIMENT 2

	LOW	MIX	CI	CB
LOW	84	1	1	Ø
MIX	11	72	Ø	4
CI	1	4	19	Ø
CB	Ø	3	Ø	43

TABLE 35, EXPERIMENT 3

	LOW	MIX	CI	CB
LOW	81	4	1	Ø
MIX	11	72	Ø	4
CI	1	4	19	Ø
CB	Ø	6	Ø	4Ø

TABLE 36, EXPERIMENT 1

	LOW	MIX1	MIX2	CI	CB
LOW	81	0	4	1	0
MIX1	6	6	73	0	2
MIX2	6	6	73	0	2
CI	1	0	4	19	0
CB	0	0	3	0	43

TABLE 36, EXPERIMENT 2

	LOW	MIX1	MIX2	CI	CB
LOW	81	0	4	1	0
MIX1	7	5	73	0	2
MIX2	7	5	73	0	2
CI	1	0	4	19	0
CB	0	0	3	0	43

TABLE 36, EXPERIMENT 3

	LOW	MIX1	MIX2	CI	CB
LOW	81	0	4	1	0
MIX1	11	1	73	0	2
MIX2	11	1	73	0	2
CI	1	0	4	19	0
CB	0	0	3	0	43

TABLE 36, EXPERIMENT 4

	LOW	MIX1	MIX2	CI	CB
LOW	81	0	4	1	0
MIX1	6	6	72	0	3
MIX2	6	6	72	0	3
CI	1	0	7	16	0
CB	0	0	6	0	40

TABLE 37, EXPERIMENT 1

	LOW	MIX	CI	CB
LOW	81	4	1	Ø
MIX	12	6Ø	7	8
CI	1	5	18	Ø
CB	Ø	8	Ø	38

TABLE 37, EXPERIMENT 2

	LOW	MIX	CI	CB
LOW	81	5	Ø	Ø
MIX	8	56	16	7
CI	1	8	15	Ø
CB	Ø	6	Ø	4Ø

TABLE 37, EXPERIMENT 3

	LOW	MIX	CI	CB
LOW	81	4	1	Ø
MIX	8	62	11	6
CI	1	5	18	Ø
CB	Ø	6	Ø	4Ø

TABLE 38, EXPERIMENT 1

	LOW	MIX	CI	CB
LOW	82	3	1	Ø
MIX	8	64	4	11
CI	1	7	16	Ø
CB	Ø	4	Ø	42

TABLE 38, EXPERIMENT 2

	LOW	MIX	CI	CB
LOW	81	5	Ø	Ø
MIX	9	51	15	12
CI	1	7	16	Ø
CB	Ø	9	Ø	37

TABLE 38, EXPERIMENT 3

	LOW	MIX	CI	CB
LOW	66	2Ø	Ø	Ø
MIX	6	73	1	7
CI	1	7	16	Ø
CB	Ø	3	Ø	43

TABLE 39, EXPERIMENT 1

	LOW	MIX	CI	CB
LOW	83	2	1	0
MIX	13	67	3	4
CI	1	7	16	0
CB	0	8	0	38

TABLE 39, EXPERIMENT 2

	LOW	MIX	CI	CB
LOW	83	2	1	0
MIX	14	66	3	4
CI	1	6	17	0
CB	0	7	0	39

TABLE 39, EXPERIMENT 3

	LOW	MIX	CI	CB
LOW	81	4	1	0
MIX	13	70	1	3
CI	1	7	16	0
CB	0	6	0	40

TABLE 40, EXPERIMENT 1

	LOW	MIX	CI	CB
LOW	81	5	0	0
MIX	12	66	3	6
CI	1	5	18	0
CB	0	5	0	41

TABLE 40, EXPERIMENT 2

	LOW	MIX	CI	CB
LOW	81	5	0	0
MIX	8	70	3	6
CI	1	5	18	0
CB	0	5	0	41

TABLE 40, EXPERIMENT 3

	LOW	MIX	CI	CB
LOW	81	4	1	0
MIX	8	71	2	6
CI	1	5	18	0
CB	0	5	0	41

TABLE 41, EXPERIMENT 1

	LOW	CI	CB
LOW	77	Ø	9
CI	24	Ø	Ø
CB	6	Ø	4Ø

TABLE 41, EXPERIMENT 2

	LOW	CI	CB
LOW	85	1	Ø
CI	1	12	11
CB	Ø	5	41

TABLE 41, EXPERIMENT 3

	LOW	CI	CB
LOW	85	1	Ø
CI	1	23	Ø
CB	Ø	Ø	46

TABLE 41, EXPERIMENT 4

	LOW	CI	CB
LOW	86	Ø	Ø
CI	1	22	1
CB	Ø	Ø	46

TABLE 41, EXPERIMENT 5

	LOW	CI	CB
LOW	84	2	Ø
CI	1	23	Ø
CB	Ø	Ø	46

TABLE 42, EXPERIMENT 1

	LOW	CI	CB
LOW	86	Ø	Ø
CI	1	22	1
CB	Ø	Ø	46

TABLE 42, EXPERIMENT 2

	LOW	CI	CB
LOW	85	1	Ø
CI	1	23	Ø
CB	Ø	1	45

TABLE 42, EXPERIMENT 3

	LOW	CI	CB
LOW	85	1	Ø
CI	1	23	Ø
CB	Ø	Ø	46

TABLE 42, EXPERIMENT 4

	LOW	CI	CB
LOW	84	2	Ø
CI	1	23	Ø
CB	Ø	Ø	46

TABLE 43, EXPERIMENT 1

	LOW	MIX	CI	CB
LOW	84	2	0	0
MIX	18	53	7	9
CI	1	2	21	0
CB	0	4	0	42

TABLE 43, EXPERIMENT 2

	LOW	MIX	CI	CB
LOW	84	2	0	0
MIX	18	40	13	16
CI	0	0	24	0
CB	0	2	0	44

TABLE 43, EXPERIMENT 3

	LOW	CI	CB
LOW	85	1	0
CI	1	23	0
CB	1	0	45

TABLE 43, EXPERIMENT 4

	LOW	CI	CB
LOW	85	1	0
CI	1	23	0
CB	2	0	44

TABLE 43, EXPERIMENT 5

	LOW	MIX	CI	CB
LOW	1	1	0	0
MIX	2	17	9	8
CI	0	0	19	0
CB	0	2	0	31

TABLE 43, EXPERIMENT 6

	LOW	CI	CB
LOW	82	0	0
CI	0	22	0
CB	1	0	43

TABLE 43, EXPERIMENT 7

	LOW	MIX	CI	CB
LOW	84	2	0	0
MIX	18	64	0	5
CI	1	8	15	0
CB	0	6	0	40

TABLE 43, EXPERIMENT 8

	LOW	CI	CB
LOW	85	1	0
CI	1	22	1
CB	2	0	44

UNCLASSIFIED

SECURITY CLASSIFICATION OF THIS PAGE (When Data Entered)

18

REPORT DOCUMENTATION PAGE		READ INSTRUCTIONS BEFORE COMPLETING FORM
1. REPORT NUMBER 19 AFOSR - TR - 76 - 1137	2. GOVT ACCESSION NO.	3. RECIPIENT'S CATALOG NUMBER 9 Technical rept.,
4. TITLE (and Subtitle) 6 CLOUD PATTERN CLASSIFICATION FROM VISIBLE AND INFRARED DATA.		5. TYPE OF REPORT & PERIOD COVERED Interim
		6. PERFORMING ORG. REPORT NUMBER 14 TR-442
7. AUTHOR(s) 10 JoAnn Parikh		8. CONTRACT OR GRANT NUMBER(s) 15 F44620-72C-0062
9. PERFORMING ORGANIZATION NAME AND ADDRESS Computer Science Center Univ. of Maryland College Park, MD 20742		10. PROGRAM ELEMENT, PROJECT, TASK AREA & WORK UNIT NUMBERS 61102F 9769-02
11. CONTROLLING OFFICE NAME AND ADDRESS Math.& Info. Sciences, AFOSR/NM A.F. Systems Command, 1400 Wilson Blvd., Arlington, VA 22209		12. REPORT DATE February 1976
		13. NUMBER OF PAGES 17 168 p.
14. MONITORING AGENCY NAME & ADDRESS (if different from Controlling Office) 11 Feb 76		15. SECURITY CLASS. (of this report) UNCLASSIFIED
		15a. DECLASSIFICATION DOWNGRADING SCHEDULE

16. DISTRIBUTION STATEMENT (of this Report)

Approved for public release; distribution unlimited.

16 9769

12 02

17. DISTRIBUTION STATEMENT (of the abstract entered in Block 20, if different from Report)

18. SUPPLEMENTARY NOTES

19. KEY WORDS (Continue on reverse side if necessary and identify by block number)

Pattern recognition
Meteorology
Cloud pattern classification
Feature selection

403018

20. ABSTRACT (Continue on reverse side if necessary and identify by block number)

This report describes progress in the development of the area classification portion of a computer vision system for cloud pattern analysis. The ultimate goal of the vision system is to extract meteorologically significant cloud regions from a time sequence of dual-channel geosynchronous satellite images. The question explored by this paper is to what extend single-stage and multistage statistical pattern recognition techniques may be

next page

DD FORM 1 JAN 73 1473 EDITION OF 1 NOV 65 IS OBSOLETE UNCLASSIFIED

SECURITY CLASSIFICATION OF THIS PAGE (When Data Entered)

Abstract (cont'd)

cont

employed in the classification of clouds from a single dual-channel image.